ON-LINE MOISTURE MEASUREMENT OF ROCKS, USING MICROWAVE TECHNIQUES

Scarre Celliers
BSc (Eng) Cape Town

Thesis submitted to the Department of Electrical and Electronic Engineering of the University of Cape Town in partial fulfilment of the requirements for the degree of Master of Science in Engineering.

ABSTRACT

On-line measurement of the moisture content of process streams in a mineral processing plant is vital for their efficient operation. Although many industrial moisture meters are available, most of these were designed to determine the moisture content of low density, fine grained, uniformly surfaced and low resistance materials. Consequently these meters operate poorly on mineral treatment plants as the measured material, rock, is dense, uneven and consists of mixtures of various minerals.

A literature survey revealed that of the many methods available, only three techniques could be used for on-line moisture determination in mineral processing operations. These were microwave attenuation, phase and frequency techniques.

Microwave transmission attenuation was attempted first due to its simplicity. In this method a signal is passed through the material and the resulting attenuation gives a measure of the moisture content, as water is highly resistive to microwaves. Normally gamma rays are used in this technique, for density compensation, but this is undesirable for safety reasons. Thus an attenuation alone system was designed and built. The operating frequency was chosen at 23GHz as this is a particularly moisture sensitive frequency. Tests on various materials revealed that 23GHz was indeed a very strong moisture sensitive frequency, however, kimberlite (a diamond ore) also attenuated the signal very strongly so that the signal could not be detected. Thus this technique was not taken further. However, for a low attenuating, homogeneous material with low moisture content, this method could be used with great success.

The moisture in a material changes the phase of a coherent signal which passes through the material because of the high dielectric constant of water (ϵ_r=80). Thus phase methods monitor the phase shift of a signal passing through the measured material. This method was not considered viable since this technique also requires a direct path through the material. A reliable system could not be developed, however, because of the high loss seen for the attenuation method. A long development time and associated high costs of the complex system excluded this method from further consideration.

The high dielectric constant of water also effects the frequency and quality factor of a resonant structure; frequency shift methods were therefore considered. Open resonant structure devices were first designed as these allow easy installation and do not interfere with the processing plant operations. The devices tested were loop antennae, resonant patch antennae, and a microstrip filter. In addition, due to low quality factors and loading problems, a partially closed structure, a hybrid loop-gap resonator, was tested. Although the results of the loop-gap resonator were more promising than for the open structures, the field distribution was not strong or uniform enough to provide sufficient sensitivity and reproducibility.

Finally an almost closed structure, in the form of a rectangular waveguide resonant cavity, was developed. Although very high moisture sensitivity was observed, the structure itself was impractical for the application due to the closed cavity. This meant that passing a large sample through the cavity was impossible. Thus the cavity was separated into two, with one half placed above the sample, and the other below. The moisture sensitivity was 0.891% frequency shift for 1% moisture change, with a correlation coefficient of 0.999. Although there were loading effects

due to the kimberlite, these problems would be ameliorated using a full size structure, as the lower frequency would provide greater penetration and sensitivity. However, since this was a feasibility project, development was not taken further.

Thus a viable on-line technique for the moisture determination of kimberlite rocks has been discovered and demonstrated.

ACKNOWLEDGEMENTS

The author wishes to thank the following for their assistance in the project:

Professor B.J Downing for his supervision and support during this project.

Mr N.Wright and Mr D.Kenyon for manufacturing the mechanical designs.

All the students in the Postgraduate Microwave Laboratory, especially Sean Mercer for his advice, old designs and components.

De Beers Diamond Research Laboratories for their financial assistance and co-operation in supplying rock samples for this project. Particular thanks to Dr D.Salter for his advice on mining applications.

Council for Scientific and Industrial Research for their financial assistance.

TABLE OF CONTENTS

LIST OF ILLUSTRATIONS

FIGURES **Page**

TABLES

PHOTOGRAPHS

GLOSSARY

Felsite	- A non diamond bearing rock
τ-rays	- Gamma rays, i.e above 300GHz
Gabbro	- A non diamond bearing rock
K-band	- Microwave signals in the range 18GHz to 26.5GHz
Kimberlite	- A diamond bearing rock
LC circuit	- A circuit using inductors and capacitors
RF	- Radio frequencies i.e between 500kHz & 1GHz
S_{11}	- Reflection coefficient at port 1
S_{21}	- Forward voltage transfer ratio

CHAPTER 1

BACKGROUND THEORY

1.1. INTRODUCTION

The moisture determination of bulk solids is required in many industries including mining, food, timber and paper. Diverse applications require a host of both direct and indirect methods used in a wide range of situations. The most common of these are outlined, with their advantages and disadvantages.

1.2. TEMPERATURE DIFFERENCE

In this method the input and output gas temperatures in a dryer or the temperature difference between the drying gas and the material being dried are determined. This method works similarly to the wet and dry bulb hygrometer. The advantage of this technique is that it is on-line, cheap, reliable and easy to maintain. However, it has poor accuracy and in the latter case contact is required for measuring the material temperature. The system is not very good in dusty environments [1].

1.3. RELATIVE HUMIDITY EQUILIBRIUM

This method assumes the relative humidity of a gas in a chamber is in equilibrium with a solid, and is thus correlated to the moisture content. This system is cheap, on-line and easy to install. Its disadvantages include temperature dependance, problems in dusty

environments and accuracy. The accuracy problem exists since the gas does not have time to reach exact equilibrium with the moist material [1].

1.4. THERMAL CONDUCTIVITY METHOD

Thermal conductivity increases with moisture content. Two measuring methods exist for this technique. In the first, a heat emitting source is buried in the material. The thermal gradient through the material is then monitored using thermo-couples. In the second method the resistance of a heating element is monitored as the temperature changes. Both these methods can not estimate the moisture content either continuously or automatically, thus not being on-line systems [2].

1.5. ELECTRICAL RESISTANCE METHOD

Resistivity decreases with moisture content due to the conductivity of water. This method measures the free moisture rather than the total moisture, where free water is not bound to the host material. Total moisture includes water that is absorbed in the fine structure of the material, so reducing the freedom of rotation of the water. This method is very dependent on the packing density, static, temperature and most strongly on electrolytes [2-5]. This is due to salts dissolved in the water setting up conduction between the electrodes. Unless all these factors are controlled, the accuracy will be poor. Since probes are required, the system is only on-line for fine grain products. A good contact between the sample and probes also needs to be maintained [4].

1.6. NUCLEAR MAGNETIC RESONANCE

Hydrogen atoms behave like small magnets, and when placed in a suitable magnetic field, the magnets can be displaced from their aligned positions by radio waves at frequencies corresponding to the quantum of energy required for the displacement. If the absorption at these frequencies is measured, it can be used to determine proton and hence water content. This is obviously not useful for organic materials where the hydrogen varies in the dry material [2]. However, pulsed magnetic field techniques seem to overcome this problem [1].

The biggest problem is that the material must be in a powerful magnetic field for measurement. In practice the maximum possible gap to sustain this magnetic field is 50mm, so the material is usually contained in a tube or leveling is required. This also solves the problem of bulk density control, that is essential for accuracy. As this technique is flow rate dependent, "on-line" applications often use stopped flow-intermittent measurements.

1.7. NEUTRON MODERATION

Fast or energetic neutrons are selectively slowed by certain atomic nuclei, usually hydrogen. So by measuring the number of slow neutrons around a fast neutron source, indicates the number of protons in the measured sample. Using this, in association with bulk density measurement, usually gamma rays, the moisture content of many non-hydrogen containing materials can be measured [1]. This technique is penetrating, so giving the total moisture, and a large volume is

sensed. However, it has poor limits of detection, needs radio isotopes and is proton selective. This means the measurement of organic materials which contain varying hydrogen content is not really possible [3,6].

1.8. INFRA-RED REFLECTANCE

This technique is based on the characteristic absorption bands of water at 1.94μm and 2.48μm [2,3]. Its advantages are easy installation, insensitive to bulk density as it is a reflection method, and wide sensitivity. Its disadvantage is that black (strongly absorbing) and shiny (specular reflecting) materials are difficult to examine. Since it is a reflection method, the reading is dependent on the surface moisture, so can only be used where the surface moisture is representitive of the bulk of the sample [1-5]. The dependence on particle size and distance from the material to the instrument [3,7] means this system should not be used for uneven conveyor applications. Since only a small part of the stream is sampled its accuracy is questionable for non-homogeneous materials [3]. Dust should also be eliminated from the systems windows [1].

1.9. CAPACITIVE METHOD

This method is based on the high permittivity of water, compared with most dry materials. Hence measurement of this parameter allows moisture to be determined in bulk solids. The advantage of this system is that it is simple, rugged with a wide range of electrode pairs, suited for a particular case. Parallel plates or fringing type sensors are commonly used. The latter

suffers from having a non-uniform field, so materials being measured should be homogeneous [2]. Capacitive systems are usually cheap and cover a wide sensitivity range [1].

The disadvantages include, maintaining a stable contact between the probe and the sample [4,7], sensitivity to temperature, bulk density, particle size and material thickness [1,2,8]. Some of the very high dielectric constants measured at low frequencies are due to electrode polarization and interfacial problems [9-12]. However, the greatest problem is due to salt concentration as this forms an electrolytic solution, so allowing conduction to take place [1-4].

1.10 MICROWAVE TECHNIQUES

The high permittivity of water extends to microwave frequencies, so influencing the dielectric properties of moist materials. An advantage is that at these frequencies the effect due to electrolytes is much smaller and almost disappears [4,5]. In addition, at microwave frequencies water shows dielectric loss due to dipole relaxation [3,13]. This allows the measurement of either permittivity or dielectric loss for moisture content determination.

Three methods can be used, namely resonators, reflection or transmission measurements.

1.10.1 Moisture determination using transmission methods:

The most common method used is that of dielectric loss determination, where the attenuation of the signal through the transmitted layer is measured. The

maximum dielectric loss for water within a practical frequency range occurs at 23GHz, due to the electric dipole moment of the molecule [3,14]. If the absorption is too high, lower frequencies are used for better penetration. This of course gives a lower moisture sensitivity. Advantages are good sensitivity, a reasonably wide range of determination, low cost, and fairly easy development. The disadvantage of this system is that the attenuation is very dependent on the bulk density. Thus all attenuation systems include a bulk density compensation by gamma radiation [3,6,7,15,16], or a second moisture dependent measurement, usually phase. The exception being for low loss, uniform density and uniform thickness samples [17].

The inclusion of phase is explained as follows. The propagation velocity of an electro-magnetic wave is influenced by the permittivity of the material it is travelling in. Hence by measuring the phase difference between a wave that has travelled through the sample, and around the sample, the permittivity can be measured [3].

Some attempts have been made to measure moisture using phase, with gamma radiation compensation for bulk density [3,7,17,18]. However, the best results have come from the attenuation and phase combination. Since both measurements are dependent on density, a quotient of the two provides a reasonably density independent moisture measurement [3,5,16,17,19,20].

Although horn antennae are commonly used for on-line transmission applications, these often deliver inconsistent results. This is due to the sample being measured the near field [21] and mismatch caused by

varying layer thickness [7]. This can be eliminated by sweeping the frequency [3]. The usual off-line method uses a waveguide or coaxial transmission line filled with either a suitably machined or pulverized sample [22-25]. The latter method, however, then gives a solid/air measurement.

1.10.2 Moisture determination using resonant methods:
Resonators are ideal for measuring thin or small samples, since this method follows from the perturbation theory. The dielectric loss can be measured by the change in quality factor, while the change in frequency allows the calculation of the permittivity. Details are given in [19,26-30]. This method provides great accuracy, especially for very high quality factor devices. However, it is very narrowband for waveguide or resonant cavities [10].

1.10.3 Moisture determination using reflection methods:
Although dielectric losses can not be measured from reflection measurement [3], permittivity is often measured this way [10,25,29-33]. Since it is a reflection measurement, it is suitable for bulky materials, but only gives an indication of surface moisture.

Open ended coaxial lines are commonly used. This allows very broadband readings to be made. Measurements are done with various terminations into the sample [29], or the sample is machined or pulverized to fit the sensor. In the latter case, as with the transmission method, a solid/air measurement is given. Even this can be overcome using a powder/liquid technique where the liquid's dielectric

constant is varied until it matches the powder [32,33].

In many cases a combination of transmission and reflection measurements are used to determine the moisture content.

1.11 OTHER METHODS

Some materials change colour depending on their moisture content, thus spectrum analysis of these materials will be a function of their moisture content.

Noise emitted by conveyed or mixed powders is a function of moisture content. Hence sonic and ultrasonic techniques have been used.

CHAPTER 2

INTRODUCTION

Mineral processing treatment operations are sensitive to changes in feed moisture contents. In addition, the knowledge of the moisture content in the rocks at many points of the process route offers valuable information about the efficiency of certain processes. Although many industrial moisture meters are available, employing a wide range of detection techniques, none have been developed specifically for the diamond mining industry. In most cases the meter is designed for a host material which is of low density, fine grain, uniform surface level, and offers low resistivity to microwave signals. In this case, however, the problem is far more complicated since the host material consists of a mixture of rock types. For example, at Premier diamond mine the rock types include kimberlite, gabbro, felsite and quartzite, with each having different properties. The rocks vary greatly in size and packing density on the conveyor belt, and the loading on the belt is not even. A leveling process is not a viable option due to the high speed and volume of the rocks. The rocks are highly attenuative to microwave signals, with the attenuation varying according to the rock type [34,35]. Finally, the moisture content of the rocks is at most 15% [36]. This is distributed between surface and absorbed internal moisture, the ratio between the two moisture types is dependent on the rock type, since some rock types absorb more water than others. Thus a moisture meter that would offer a resolution of 1% for a range of 0-15% moisture content is required. Since many moisture meters would be required around the plant, the meter should be both cheap and versatile.

As throughputs of 1000 tonnes per hour are common in many plants, it is essential that the moisture measurement system be on-line and non-intrusive. This eliminated many of the techniques discussed in the previous chapter, including temperature, humidity, and resistive methods. Nuclear methods were not considered due to the hydrogen content problems, as discussed before, as well as safety regulations in industrial environments. This also eliminated gamma ray compensation for many moisture meters using microwave techniques.

Infra-red moisture meters give unsatisfactory results with kimberlite. This would probably be due to the dark kimberlite, which is shiny when wet [1]. In addition, the material thickness on the conveyer belt varies considerably, which means that the distance between the rocks and the meter changes. This leads to inaccurate results [3,7]. Since only the surface moisture is measured, this would lead to further errors as the kimberlite is highly adsorbent [36].

Investigating microwave techniques, the attenuation transmission method was first attempted because of simplicity. Since gamma ray compensation was undesirable for safety reasons, and phase measurement would increase development time and cost due to its inherent complexity, an attenuation alone system was designed and built. Moisture sensitivity at 23GHz was compared with measurements at 10GHz and 35GHz. More tests were then carried out at 23GHz on various materials, to establish viability of the system. The results were analysed and conclusions drawn.

Both capacitive and microwave permittivity measuring techniques were also investigated. Open structure devices were first attempted as these allow easy installation and do not interfere with the processing plant. The open structure resonant devices tested were loop antennae, resonant patch

antennae, and a microstrip filter. Due to low quality factors and loading problems, a partially closed structure, a hybrid loop-gap resonator, was tested. Finally various rectangular waveguide resonant cavities, an almost closed resonant structure, were tested.

All these methods were tested for their moisture sensitivity and more extensive tests were then carried out on the most promising devices. The results were then analysed and conclusions drawn.

The scope of this thesis project was:

1. To conduct a literature survey to establish possible ways of determining the moisture content of bulk solids.

2. To determine the best frequency at which attenuation and phase shift readings could clearly show moisture content.

3. To build and test hardware at this frequency and compare moisture sensitivity to similar systems working at different frequencies.

4. To establish whether a moisture meter working at this moisture sensitive frequency would be viable using the attenuation alone technique.

5. To look at alternative methods of performing moisture measurements using dielectric constant determination techniques. Phase shift methods and frequency shift techniques should be considered as discussed in section 1.10.2.

6. To make recommendations based on the findings.

CHAPTER 3

MICROWAVE ATTENUATION TECHNIQUE

3.1. INTRODUCTION TO ATTENUATION TECHNIQUE

Since a cheap, simple, low maintenance moisture meter was required, an attenuation alone design was developed. This is in contrast to most attenuation type industrial moisture meters, which have an additional measurement, commonly phase or gamma rays, as discussed in Chapter 1. The operating frequency of these meters is usually between 1GHz and 10GHz.

In an attempt to overcome the bulk density problem generally encountered, the operating frequency was chosen to be at a moisture attenuation peak. Figure 3.1 shows a plot of water attenuation against frequency.

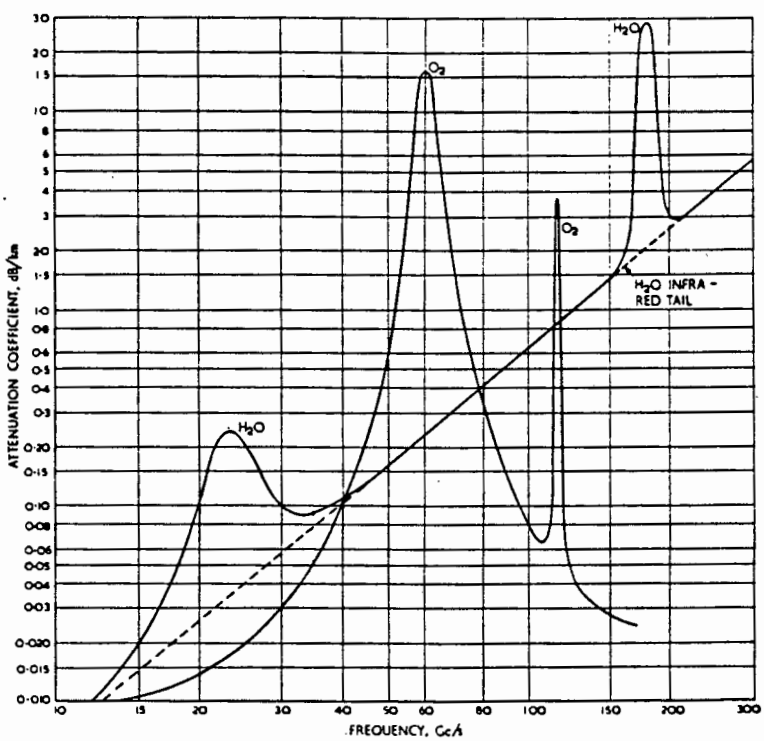

Figure 3.1: Graph of water attenuation verses frequency

The chosen operating frequency was 23GHz since this is where a moisture attenuation peak occurs [3,14]. Using this frequency as well as time averaging the results, it was hoped to overcome the usual bulk density and surface unevenness problems.

3.2. DESIGN OF MICROWAVE TRANSMITTER AND RECEIVER

The design of the transmitter and receiver was reported by Mercer [34] and Aldera [35].

3.2.1. Transmitter design:

The transmitter power supply is modulated by a 1kHz oscillator followed by an adjustable attenuator. This allows the output voltage to be altered so that a variety of Gunn oscillators, requiring different bias voltages, can be used after the current driving stage. The block diagram of the transmitter is shown in Figure 3.2 and the circuit diagrams of the power supply and the transmitter are given in Figures 3.3 and 3.4 respectively.

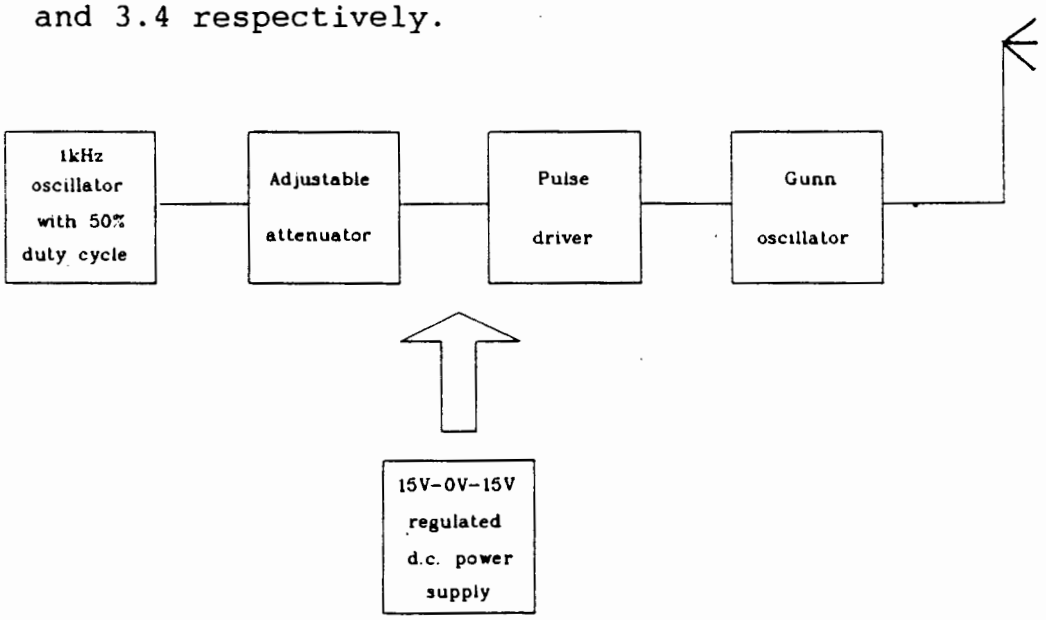

Figure 3.2: Block diagram of transmitter circuit.

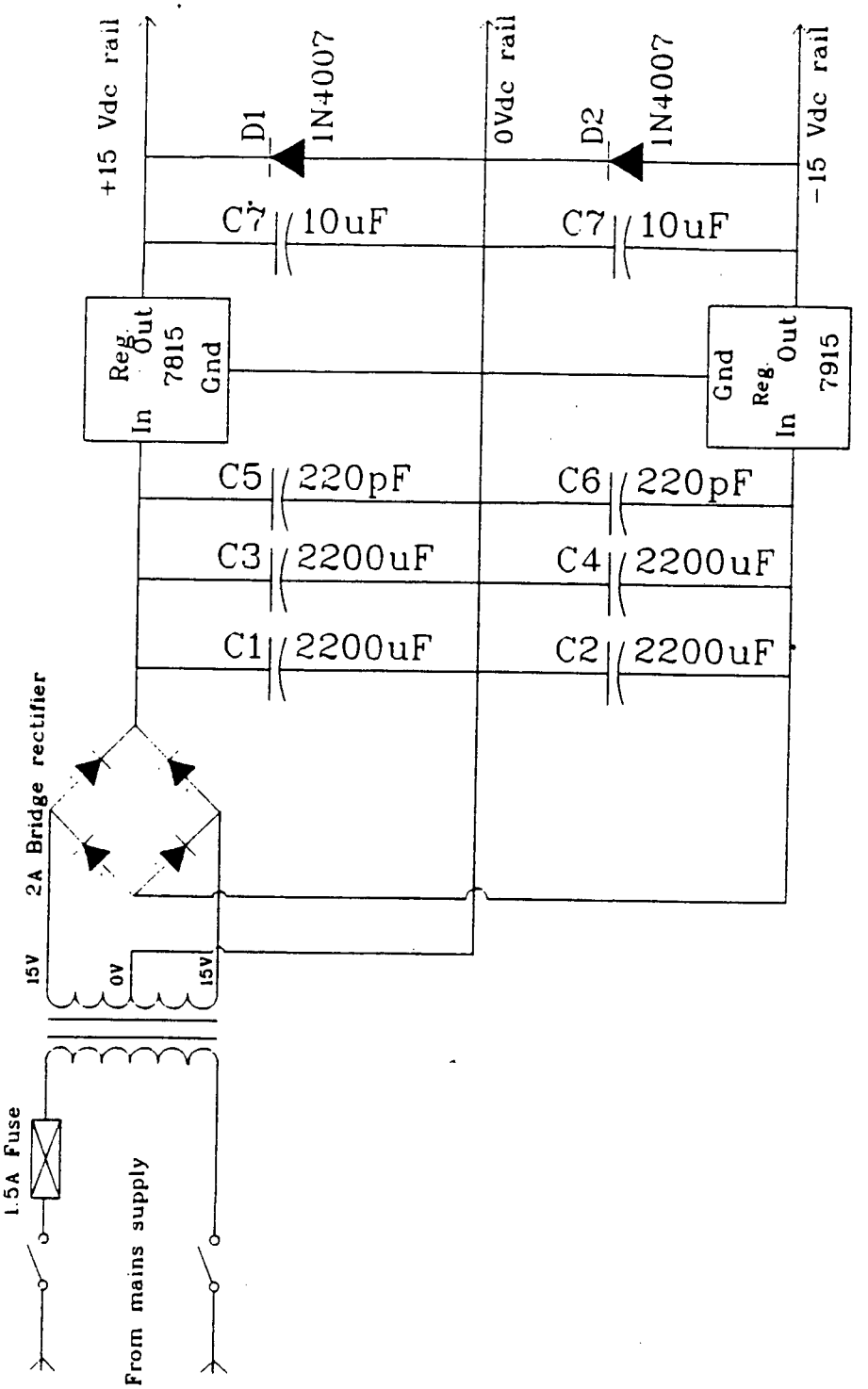

Figure 3.3: Circuit diagram of transmitter power supply.

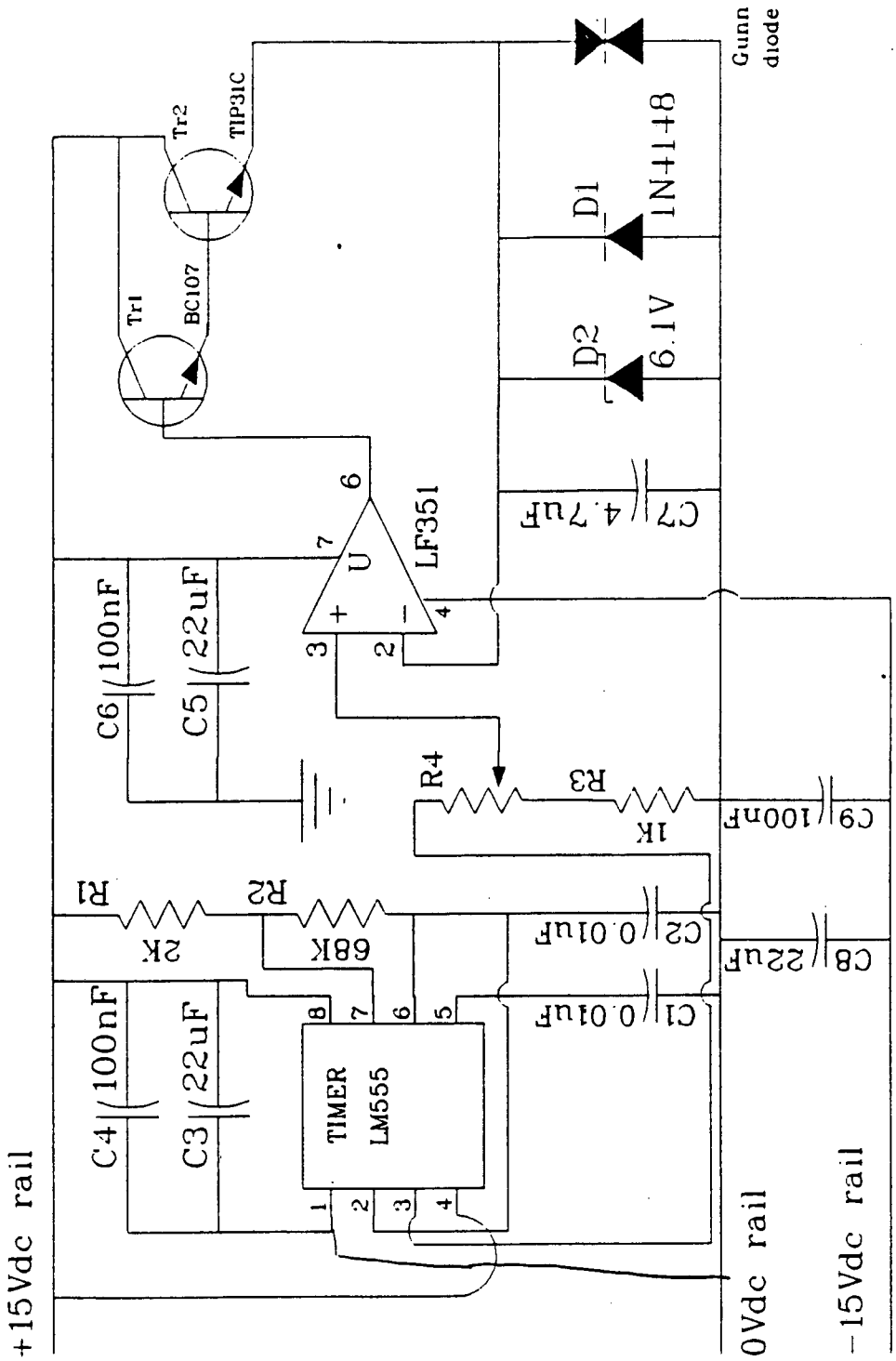

Figure 3.4: Transmitter circuit diagram.

Since no oscillators were available for 23GHz, one had to be developed. The Gunn diode was mounted in a K-band waveguide section, especially designed to allow D.C bias to be applied to the diode, while not allowing the R.F to escape. The details are given in Appendix A. The final design is shown in Figure 3.5.

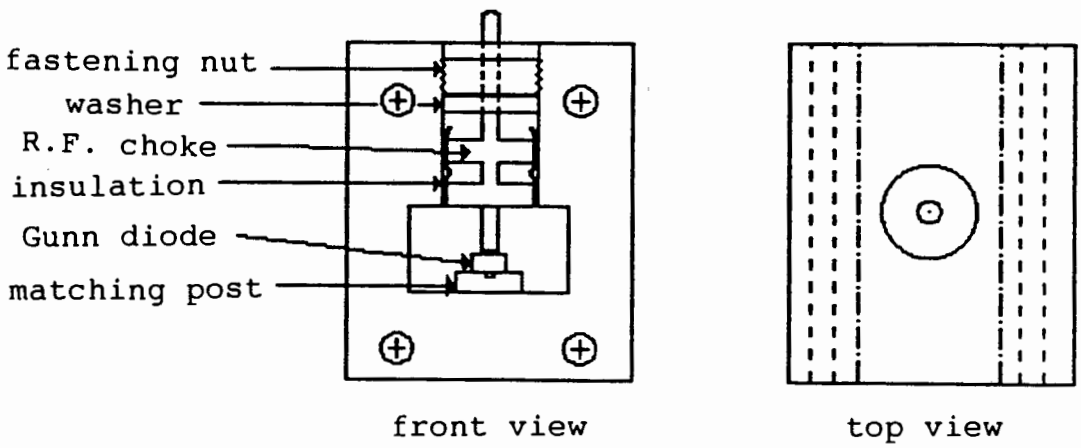

Figure 3.5: Final waveguide cavity design.

The oscillator frequency is determined by the position of the diode from the short circuit side of the waveguide cavity. The frequency was tuned by varying this waveguide transmission line distance using four `spacers'. These are brass plates which have slot dimensions identical to the waveguide cavity. They must also be attached to the transmitter cavity, hence the bolt hole positions are predefined. The spacers are shown in Figure 3.6

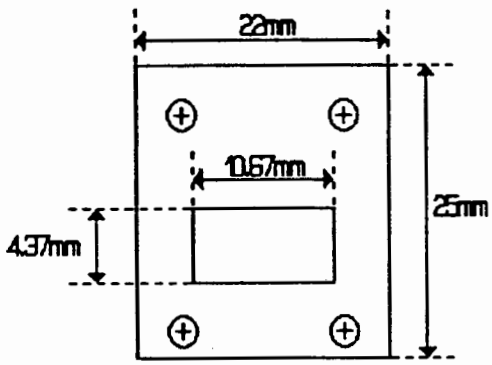

Figure 3.6: Spacer design.

The thickness of these spacers are 1, 2, 4, 8mm so that any waveguide transmission line distance may be extended between 1 and 15mm. Finally a blank plate was fabricated, which acts as a short circuit. This allows the waveguide distance between the diode and the short circuit to be altered to give the correct frequency. The results for the different spacer distances are given in Table 3.7.

Table 3.7: Frequency and power outputs.

DISTANCE (mm)	FREQUENCY (GHz)	POWER OUTPUT (mW)
0	23.894	29.0
1	22.914	31.0
2	21.776	27.5

From the results shown in Table 3.7 the spacer chosen was 1mm. This makes the total distance between the Gunn diode and the short circuit equal to $l \approx 12$mm.

The reactive impedance of the short circuit length of waveguide = $+jZ_1 \text{TAN}\ (2\pi l\ /\ \lambda_g)$

where $\lambda_g = \lambda\ /\ \sqrt{1 - (\lambda\ /\ 2 * a)^2}$

$= 16.48\text{mm}$ since $= c\ /\ f$

$= c\ /\ 23\text{GHz}$

$= 13.04\text{mm}$

and $a = 10.67\text{mm}$

and where Z_1 is the waveguide characteristic impedance given by $Z_1 = 377 * (\lambda_g\ /\lambda) * (b\ /\ a)$

$= 192.85\Omega$ as $b = 4.32\text{mm}$

Hence the reactive impedance of the short circuit length of waveguide = $+jZ_1 TAN\ (2\pi l\ /\ \lambda_g)$

$= +j192.85*TAN\ (2\pi*12\ /\ 16.48)$

$= +j1396$

This inductive reactance resonates with the capacitive reactance of the packaged Gunn diode at a frequency of 23GHz.

Since the output power also peaked at the required frequency, no alterations were made to the matching posts.

3.2.2. Antenna design:

Antennae had to be designed for both the transmitter and the receiver. Although high gain was desirable, horn antennae could not be used because of the nearfield inconsistency [21]. Thus slightly undersquare open waveguide antennae were used. This allows the antennae to be brought closer to each other as the far field of $2D^2/\lambda$ is only about 2cm. The antennae are well matched to the impedance of free space as shown below:

Antenna impedance = $Z_A = 377 * (\lambda_g\ /\ \lambda) * (\ b\ /\ a\ )$

Thus for the dimensions and frequencies used here, a = 10.67mm and b = 8.47mm, Z_A = 377Ω, which is the impedance of free space.

Waveguide matching transformers are required, so that the antennae are matched to the K-band rectangular waveguide cavity. Figure 3.8 shows the final design.

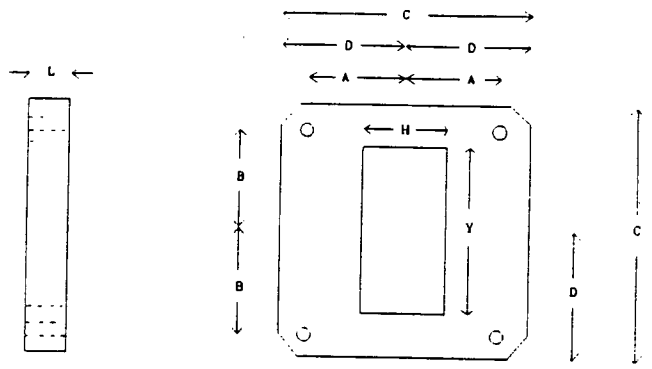

	A	B	C	D	L	H	Y	Hole diameter
K band	8.1	8.5	22.2	11.1	4.1	6.8	10.7	2.9

Figure 3.8: K-band waveguide matching transformer.

The waveguide antenna's internal dimensions are given by 10.67 * 8.47mm. The length of the antenna is not electrically critical and so a length of 5cm was chosen for convenience. The antenna design is shown in Figure 3.9.

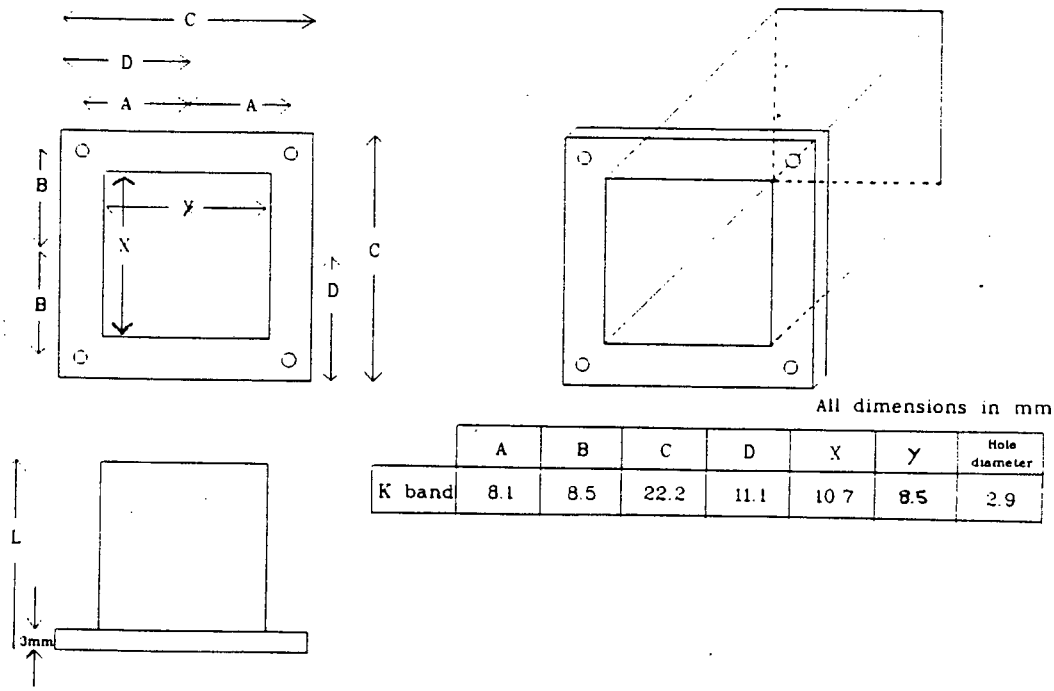

All dimensions in mm.

	A	B	C	D	X	Y	Hole diameter
K band	8.1	8.5	22.2	11.1	10.7	8.5	2.9

Figure 3.9: A waveguide antenna.

Note that an isolator could be included between the rectangular waveguide cavity and the antenna. This prevents any possible impedance mismatch, due to a sample, from interfering with the operation of the Gunn oscillator. However, the performance of the oscillator was satisfactory without the use of the isolator.

3.2.3. Receiver design:

The receiver consists of a detector diode, mounted in a waveguide cavity, followed by a low noise amplifier. The detector diode was matched into the waveguide cavity in much the same way as the Gunn diode. The signal is then bandpass filtered to remove the 1kHz fundamental, A.C amplified, rectified and finally low pass filtered to produce a D.C level. This D.C level is then displayed on an analogue ammeter. The block diagram is given in Figure 3.10 and the circuit diagrams of the receiver and its power supply are given in Figures 3.11 - 3.13.

The hardware was fabricated, assembled, tested and finally mounted in boxes. The transmitter and receiver were kept separate so they could be moved around as required. The final product is shown in Photograph 3.14.

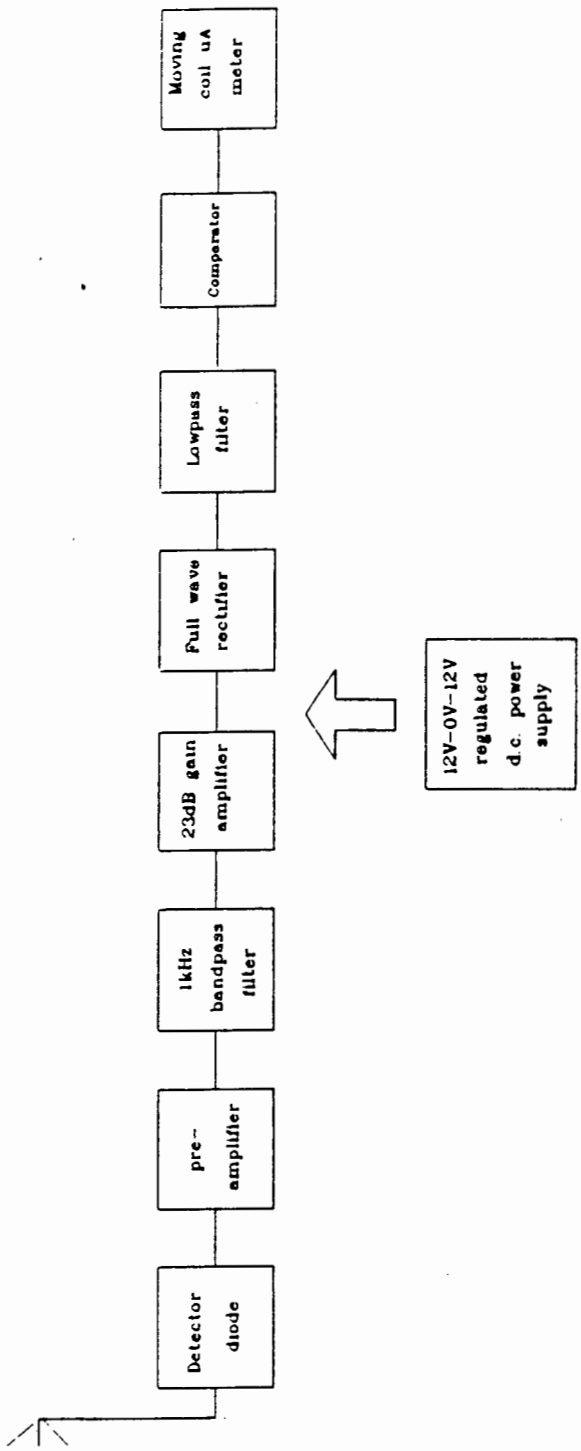

Figure 3.10: Block diagram of receiver circuit.

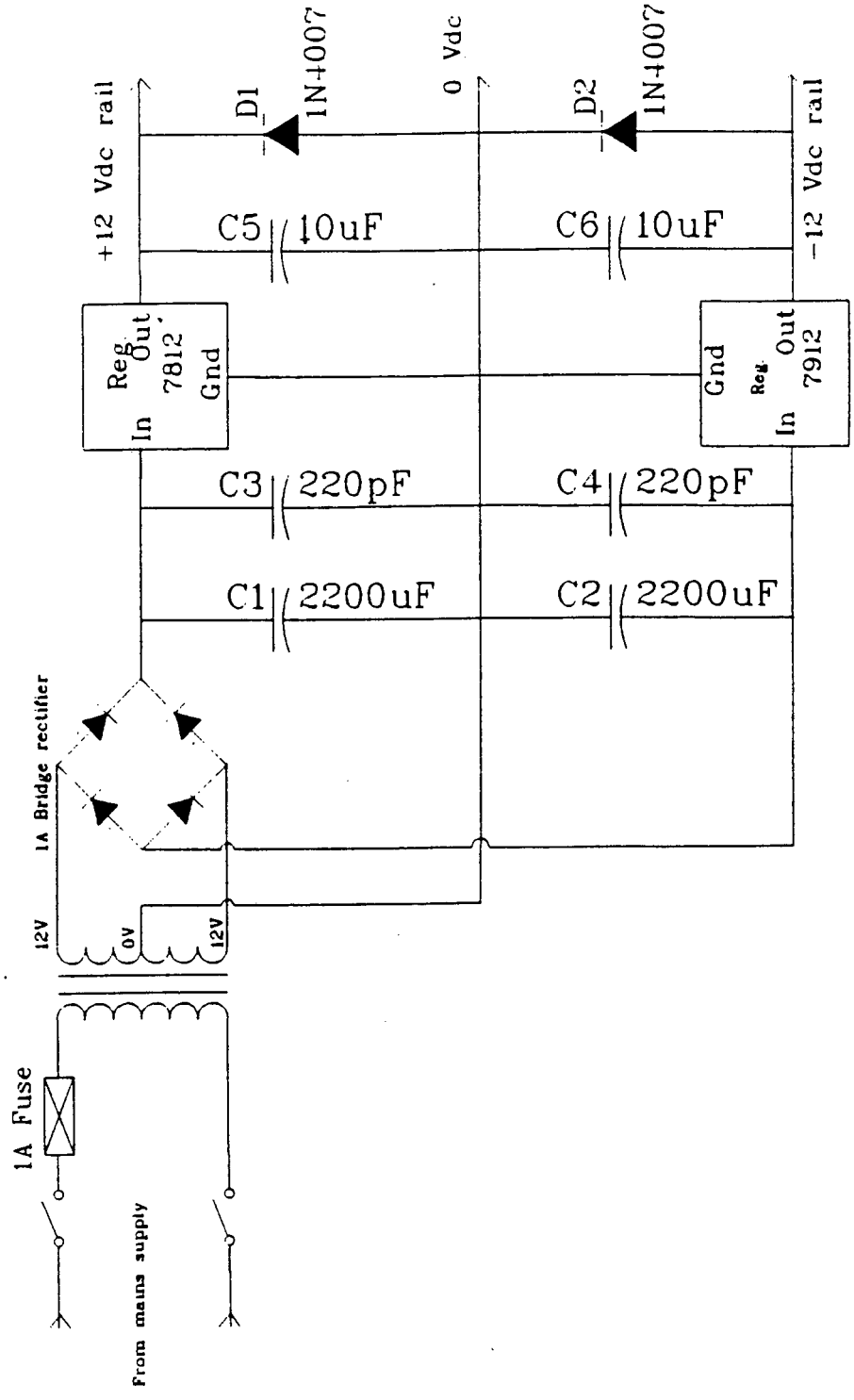

Figure 3.11: Receiver power supply.

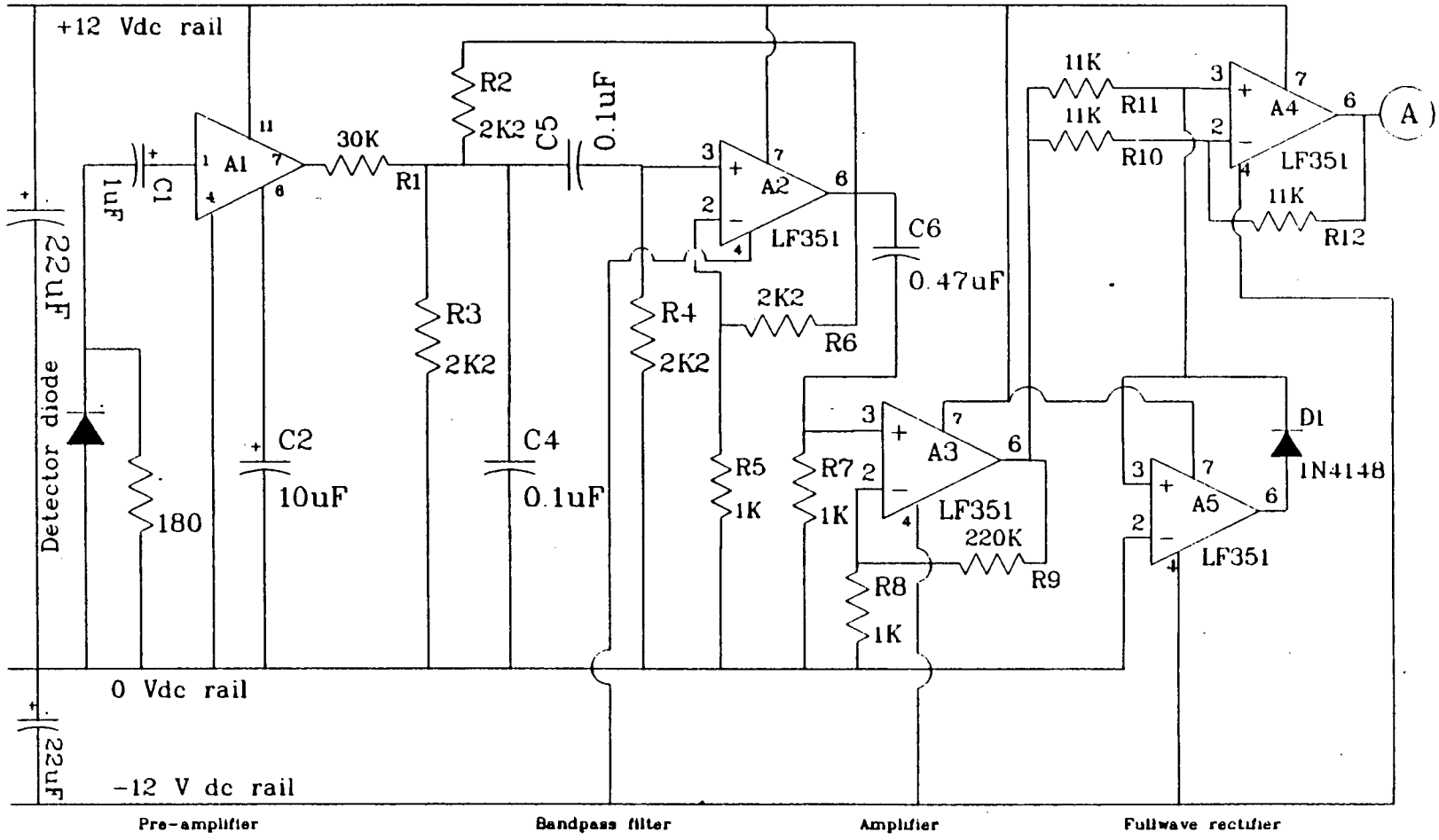

Figure 3.12: Initial stages of receiver circuit.

Note that an isolator could be included between the rectangular waveguide cavity and the antenna. This prevents any possible impedance mismatch, due to a sample, from interfering with the operation of the Gunn oscillator. However, the performance of the oscillator was satisfactory without the use of the isolator.

3.2.3. Receiver design:

The receiver consists of a detector diode, mounted in a waveguide cavity, followed by a low noise amplifier. The detector diode was matched into the waveguide cavity in much the same way as the Gunn diode. The signal is then bandpass filtered to remove the 1kHz fundamental, A.C amplified, rectified and finally low pass filtered to produce a D.C level. This D.C level is then displayed on an analogue ammeter. The block diagram is given in Figure 3.10 and the circuit diagrams of the receiver and its power supply are given in Figures 3.11 - 3.13.

The hardware was fabricated, assembled, tested and finally mounted in boxes. The transmitter and receiver were kept separate so they could be moved around as required. The final product is shown in Photograph 3.14.

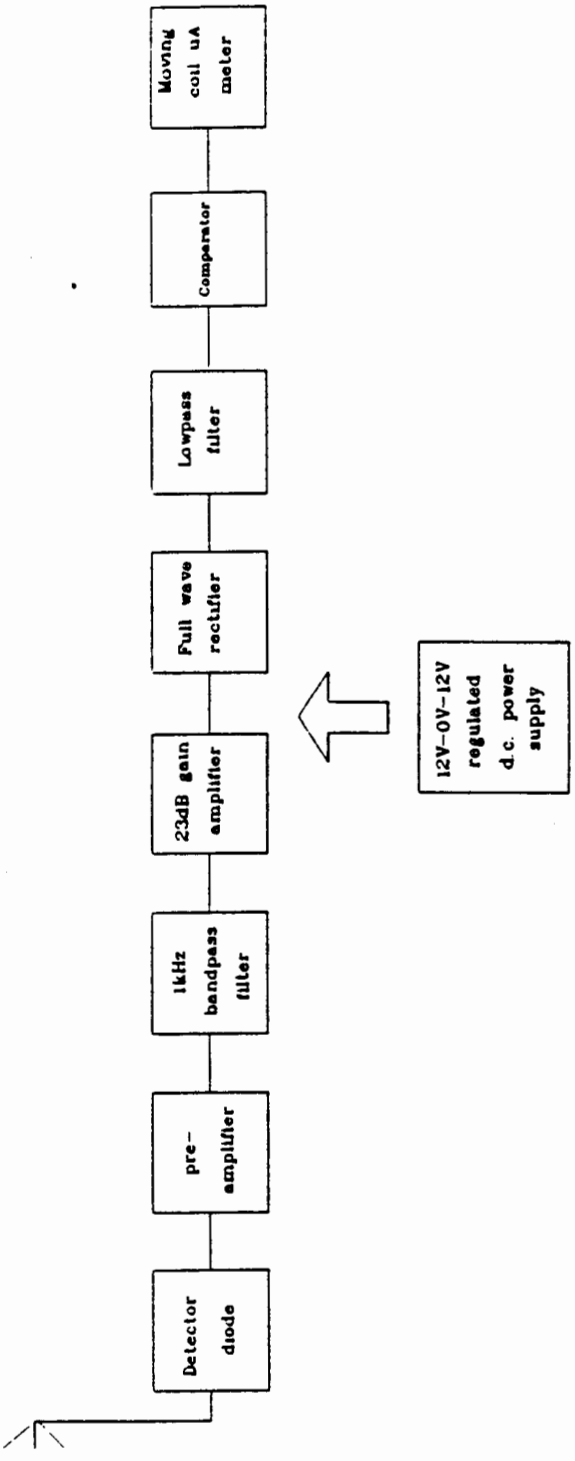

Figure 3.10: Block diagram of receiver circuit.

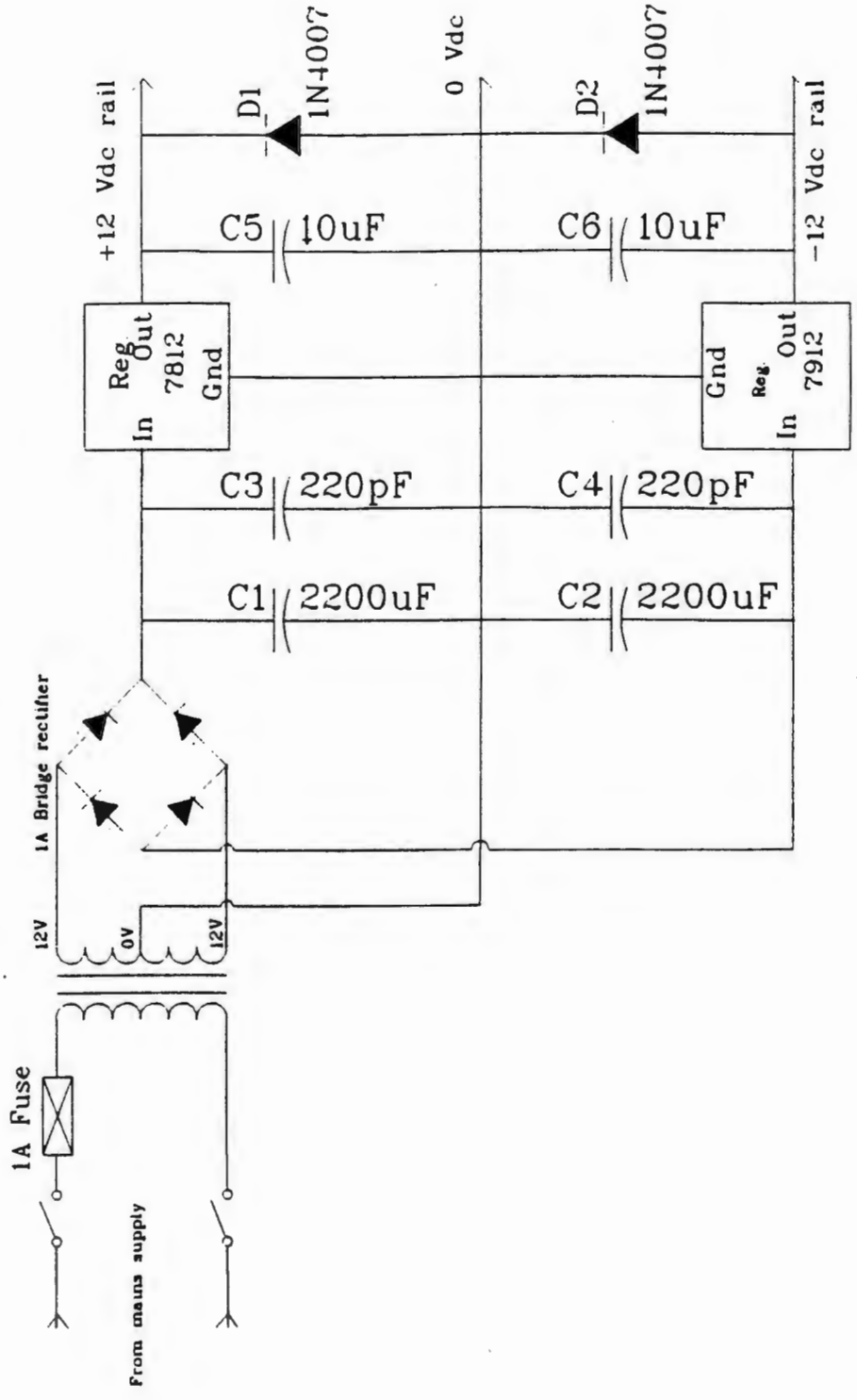

Figure 3.11: Receiver power supply.

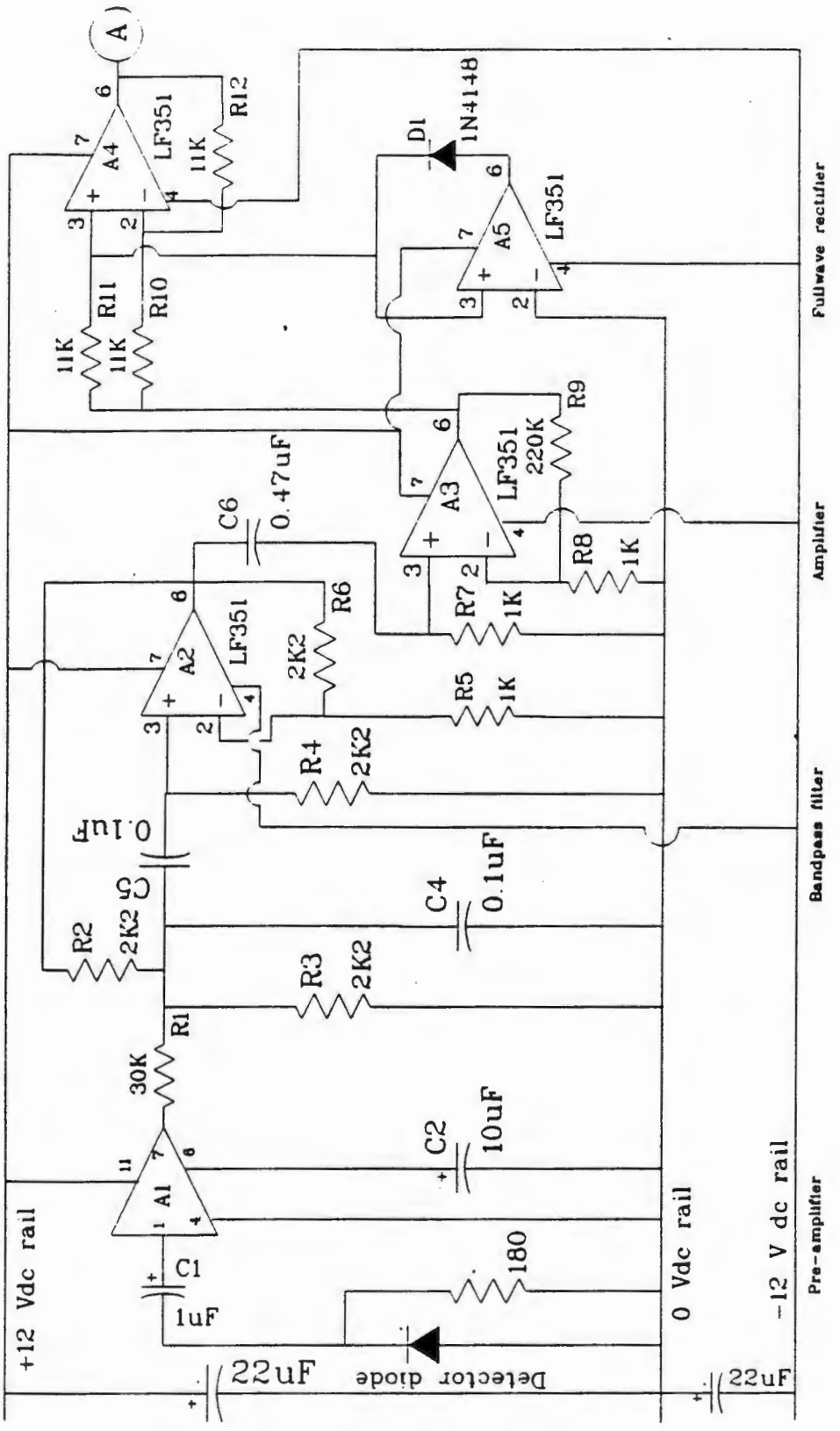

Figure 3.12: Initial stages of receiver circuit.

Note that an isolator could be included between the rectangular waveguide cavity and the antenna. This prevents any possible impedance mismatch, due to a sample, from interfering with the operation of the Gunn oscillator. However, the performance of the oscillator was satisfactory without the use of the isolator.

3.2.3. Receiver design:

The receiver consists of a detector diode, mounted in a waveguide cavity, followed by a low noise amplifier. The detector diode was matched into the waveguide cavity in much the same way as the Gunn diode. The signal is then bandpass filtered to remove the 1kHz fundamental, A.C amplified, rectified and finally low pass filtered to produce a D.C level. This D.C level is then displayed on an analogue ammeter. The block diagram is given in Figure 3.10 and the circuit diagrams of the receiver and its power supply are given in Figures 3.11 - 3.13.

The hardware was fabricated, assembled, tested and finally mounted in boxes. The transmitter and receiver were kept separate so they could be moved around as required. The final product is shown in Photograph 3.14.

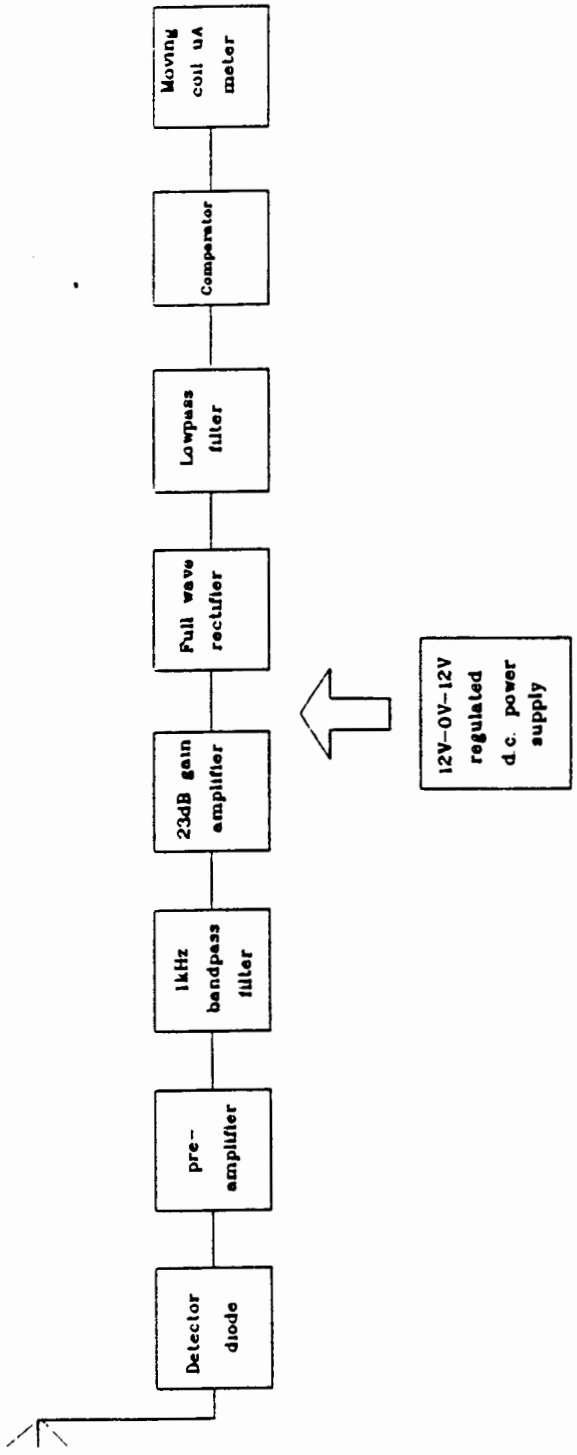

Figure 3.10: Block diagram of receiver circuit.

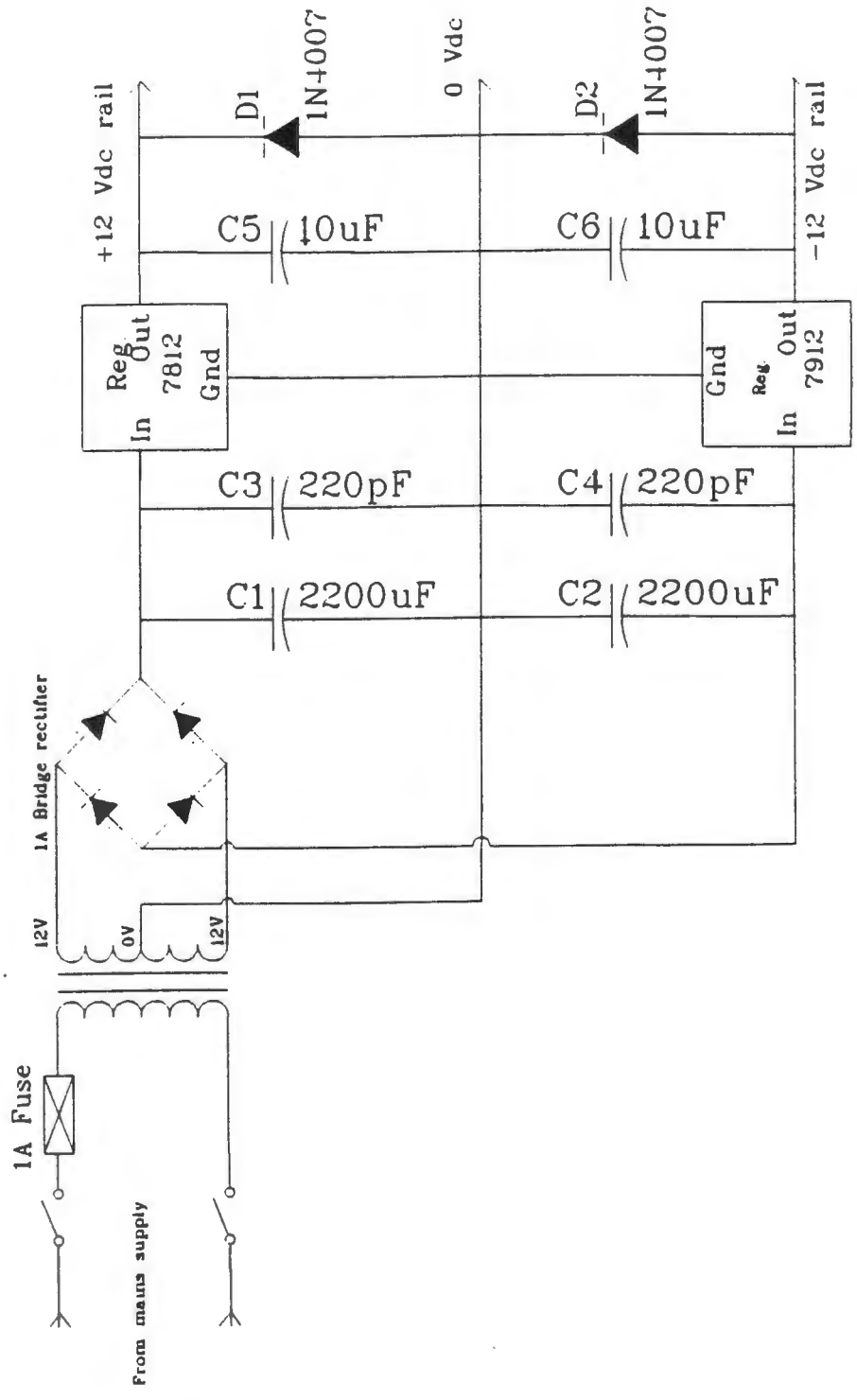

Figure 3.11: Receiver power supply.

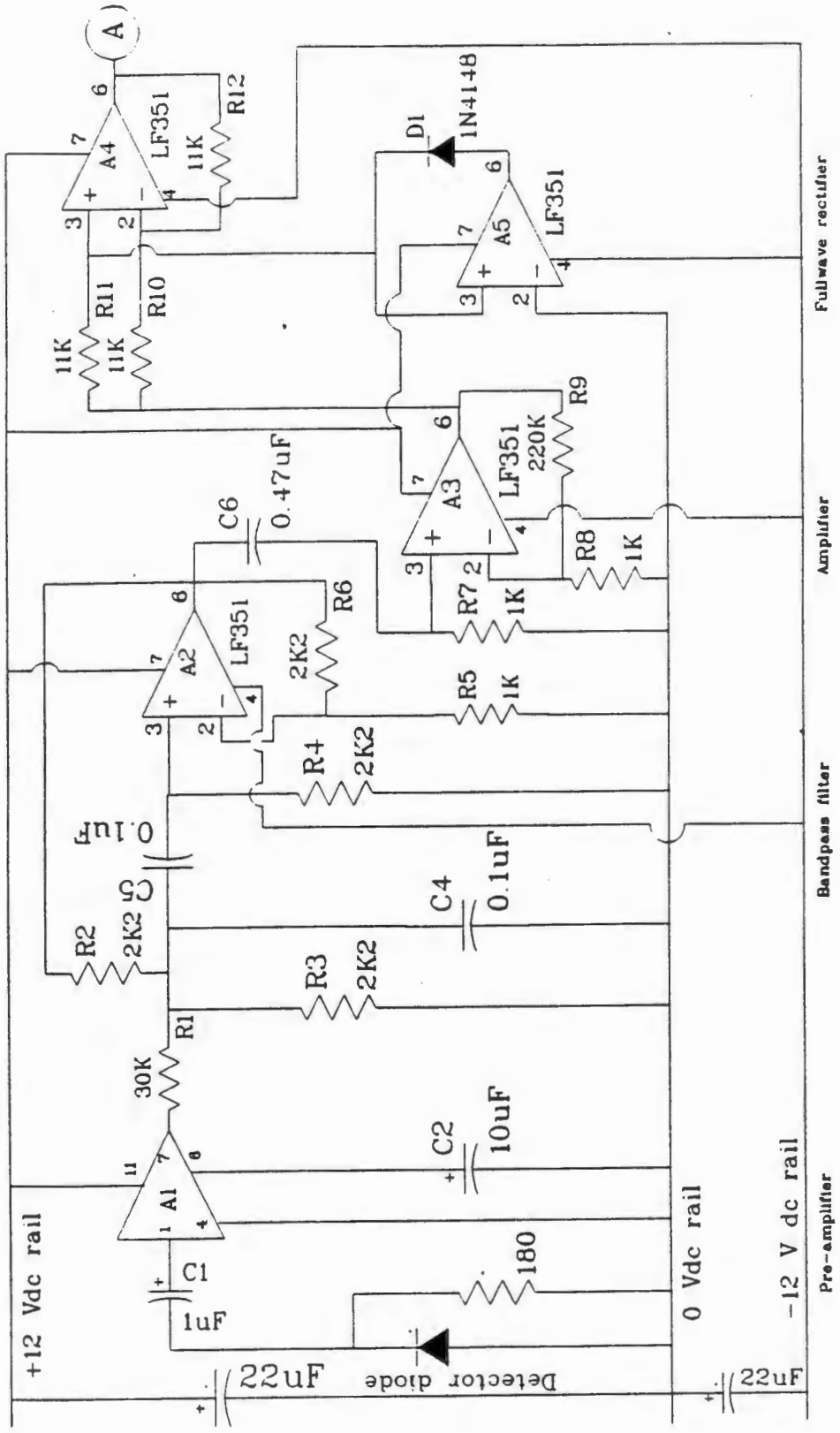

Figure 3.12: Initial stages of receiver circuit.

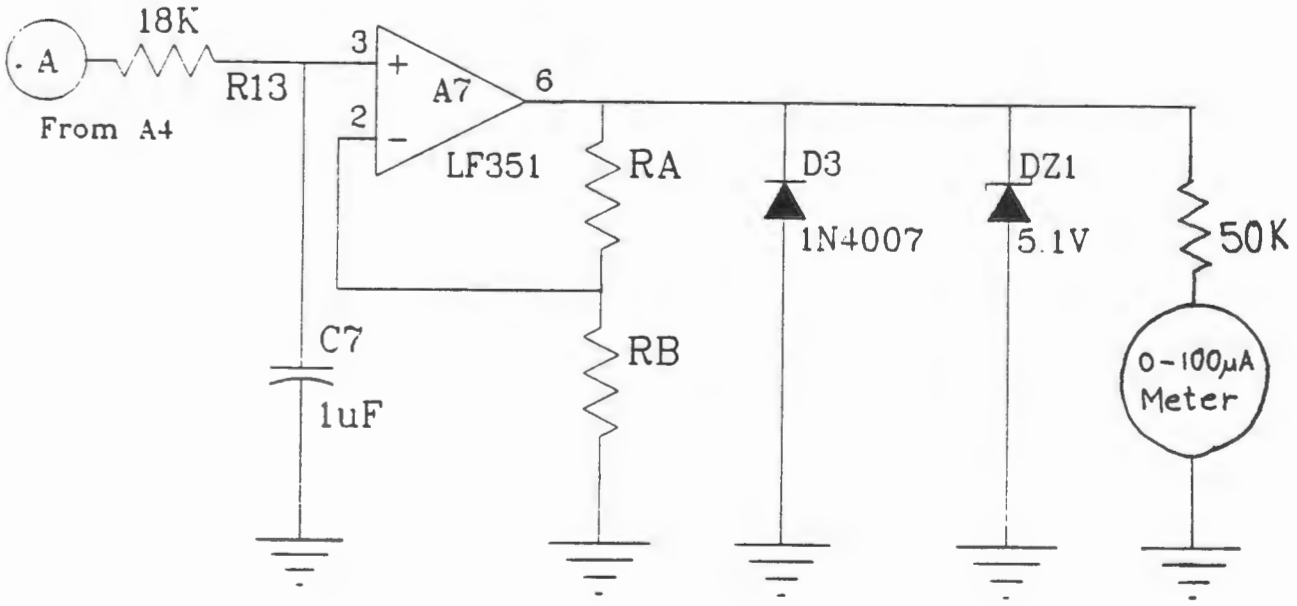

Figure 3.13: Receiver circuit diagram.

Photograph 3.14: Mounted transmitter and receiver.

3.3. EXPERIMENTAL METHOD

The attenuation of the signal through the material is measured as follows. Firstly the amplitude of the received signal is recorded with no material between the antennae. Then the sample is placed between the antennae and the signal amplitude recorded. The attenuation can then be calculated.

For measurements to be taken, the alignment of the antennae was crucial. To ensure this, a wooden test jig was used. This was designed and built by Mercer [34] and Aldera [35]. The test jig is shown in Photograph 3.15.

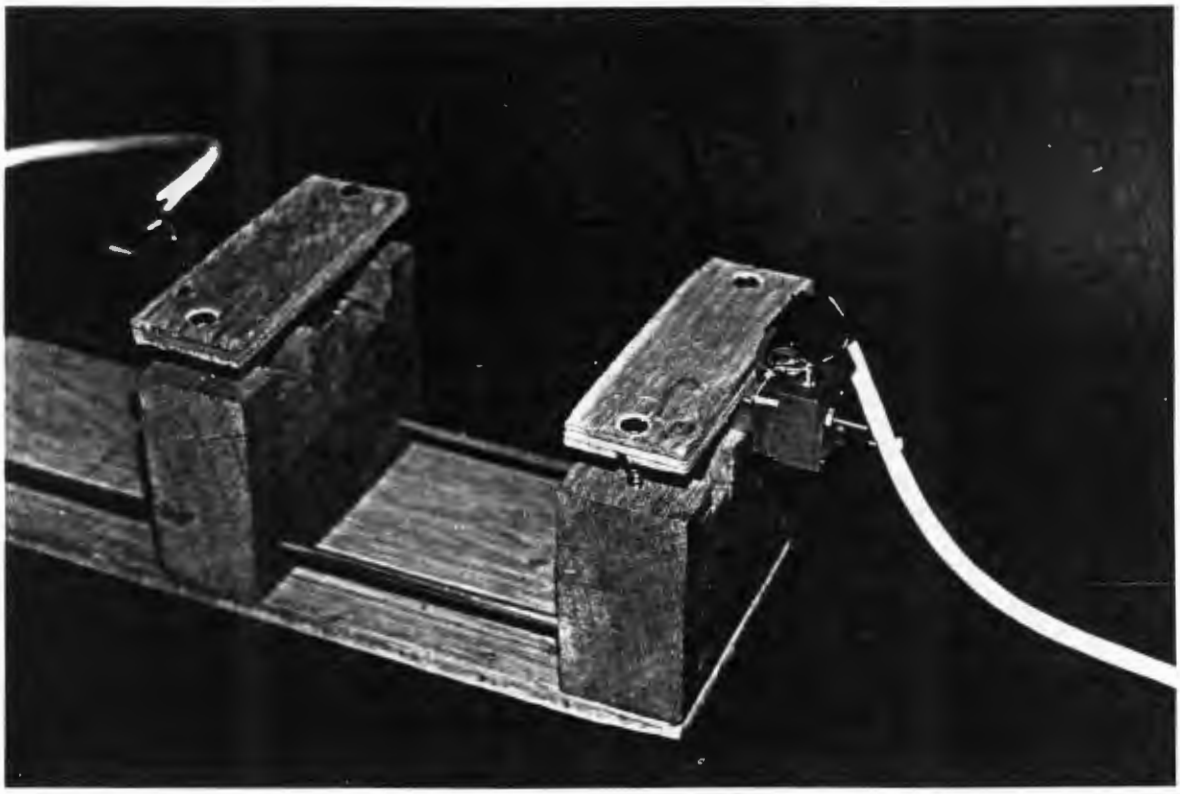

Photograph 3.15: Wooden test jig.

The experimentation consisted of two main sections. The first was to justify the use of 23GHz as the working frequency. This was done by taking dry attenuation

readings of several materials, namely gabbro, kimberlite, bricks, wood and paper. The readings were taken at 23GHz as well as at 10GHz and 35GHz, since equipment was already available at these frequencies. Attenuation readings for the latter two cases were particularly easy as rotary vane attenuators were available. This allows one to match the signal amplitude due to the sample, with the amplitude through the attenuator. The attenuation can then simply be read off.

3.4. RESULTS

As mentioned earlier, the experimentation consisted of two sections. The first is to justify the use of 23GHz as the working frequency. Results of the various dry material readings for 10, 23 and 35GHz are given in Table 3.16.

Table 3.16: Dry attenuation readings.

		10GHz dB	35GHz dB	23GHz dB
2cm kimberlite samples	No.1	11.1	> 20	31.5
	No.2	13.1	> 20	34.5
	No.3	7.7	> 20	16.1
2cm gabbro samples	No.1	2.2	6.6	3.0
	No.2	4.3	3.6	1.4
	No.3	4.1	4.7	1.3
	No.4	3.8	6.9	2.0
14cm kimberlite		11.6	> 20	30.0
12cm kimberlite		13.1	> 20	*
11cm kimberlite		13.0	> 20	*
8cm gabbro		4.8	11.2	11.5
14cm gabbro		10.3	19.0	*
8cm felsite		7.5	16.0	11.9
12cm felsite		10.6	> 20	*

Brick width length	1.0 +3.5	12.5 7.0	# #
Wood width length	21.0 16.0	> 20 > 20	32.1 *
Paper 10 20	0.8 1.7	0.3 1.2	0.3 1.0

* means that the output was too small to be recorded.

means that the readings were inconsistent, details are give later.

Before continuing with the wet readings, some comment should be made about the dry material results:

1. High attenuation readings could not be made using the 35GHz hardware. This is because the dynamic range of the detector diode is about 20dB. Any readings above this attenuation are consequently invalid.

2. Inconsistent results occurred when measuring the brick and wood samples. The readings could vary by up to 10dB depending on the position of the sample. This was probably due to the material not being homogeneous.

3. The readings for the 2cm rock samples were initially done with the square antennae placed 2cm apart. However, some of the gabbro samples then showed a gain rather than a loss. This is due to high reflections between the square antennae without the gabbro samples. Thus the antennae were shifted 20cm apart for consistent readings.

4. The 14cm felsite sample exhibited an unusually high attenuation. This is not due to attenuation alone, but also as a result of the surface reflections as this sample's sides were not completely parallel. Further, the attenuation recorded was a function of the rock orientation [37].

Due to the very high attenuation of the large rock samples, and the inconsistent results obtained for the wood and brick samples these were not used for the wet test. Thus wet measurements were only performed on the 2cm rock samples and paper. The results are given in Table 3.17.

Table 3.17: Wet samples attenuation readings.

SAMPLE	10GHz	23GHz	35GHz
K 1	15.3	*	*
K 2	17.4	*	*
G 0	4.1	3.0	7.0
G 1	5.4	3.0	4.7
G 2	5.3	5.4	7.6
G 3	4.9	4.1	6.7
Paper with 25% water	8.7	33.9	17.6

* means that the output was too small to be recorded.

The results above do not show that 23GHz is a good working frequency. This is because the kimberlite attenuation was too large to be measured for two of the cases. The 10GHz readings increased by 4dB showing that the kimberlite absorbs quite a lot of water.

The gabbro readings only really show that gabbro does not absorb much water, since the wet samples do not attenuate much more than the dry ones.

The only readings that show 23GHz to be an effective working frequency are those for wet paper. This is because dry paper does not attenuate the signal much and is also highly absorbant. This means that the actual water attenuates the signal rather than the base material, as in the case of the rocks.

Thus more comprehensive measurements were taken for wet paper. For these experiments, 20 sheets of paper were used. One page was soaked in water and then placed in the middle of the stack. This was done to avoid surface reflections due to the water. The actual moisture content was not measured as the same sample was used for all three frequencies. The results are given in Table 3.18. and plotted in Figure 3.19.

Table 3.18: Wet paper samples attenuation readings.

	10GHz dB	23GHz dB	35GHz dB
20 dry sheets	1.5	0.4	3.9
1 wet sheet	3.6	8.0	3.3
2 " "	5.6	16.0	9.3
3 " "	6.6	23.1	14.3
4 " "	7.5	28.9	14.9
5 " "	8.0	31.4	16.6
6 " "	8.7	33.9	17.6
7 " "	9.3	36.9	*
8 " "	11.2	*	*

* means that the output was too small to be recorded.

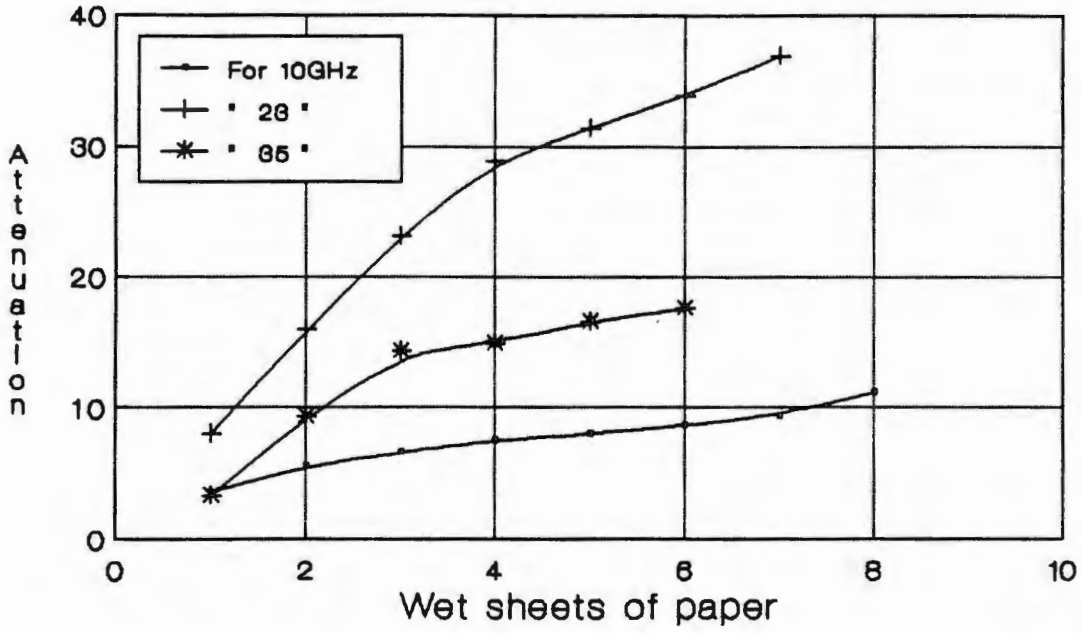

Figure 3.19: Plot of attenuation for wet paper at 10, 23, and 35GHz.

The readings for wet paper have had the dry attenuation readings subtracted from them, thus the readings shown in Table 3.18 are due to the moisture alone.
The results of Table 3.18 show conclusively that the attenuation due to water at 23GHz is much higher than surrounding frequencies. Thus the use of 23GHz for a moisture meter has been justified.

Also notice that the attenuation at 35GHz is higher than at 10GHz, which confirms the theory discussed in Section 3.1.

The second stage of experimentation was to calibrate the 23GHz system. Again moist paper was used for reasons discussed earlier. The results for this section give the moisture content and the attenuation. The moisture content is given by the following formula:

$$\% \text{ MOISTURE CONTENT} \equiv \tau = M_{water} / (M_{water} + M_{dry})$$

This formula can be rearranged to give

$$\% \text{ MOISTURE CONTENT} = \tau = (M_{total} - M_{dry}) / M_{total}$$

where M_{total} = Total mass including water
M_{water} = Mass of water alone
M_{dry} = The dry mass i.e. with no water.

The results are given in Table 3.20.

Table 3.20:Attenuation verses moisture content results.

COMPUTER PAPER				NEWSPAPER		PHOTOSTAT PAPER	
τ	dB	τ	dB	τ	dB	τ	dB
0.0	1.6	0.0	0.4	0.0	1.4	0.0	0.2
7.5	5.3	6.2	2.7	9.3	5.6	11.1	7.1
12.3	8.5	11.6	6.0	16.9	9.7	20.0	10.5
18.4	11.5	16.4	8.7	23.4	14.3	29.8	15.3
21.5	14.5	21.8	13.0	29.0	21.7	36.5	16.2
25.5	19.0	25.6	17.7	33.8	27.5	42.9	20.0
28.7	23.6	29.9	24.4	38.0	32.7	*	*
32.2	29.6	33.0	29.3	*	*	*	*
35.4	34.7	36.5	35.7	*	*	*	*

These results were plotted and are shown Figure 3.21.

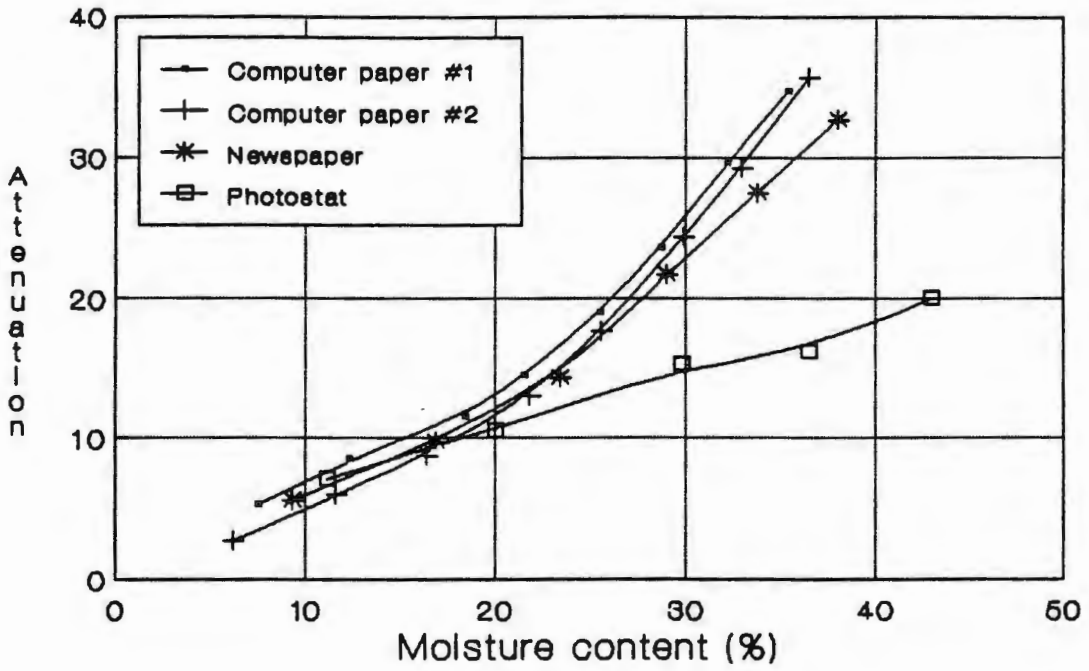

Figure 3.21: Plots of moisture content against attenuation for various types of paper.

From these results it is clearly seen that the moisture curves are very material specific. Thus for this system, different calibration curves would be necessary for each material being measured.

3.5. CONCLUSIONS FOR ATTENUATION TECHNIQUE

In view of the results, the following conclusions may be drawn.

3.5.1. The moisture attenuation peak at 23GHz was confirmed. In addition the attenuation at 35GHz is higher than at 10GHz, which also conforms with theory.

3.5.2. Despite working at a moisture sensitive frequency, attenuation readings alone can not be used to determine moisture content generally. However, in the case where the material has uniform height and an even surface, as well as a homogeneous composition, eg. paper, this system could be used very successfully.

3.5.3 This system would then be specifically calibrated to the material being measured.

3.5.4 The use of a microprocessor to sample and process the measurements would be required since many readings should be averaged so giving more consistent results. This would help overcome the problems of surface unevenness, variable conveyor belt attenuation and non-homogeneous base materials.In addition, calibration curves could be stored, so allowing the software to calculate actual moisture values.

3.5.5 For the specific application of rock moisture measurement for kimberlite, the system was not considered viable for the following reasons: The great unevenness of the rocks, the difference in attenuation between gabbro and kimberlite, and the variation of the level on the conveyor belt will lead to a great variation in the readings. These problems would be eased using the microprocessor averaging system in conjunction with a level sensor, but even so the results would not be very accurate.
The greatest problem, however, is that of the attenuation. The rocks on the conveyor belt are approximately 30cm deep and the attenuation for a 15cm kimberlite sample alone is too large to be measured. So if moisture was now included, as well as the belt attenuation, the signal would never be

detected using this system. The system receiver sensitivity could be improved by about 40dB using a superhetrodyne receiver. However, with such a direct attenuation path, signals of similar or larger magnitudes may enter the receiver via another reflected path. This would then produce erroneous and unreliable readings.

CHAPTER 4

PHASE TECHNIQUES

Since the attenuation of water at 23GHz is so high, it is difficult to get accurate readings if the material containing the water also has a high attenuation. This is the case with the rocks, so a different approach had to be taken.

A second property that distinguishes water from the host material is its relative permittivity or dielectric constant. The dielectric constant of water is very high, ϵ_r=76.5 + j11.2 at 3 GHz [31], compared to kimberlite (ϵ_r=4) and gabbro (ϵ_r=6-7) [36]. The high dielectric constant is due to the freedom of rotation of the liquid molecules in an electric field [12].

The dielectric constant can be determined by measuring the phase change of a signal through the sample compared to a reference signal travelling via another path. However, this requires the construction of a network analyser which is complex and expensive. The high cost is due to long development times and the need for very stable, accurate components. Such components are required as the received signal is compared to the original signal for phase measurement. The phase of the two signals can not be compared at this high frequency, so they are mixed down to a much lower frequency where phase measurements can take place. Ambiguity in phase is overcome using a modulated subcarrier technique as proposed by Kalinski [38], as shown in Figure 4.1.

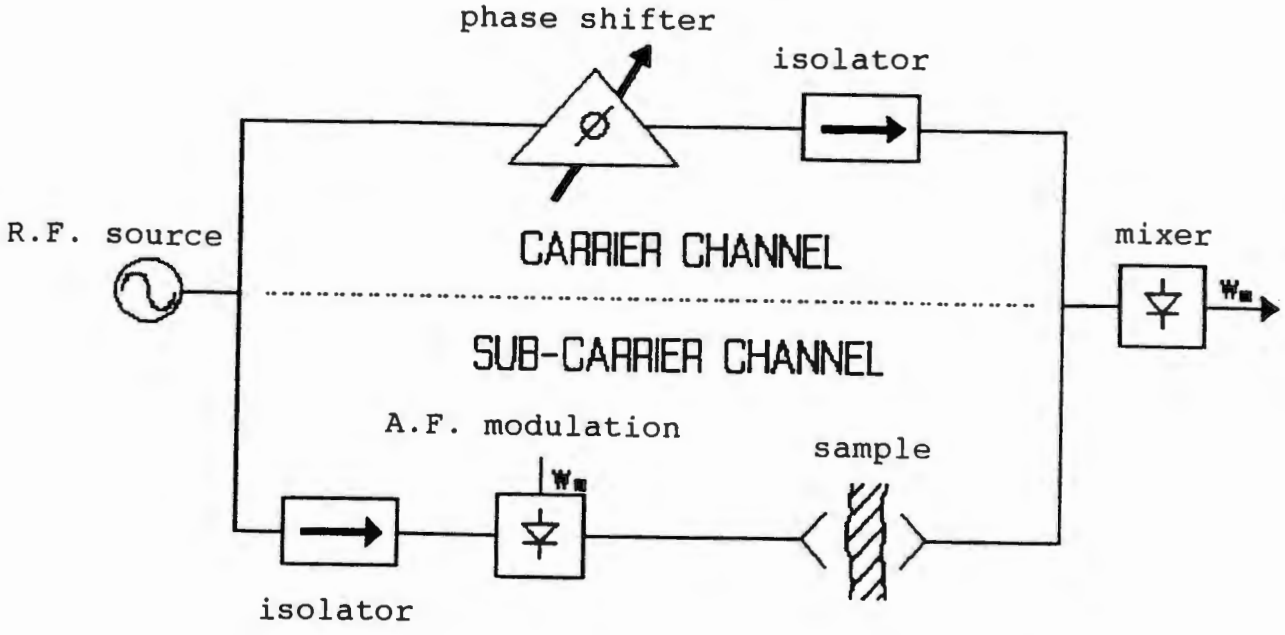

Figure 4.1: Dielectric constant determination using phase shift techniques.

Although phase combined with gamma-ray measurements have been used for moisture measurement [3,7,17-18], the results have varied greatly. The biggest problem, however, is the high attenuation of the rocks and water, as seen in Chapter 3. This is because phase measurement still requires a direct path through the sample, thus the high attenuation of the rocks would make this difficult.

Since these systems are commercially available, this method was not attempted. The high cost of such a meter also excluded it from consideration.

CHAPTER 5

FREQUENCY TECHNIQUES

5.1. INTRODUCTION TO FREQUENCY SHIFT TECHNIQUES

Although the dielectric constant can be determined by measuring the phase change, as seen in the previous chapter, the change in frequency of a resonant structure will also give a measure of the dielectric constant, as discussed in Chapter 1. In addition, the change in quality factor can be used to determine the dielectric loss. The exact mathematical relationships between the measured frequency shifts and quality factor changes, and the permittivity are given in many papers [19,27,28,31]. The development of the mathematics follows from the perturbation theory. The measure of the permittivity, using the change in frequency, can be performed using either capacitive or microwave resonant structures. The accuracy of measurement depends strongly on the quality factor of the structure; the higher the quality factor, the greater the accuracy [39].

Although very high quality factor devices are available at microwave frequencies, the difference in the permittivity of water as compared to the base material, increases at lower frequencies [37,40,41]. Another advantage of using a low frequency is that the penetration through the material is better. The attenuation due to dry kimberlite is very high, as shown in Chapter 3, so using a lower frequency should alleviate this problem. Thus a compromise must be reached between a low frequency, high quality factor structure as this will allow good penetration and

sensitivity while maintaining accuracy due to the high quality factor.

One of the biggest constraints was to make the system on-line, so the measuring device should not interfere with the conveyed material. Several different resonant structures were tested. First open resonant devices, loop antennae, resonant patch antennae and a low frequency microstrip filter were tested. This was followed by a partially closed structure, a hybrid loop-gap resonator, and finally resonant cavities, an almost closed device.

These structures were tested using a HP 8350B Frequency sweeper and a HP 8410C Network Analyser, if the resonant frequency was above 500MHz. If the resonant frequency was below this, the HP 4195A Network/Spectrum Analyser was used.

5.2. OPEN RESONANT STRUCTURES

5.2.1. Introduction to open resonant structures:

Open resonant devices have the ideal structure for on-line applications, as the conveyed material can pass the measuring device unhindered. This allows easy installation into an existing plant, as well as easy maintenance. It also does not force the material through a control point, which would be very difficult in a high volume processing application such as a mine. Thus open resonant structures were tested including loop antennae, resonant patch antennae, and a low frequency microstrip filter.

5.2.2. Loop antennae:

A loop has the ideal structure for a conveyor application since the belt can pass through it very easily, as shown in Figure 5.1.

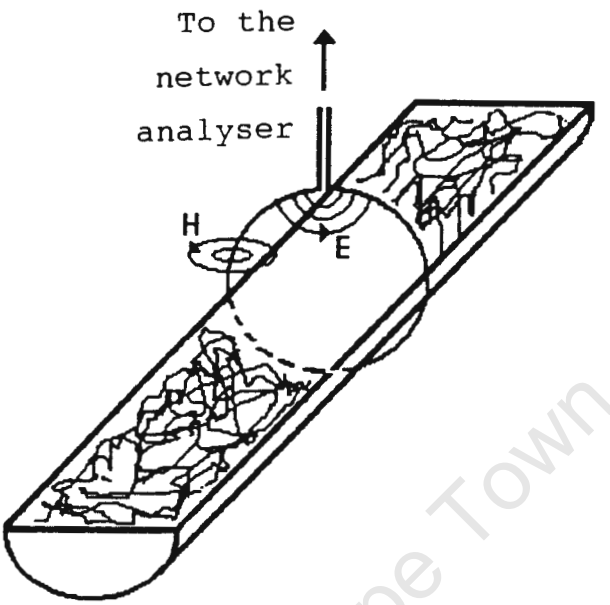

Figure 5.1: Loop antenna construction.

A loop antenna was made and tested on the network analyser but there were two main problems.

Firstly, quite a lot of the field radiated outwards, and so the readings were dependent on the surrounding environment. This could be overcome by using reflectors to redirect the field towards the centre.

Secondly, the quality factor of the loop was very low, with a bandwidth of 80MHz in the 400MHz region (Q=5). This was increased by using a stub tuner to improve the match between the network analyser and the antenna. However, even with this improvement, the frequency shift for a cup of water was only about 1%. This shift would be too small for good resolution readings.

The field within the loop was also very non linear, thus the frequency shift was highly dependent on the position of the sample in the loop.

5.2.3. Resonant patch antennae:

Resonant patch antennae have a much higher quality factor than loop antennae and are also more directed, thus they were tested next. A resonant patch antenna consists of two radiating slots separated by a $\lambda/2$ low impedance microstrip transmission line. The radiation from the two slots adds in phase at a frequency determined by the $\lambda/2$ section. A resonant patch antenna is shown in Figure 5.2.

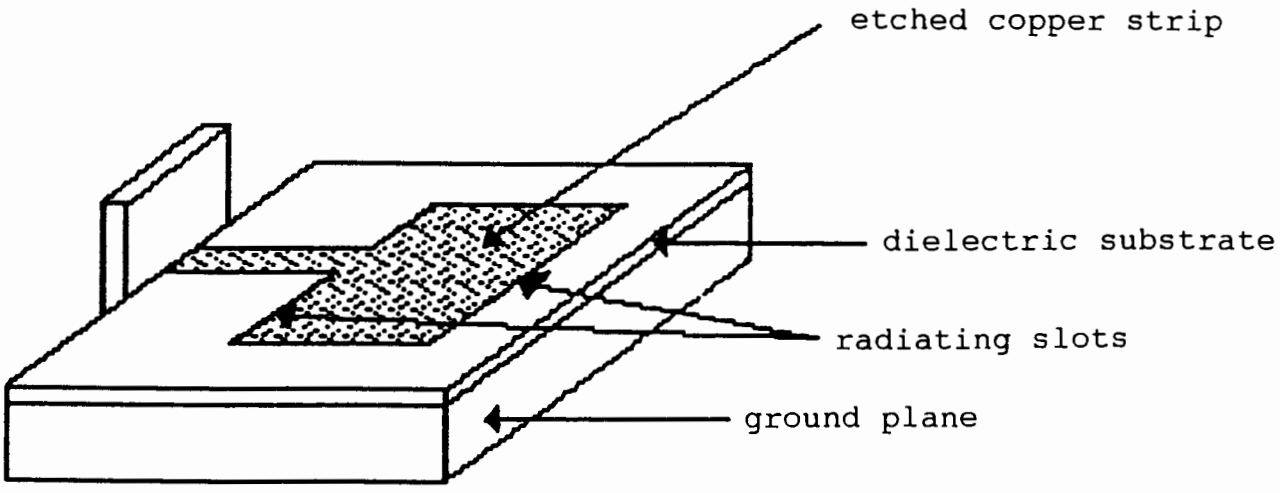

Figure 5.2: A resonant patch antenna.

The possibility of using this antenna as a moisture meter exists since the resonant frequency of the antenna is also determined by the coupling of the field to the environment. The frequency shift will depend on the dielectric constant of the material, thus a large shift is anticipated for water. For the final industrial moisture meter, the antenna would be

arranged above or below the conveyor belt so that the field would couple with the conveyed material, as shown in Figure 5.3.

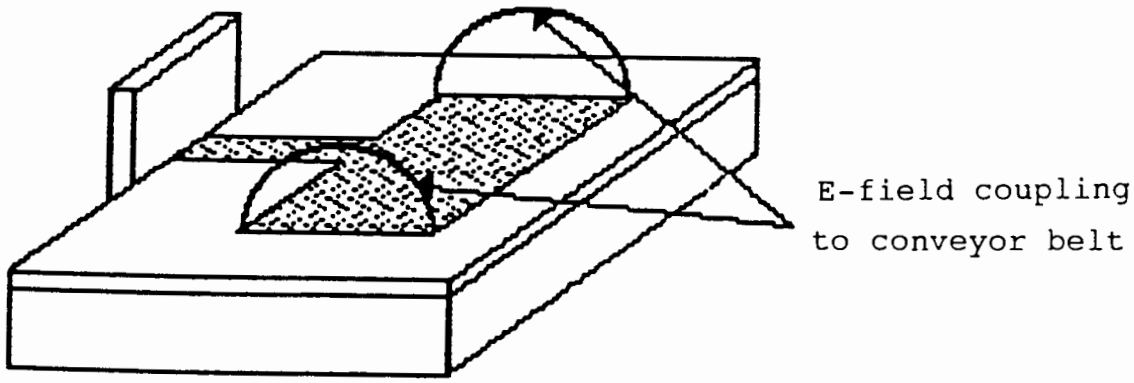

Figure 5.3: Resonant patch antenna configuration.

The concept was tested on the network analyser, using a 9GHz resonant patch antenna. The equipment was set up with the antenna connected to a circulator so that the input and output are separated. This is shown in Figure 5.4.

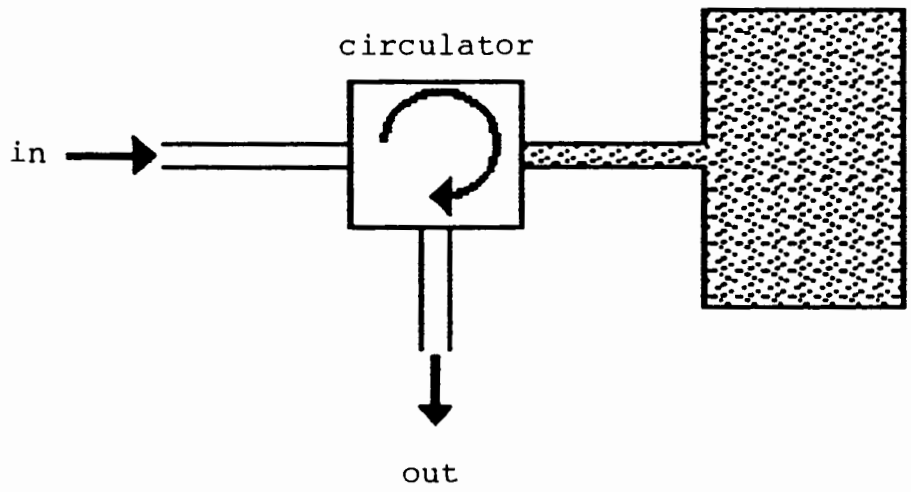

Figure 5.4: Usual arrangement for resonant patch.

The reflection coefficient of the unloaded antenna is given in Figure 5.5. The dip which occurs at 8.992GHz shows the frequency at which the antenna radiates.

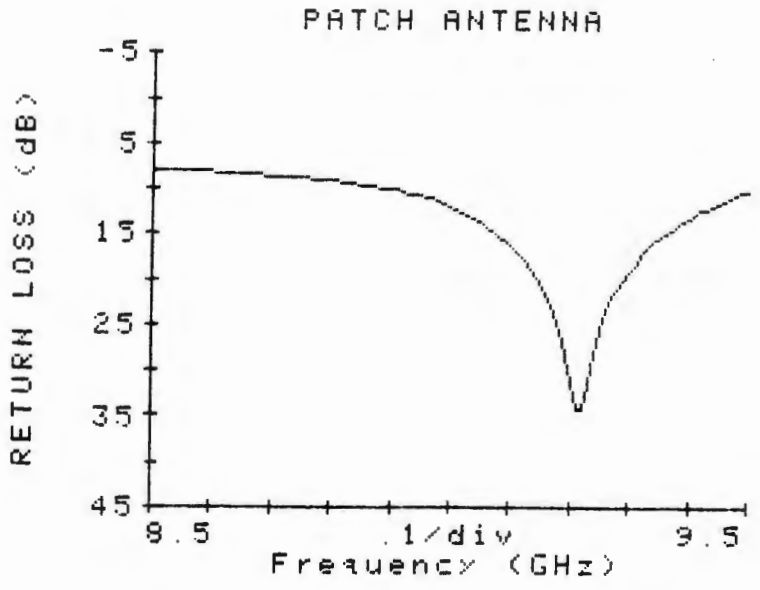

Figure 5.5: Reflection coefficient of unloaded resonant patch antenna.

Some moist paper was placed above the patch antenna, and the frequency shifts were noted.The most significant shift was to 8.841GHz, i.e 151MHz, which is a 1.68% shift. However, this was recorded for a distance of only 1cm between the paper and the antenna. The results are shown in Figure 5.6.

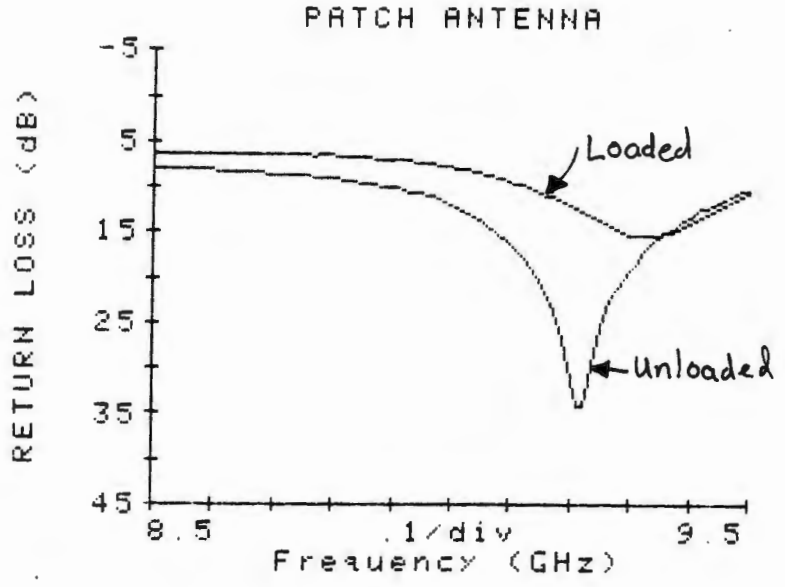

Figure 5.6: Resonant patch antenna loaded with paper.

The measurements were very dependent on the distance between the sample and the antenna, and for large heights the coupling was not so strong. This meant that the shift was not as great. If the distance was reduced too much, then the sample would overcouple to the antenna, so reducing the quality factor and the amplitude.

Thus for a practical system, where the antenna is held under the conveyor belt, the distance is critical. The frequency would have to be reduced to increase the critical height to a reasonable size, and the system carefully set up.

This system was not considered viable due to the small frequency shift and the low quality factor of the antenna, giving insufficient resolution and accuracy. A large amount of rock also loads the antenna. This is all because the sample only passes through the resonant patch antenna's fringe field.

Most of the microstrip field is concentrated between the copper conductor and the ground plane. Ideally one would like to run the conveyor belt through this high concentration field. However, the distance between the ground plane and the conductor is small and filled with a high dielectric substrate. This is because the E-field in the conductor and ground plane must be in phase for the microstrip to behave as a transmission line. This distance is thus restricted to be less than one tenth of the wavelength. So for a system to be developed where the conveyor belt is to run through the high field concentration, the frequency must be reduced. This increases the wavelength, so allowing the sample to pass between the conductor and the ground plane. Thus low frequency microstrip was tested next.

5.2.4. Low frequency microstrip:

For normal microstrip the distance between the ground plane and the conductor is quite small, as explained in Section 5.2.3. Most of the field is concentrated between the two planes but there are also some stray field effects. As the frequency reduces, the height of the dielectric can be increased. The idea for the low frequency microstrip design is to reduce the frequency to a point where the conveyor belt can run between the conductor and the ground plane. This means that the material will pass through the main E-field instead of the fringe field, as in the resonant patch case. Thus this method can almost be regarded as a capacitive technique.

Since the maximum height of the conductor above the ground plane is 3mm at 10GHz, using the one tenth wavelength rule, for a conveyor belt of 30cm, the

frequency should be 100MHz. However, the principle had to be tested at a higher frequency due to the size constraint for the prototype design.

As a high quality factor structure was required for accurate measurements, a filter design was considered. This is because multi-element filters can be designed to provide high quality factors and good bandwidths. Either a band-pass or band-stop filter could be used. The latter was chosen since a band-stop filter has a higher quality factor. For this design radical mismatching is required between the elements. This is done by using alternate high and low impedance quarter wavelength sections, as the referred impedance for a quarter wavelength section is given by Z_1^2 / Z_2 as shown in Figure 5.7.

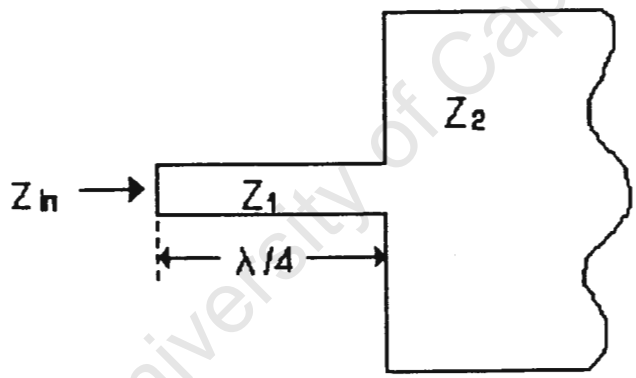

Figure 5.7: Quarter wavelength impedance transformation.

The complete design of the filter is given in Appendix B, and the final arrangement is shown in Photograph 5.8.

Photograph 5.8: Final microstrip band-reject layout.

The expected output is a transmission dip of 30dB at 600MHz. The output of S_{12} is shown in Figure 5.9.

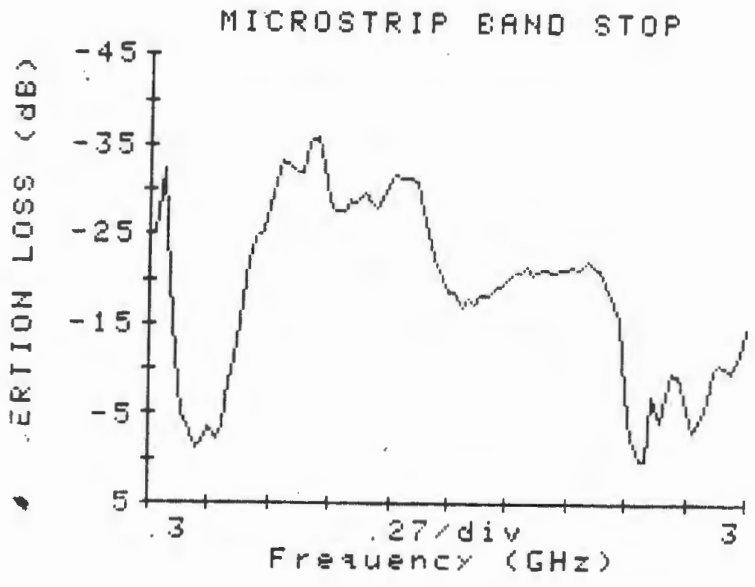

Figure 5.9: Transmission loss of the band-stop filter design.

The results show the expected insertion loss occurred at 540MHz, but the quality factor of the system was not nearly as high as desired.

Notice the third harmonic occurs at about 1.78GHz. Because of the low quality factor, the maximum frequency shift, seen when water was placed between the conductor and the ground plane, was insufficient to give accurate readings.

To improve the response, the filter was converted from microstrip to stripline, by placing another ground sheet above the filter. The resulting response is given in Figure 5.10.

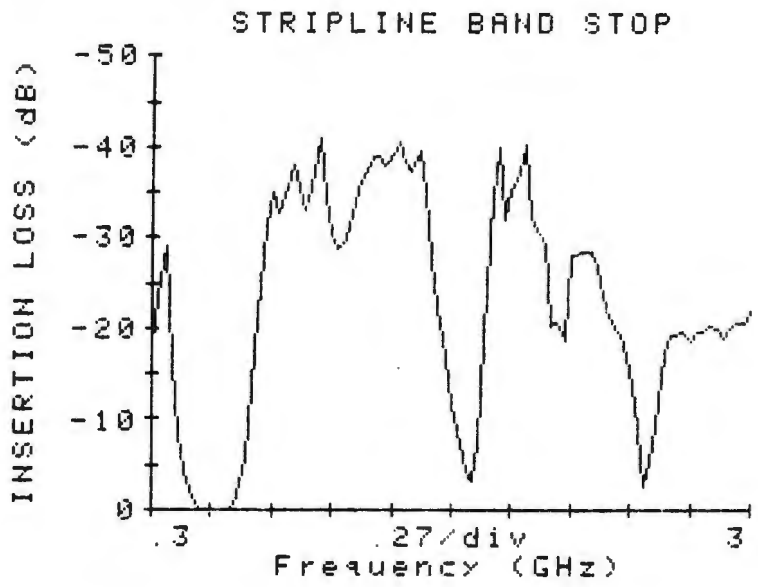

Figure 5.10: Insertion loss for stripline band stop filter.

This response was much better than for microstrip, with the third harmonic particularly well defined. However, the response to moisture did not give sufficient improvement as the quality factor was still too low.

5.2.5. Conclusions for open resonant structures:

In view of the results of the devices tested, the following conclusions can be drawn.

1. Although a loop antenna has the ideal structure for conveyor applications, its low quality factor and non-directivity meant that it was insensitive to moisture, easily loaded and affected by the surrounding environment.
2. Resonant patch antennae have a better quality factor and directivity, but the sample passes through the fringe field of the microstrip device. Thus it is easily loaded, highly position dependent, and not very moisture sensitive.

3. Finally, using a low frequency microstrip filter design, the sample was passed through the main E-field of the device. However, this device was still too moisture insensitive due to the low quality factor.

4. Open structures are not generally moisture sensitive and are easily loaded. This is due to their low field concentration and low quality factors.

5.3. LOOP-GAP RESONATORS

5.3.1. Introduction to loop-gap resonators:

The biggest problem that has been encountered with all the previous methods has been low field concentration and/or low quality factor. This is mainly due to the open structure of these devices. In an attempt to solve these problems, a partially closed device known as a loop-gap resonator (LGR) was tested. A LGR is a resonant structure with a field distribution that is intermediate between lumped and distributed [42]. Figure 5.11 shows the device.

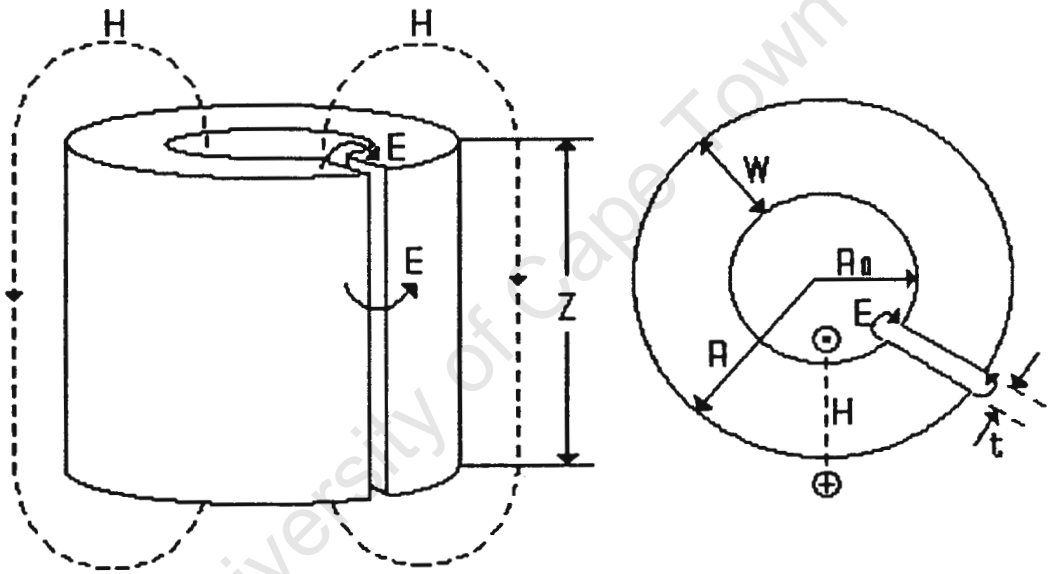

Figure 5.11: The LGR and cross-section view.

The question now arises; how could this device be used as a moisture meter? In simple terms, the LGR may be regarded as a LC parallel tuned circuit, with the capacitor being the parallel gap. The LGR frequency can be tuned by altering the dielectric in the gap. In the case of a moisture meter, the high dielectric constant of water would hopefully generate sufficient change in frequency to determine the moisture content of the host material.

5.3.2. Development procedure of LGR:

Since the characteristics of the LGR were not known, a few were designed and built to allow a better understanding of them. Design equations for the frequency and quality factor of the LGR were fairly complicated and a closed set of equations do not exist [42]. Thus an iterative program was written to determine optimum design dimensions. These dimensions are given in Table 5.12.

Table 5.12: Design dimensions of first phase LGR.

Res.No.	R_0	R	W	t	Z
A	10.0mm	19.0mm	9.0mm	2mm	20m
B	15.0	17.5	2.5	3	40
C	21.0	21.5	0.5	4	40

As can be seen from Table 5.12, these devices are very small compared to the conveyor belt. It is also obvious that if the conveyor belt were to pass through the gap, then the LGR would be several meters in dimension. However, it was hoped that by passing the conveyor through the centre of the resonator the fringing field from the gap would penetrate the measured material strongly enough to allow readings to be made. Thus initial work was to determine the dimensions of the LGR which had the strongest E-field near the gap. Photograph 5.13 shows the three resonators.

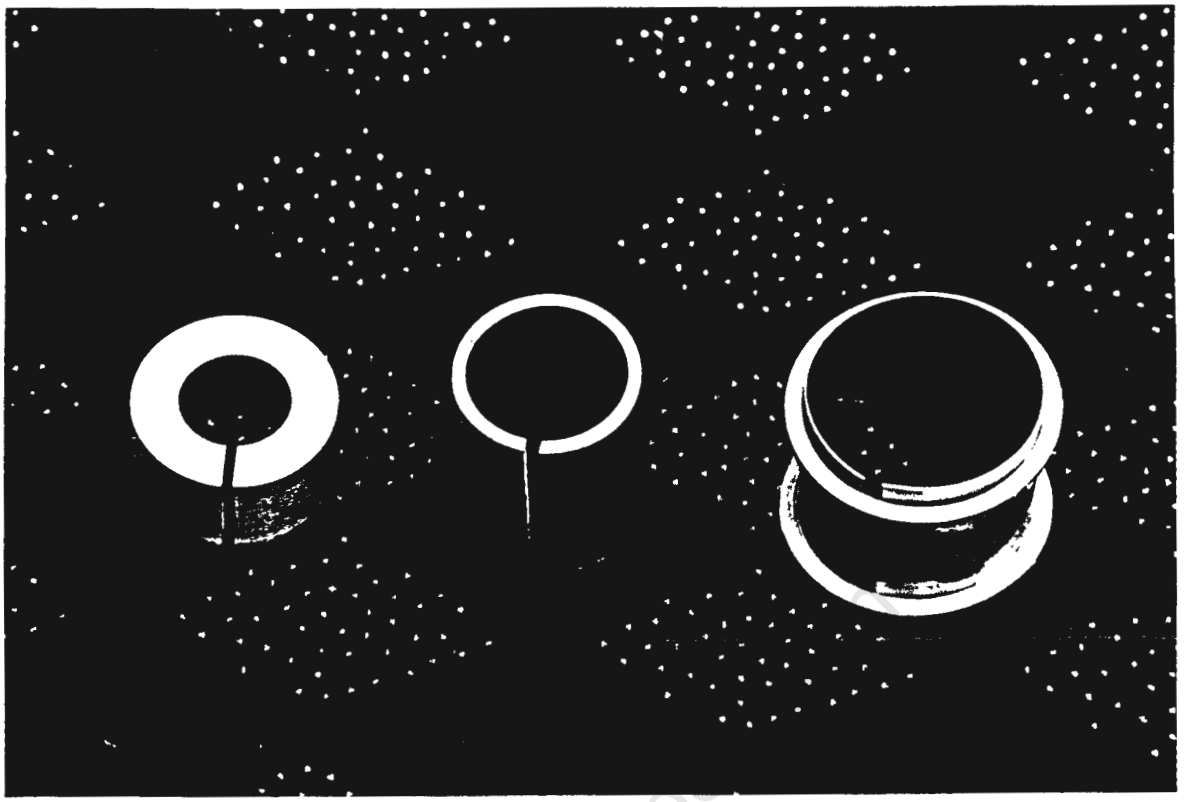

Photograph 5.13: First phase loop-gap resonators.

The LGR can be coupled to external circuits using either an inductive loop coupling, or a monopole probe for capacitive coupling, or a microstrip line for magnetic coupling. Since the characteristics of the LGR were not known, the microstrip method was used for initial testing, as this is the easiest coupling method. This is shown in Figure 5.14.

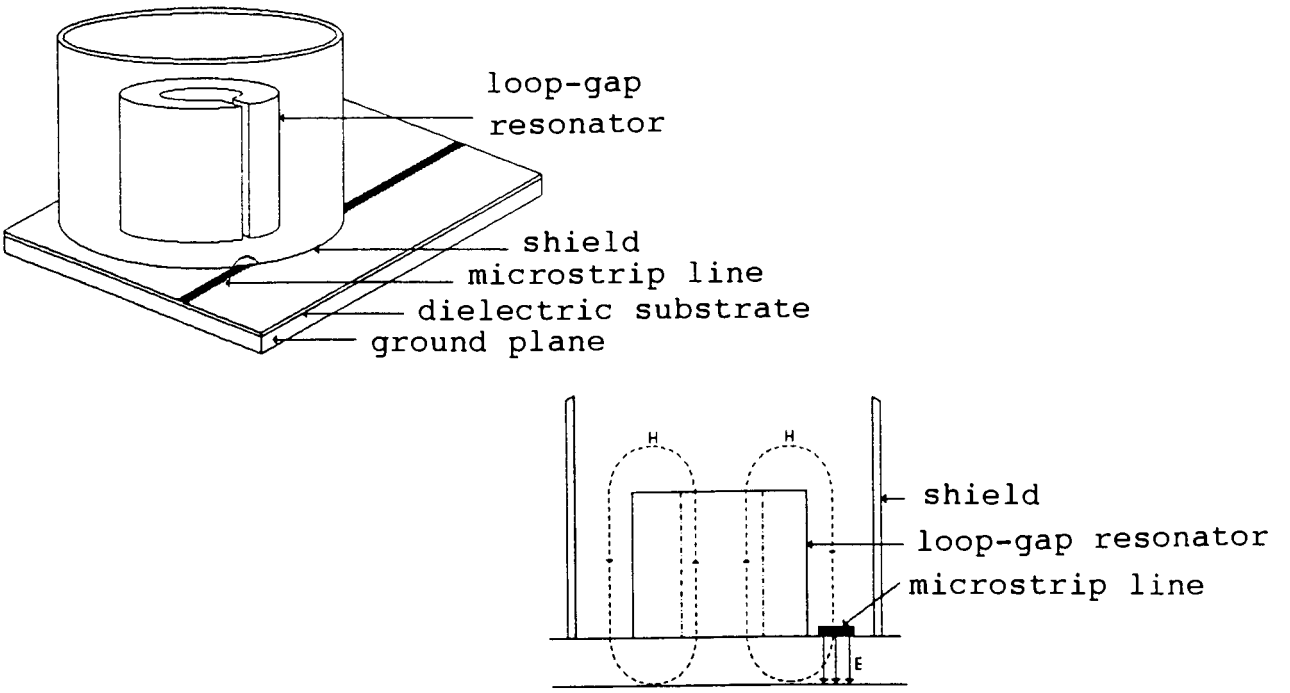

Figure 5.14: Coupling of a LGR to microstrip line a) schematic view b) electromagnetic field configuration.

Three different microstrip boards were used. They varied in their dielectric substrate thickness, 0.254mm, 0.813mm, and 1.575mm, so giving line width variations. The board with the thinnest substrate, 0.254mm, gives a line width of 0.76mm, while the widest line is 4.79mm. The resonators were tested by connecting the 50Ω microstrip boards to the HP 8410C Network Analyser. The frequency is swept using a HP 8350B Frequency Sweeper. The transmission loss, S_{12}, was observed for various LGR positions on the boards. Although a shield is normally used with the LGR, to increase the quality factor and reduce environmental effects, tests were done without one. This is because the ultimate moisture meter would not be able to use a shield, due to practical size constraints. The results are given in Table 5.15.

Table 5.15: Frequency and coupling results for initial loop-gap resonators.

Resonator	0.254	0.813 (GHz / dBs)	1.575 (GHz / dBs)
A	*	1.195-1.251	1.362-1.894
	*	20	40
B	*	1.092-1.158	0.680
	*	15	15
C	*	0.815-0.837	1.410
	*	7	5

* No distinguishable, consistent resonance.

In view of the results, the following points should be made.

1. For the 0.254mm board, none of the LGR appear to resonate. This is because there is only very small coupling into the resonators. Thus the energy transferred to the LGRs is not large enough to allow them to resonate properly.

2. In contrast to point 1, the best results were observed for the wide line, 1.575mm, board. Obviously in this case there is enough coupling to allow the LGRs to resonate.

3. The frequency variation is due to the different positions of the LGR on the board.

4. The strongest coupling was seen for resonator A. This was expected since it has the greatest capacitive area.

The best results were observed for Resonator A, as noted in point 4. Since the LGR would be scaled up almost 100 times for the full size model, such a design would be completely impractical due to size, mass, and cost. Thus two hybrid resonators were designed having the same basic dimensions as Resonator A. Hybrid 1 was a hollow version of the original, while Hybrid 2 consisted of the inner cylinder and the parallel gap. These are shown in Photograph 5.16 with the original Resonator A.

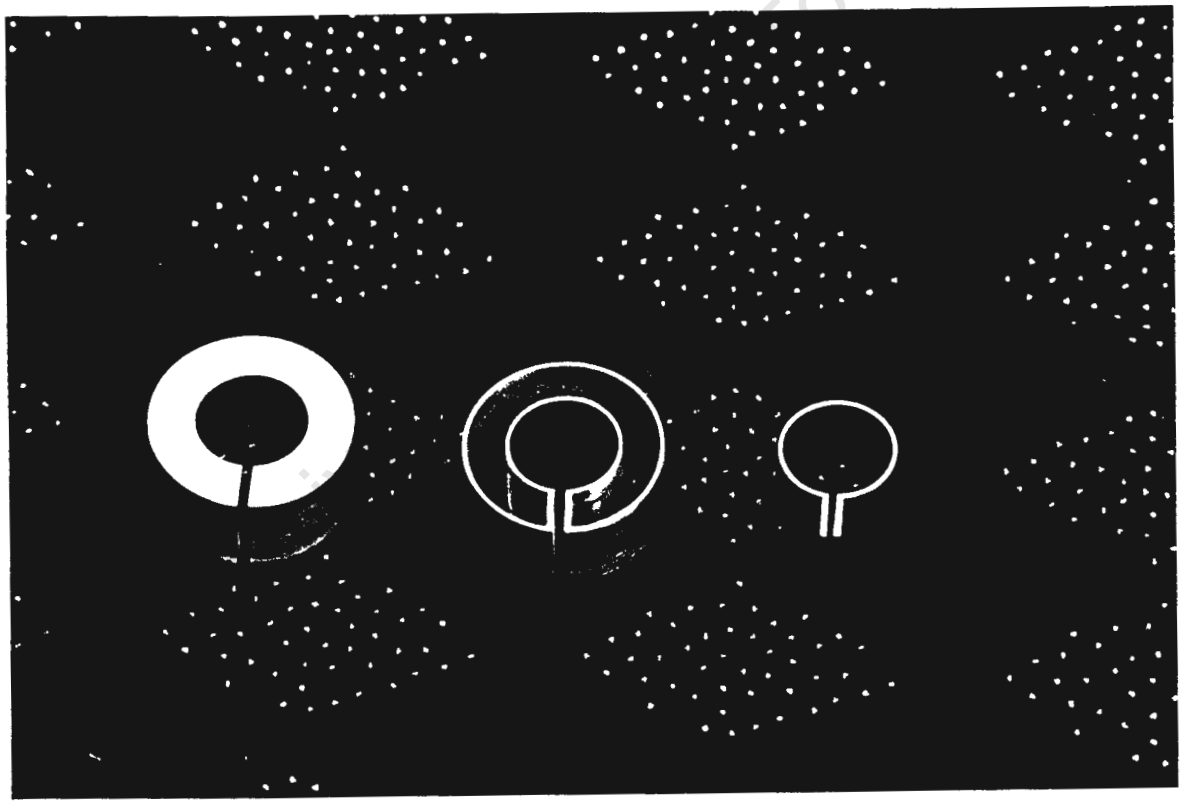

Photograph 5.16: Resonator A with the two hybrids.

These were tested in the same way as before. The results are given in Table 5.17.

Table 5.17: Frequency and coupling results for Resonator A and the two hybrids.

Resonator	0.254 (GHz/dBs)	0.813 (GHz/dBs)	1.575 (GHz/dBs)
Original	*	1.195-1.251	1.362-1.894
	*	20	40
Hybrid 1	2.76 & 1.27	1.092-1.158 & 2.700-2.740	1.133-1.206 & 1.514-1.580
	6	20	15
Hybrid 2	1.33	1.26	1.208-1.275
	7	16	18

* No distinguishable, consistent resonance.

From Table 5.17 it can be seen that although the original resonator performs the best of the three, the hybrid designs perform better than Resonators B and C. It is interesting to note that Hybrid 1 resonates at two frequencies. This is due to the coupling into both cylindrical sections of this resonator.

Although microstrip was useful for preliminary testing, it is obviously impractical for the final product. Thus inductive and capacitive techniques were tested. Various capacitive probes were used, but results were not very promising as the probe positioning was extremely critical. This would be useless for the final product, which must withstand a harsh environment.

Inductive coupling gave more promising results. The loops radii, wire thickness, as well as the number of turns were varied to optimize the coupling. This technique also proved less sensitive to positioning. The coupling to the LGR was as strong as for the microstrip case.

Having determined that the hybrid LGR was a viable structure for practical implementation, it had to be tested for moisture sensitivity. The LGRs being used were too small for such tests, so a larger one was made. The Hybrid 2 design was used as this was the most viable structure. For this design the diameter of the "loop" was 9.0cm, while the parallel "legs" were 7.5cm. Optimum coupling was obtained inductively with two double loop couplers placed about 1cm from either end of the resonator, as shown in Figure 5.18.

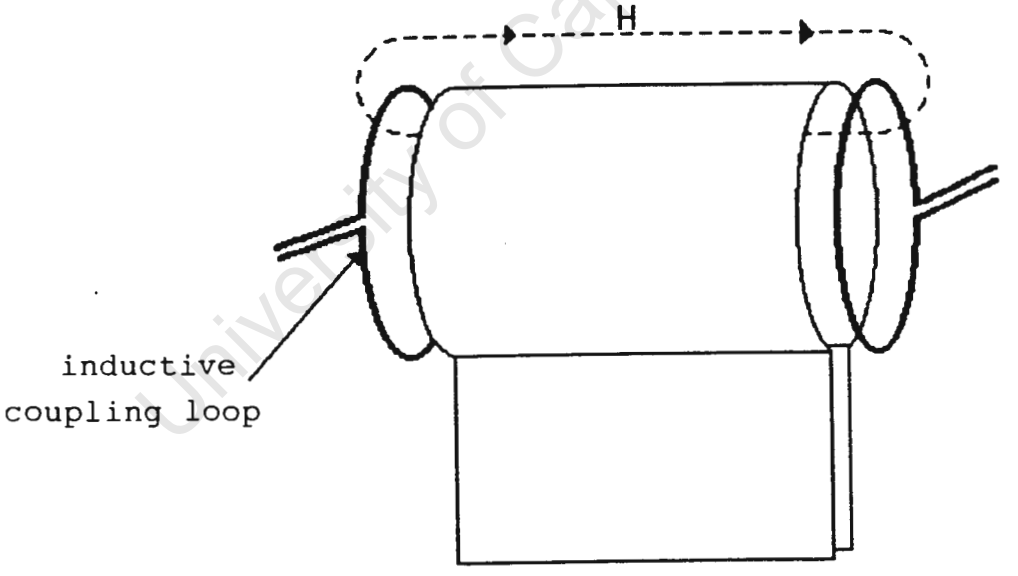

Figure 5.18: Intermediate LGR inductively coupled.

This LGR was first tested for moisture sensitivity. The resonator was held in a vertical position and a 400ml glass beaker was placed inside the resonator. Water was then added to the beaker in a controlled

manner. The change in frequency is measured to give an indication of the water sensitivity. The shift is expressed as a percentage change from the empty resonator frequency. Two frequencies were tested to compare the sensitivity. The frequency was altered by changing the width of the gap. The results are given in Table 5.19 and then plotted in Figure 5.20.

Table 5.19: Water sensitivity results for intermediate LGR at two frequencies.

Empty	150.25 MHz	172.85 MHz
50ml	2.3%	1.7%
100	4.5	3.4
150	6.5	5.1
200	8.3	6.6
250	9.7	8.0
300	11.0	9.4
350	12.1	10.6
400	12.8	11.4

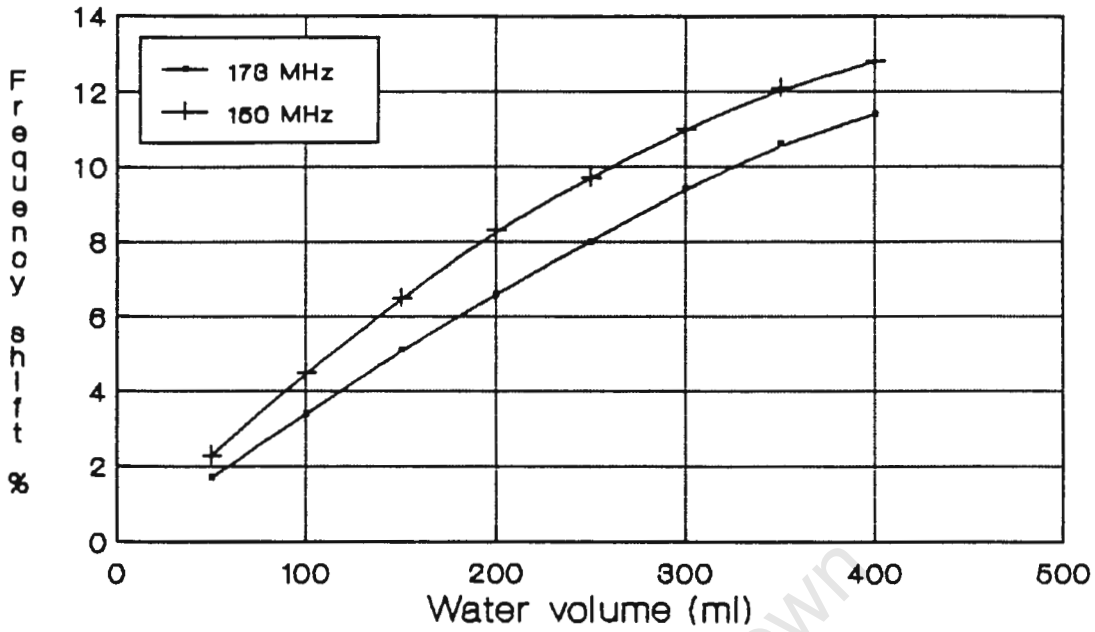

Figure 5.20: Plot of frequency shift against volume of water for intermediate LGR, at two frequencies.

As can be seen from Figure 5.20, the sensitivity is greater at the lower frequency. This is because the 150MHz case had a narrower gap than the 173MHz case, which allows a stronger E-field around the gap of the LGR. This is also enhanced because greater dielectric sensitivity is shown at lower frequencies as reported by Parkhomenko [37] and Nelson [40].

Although these initial results proved encouraging, they were not a true reflection of a realistic system. This is because the water was very close to the gap, which is the most sensitive area of the resonator. In fact, frequency shifts varied by an order of magnitude depending on the position of the sample in the resonator. At first it was thought that this could be used to the systems advantage, as this would make it less sensitive to height variation of

the material. Since the conveyor belt would be held in a fairly constant position in the final application, final tests were done as follows. A polystyrene board ($\epsilon_r \approx 1$) was placed in the resonator to separate the sample being measured from the gap. The samples were then placed in a polystyrene container and measurements taken. The configuration is shown in Figure 5.21.

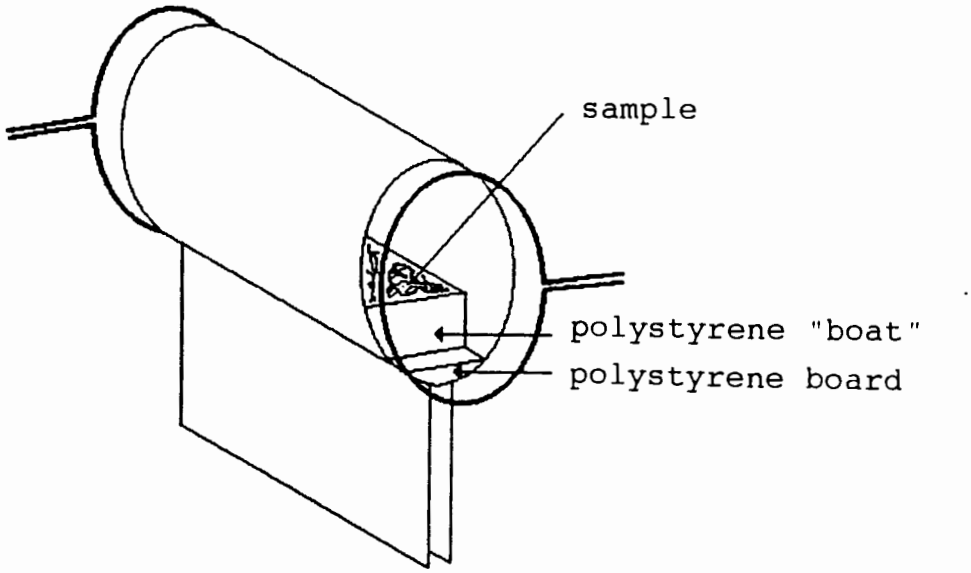

Figure 5.21: Test configuration for intermediate LGR.

The system sensitivity was tested for three cases. The first was for water alone, then for kimberlite gravel alone, and finally for a combination of water and gravel. In all cases an attempt was made to keep the sizes of the samples proportional to the final application specifications. The results are given in Table 5.22.

Table 5.22: Frequency shift measurements using intermediate LGR.

Water alone		Kimberlite		Mixture		
ml	%	g	%	τ	%	%
2.5	0.02	20	0.08	1.14	0.65	0.05
10	0.04	100	0.32	4.41	0.93	0.33
20	0.06	200	0.53	8.44	1.13	0.53
60	1.04	217	0.55	21.66	1.46	0.87

Notice that two sets of frequency shift data are given for the mixture case. The first set is the total percentage frequency shift, thus including the shift for both the water and the gravel. The second set is the shift due to the water alone. This means that the reference frequency is that of the resonator loaded with the gravel.

From the results in Table 5.22, it is seen that the responses are not very uniform, particularly for the water alone. However, once the cavity is loaded slightly the response becomes more linear, as seen for the mixture measurements. This is due to the uneven field distribution at the gap. Most importantly though, is the frequency shifts are very small showing that the field is confined very close to the gap.

To complete the investigation into LGRs, a full scale model was built. The dimensions of this resonator, diameter of 0.7m and parallel plates of 0.7m, allow a conveyor belt to pass through the centre quite easily. The resonator is shown in Photograph 5.23.

Photograph 5.23: Final full scale LGR design.

Again the coupling had to be optimized. Best results were obtained for double loop transmitter and receiver. The gap width also had to be optimized. This was adjusted by Teflon bolts which kept the plates parallel. The samples were placed 1cm above the gap for maximum response. This time the samples consisted of 1.5 litres of water, 6.5kg of kimberlite stones, and finally a section of conveyor belt. The results are given in Table 5.24 and plotted in Figure 5.25.

Table 5.24: Frequency shifts for various samples in full scale LGR, for different gap widths.

Width cm	Frequency MHz	Q	Water %	Kimberlite %	Conveyor %
1.0	12.065	67	0.58	0.00	0.37
1.5	13.610	53	0.73	0.07	0.29
2.0	15.920	51	0.97	0.22	0.66
2.5	17.225	45	1.22	0.44	0.70
3.0	18.115	35	0.97	0.36	0.06
3.5	18.455	29	0.60	0.30	0.49
4.0	18.560	27	0.32	0.13	0.11
4.5	18.635	27	0.13	0.00	0.11

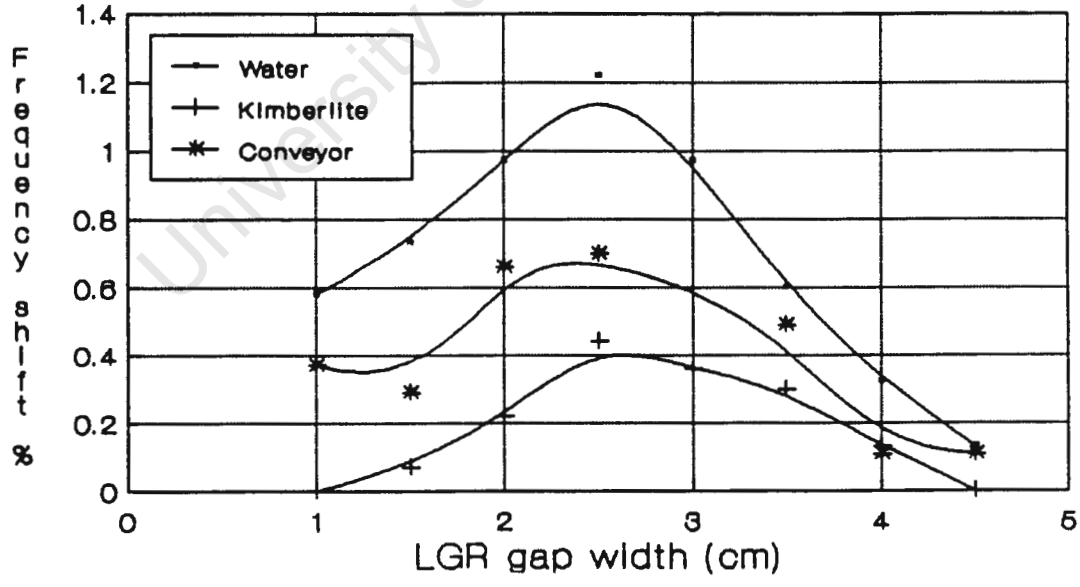

Figure 5.25: Plot of percentage frequency shifts for various samples in full scale LGR.

From Figure 5.25 it can easily be seen that the most sensitive resonator gap is for about 2.5cm. At this gap the separation of the water above the kimberlite and conveyor belt sample is also greatest. However, the frequency shifts are again very small.

5.3.3. Conclusions for loop-gap resonators:

From the results of the various tests, the following conclusions may be drawn.

1. Although a standard LGR design was not a suitable structure for a large scale industrial moisture meter, a hybrid design proved to be a viable device.

2. The LGR showed very strong moisture sensitivity when a sample was placed close to the gap. However, the moisture sensitivity is not uniform across the resonator.

3. Due to the small, non-uniform field distribution of the LGR, it was not considered a suitable device for further development.

4. This partially closed high quality factor structure performed far better than the open structures described in section 5.2. However, the device that is finally needed is a closed, high quality factor resonant structure with a more suitable field distribution.

5.4. ALMOST CLOSED RESONANT CAVITIES

5.4.1. Introduction to resonant cavities:

Despite using a partially closed structure, the field in the loop-gap resonator was not strong and uniform enough in the loop section to obtain reliable results, as seen in Section 5.3. Thus, the final devices tested were various resonant cavities. These are almost closed resonant structures with very high quality factors and well understood field patterns. The cavity chosen here was a rectangular waveguide operating in the fundamental TE_{01} mode. This structure has the advantage of a high unloaded quality factor, with higher order modes being suppressed within the cavity thus behaving in a predictable way.

For this technique the frequency and quality factor of an unloaded cavity is known. The sample is placed in the cavity, and the new frequency and quality factor are measured. From the changes, the dielectric constant and loss may be determined. This is an extension of the perturbation theory. The smaller the sample, the more accurate the technique, but here there must be a compromise. Since a realistic size structure is required for the ultimate moisture meter, the sample must be allowed to occupy a reasonable volume of the cavity. Thus, a wide range of rectangular waveguide resonant cavities were tested to try and find a water sensitive cavity, while still being a practical structure.

5.4.2. Development of resonant cavities:

For the application of measuring the moisture content of rocks, the conveyor belt is 1.5m wide with a maximum loading height of 0.5m. In order to pass the conveyor belt loaded with kimberlite rocks through the waveguide cavity, a 100MHz TE_{01} mode cavity would be required. For convenience a five times scaled model, at a frequency of 500MHz, was designed and constructed. To maintain proportion, the effective conveyor slot cut in the resonant cavity had to be reduced five times to 30cm wide and 10cm high. The microwaves are launched using H-field coupling loops, while the rocks move in and out of the cavity through slots cut in the sides in non-radiating positions. The configuration is shown in Figure 5.26.

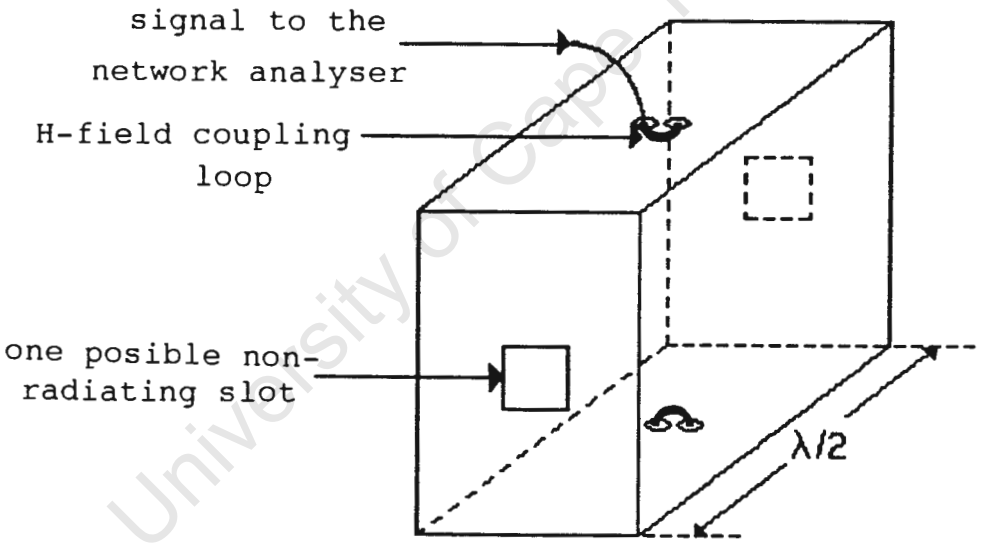

Figure 5.26: Rectangular waveguide resonant cavity configuration.

In an ideal closed cavity the field distribution is known and is shown in Figure 5.27. However, the presence of a slot, to enable the conveyor belt loaded with kimberlite to pass through the cavity, will distort the field even if the slot is in a non-radiating plane.

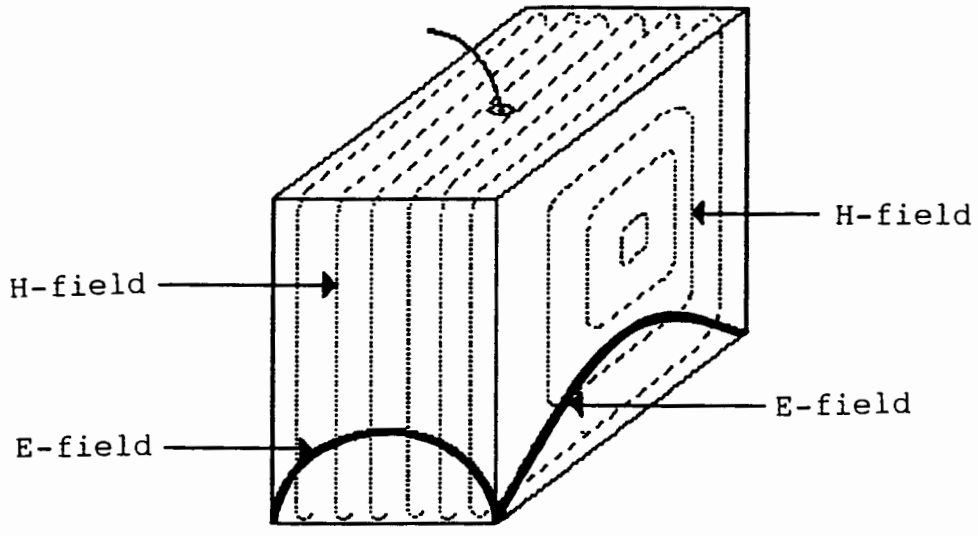

Figure 5.27: Field pattern in a resonant cavity.

Three slot orientations were tested, all in non-radiating planes. Figure 5.28 shows these three cavities.

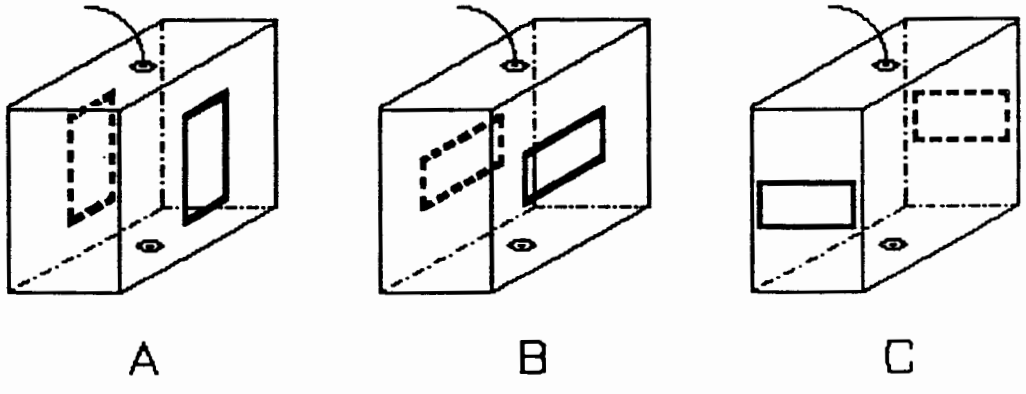

Figure 5.28: The three resonant cavities.

All three cavities were then tested using identical test samples consisting of water, kimberlite gravel, and then a gravel/water mixture. The results are given in Tables 5.29, 5.31 and 5.33 and plotted in Figures 5.30, 5.32 and 5.34.

Table 5.29 and Figure 5.30: Percent frequency shift for water for cavities A-C.

Water	Cavity A	Cavity B	Cavity C
(MHz)	513.0	515.7	492.75
(Q)	190	147	177
(dBm)	-12.0	-14.0	-12.6
2.5ml	0.292%	0.252%	0.406%
5.0	0.585	0.634	0.873
7.5	1.053	1.202	1.086
10	1.384	1.532	1.542
15	2.125	2.308	2.182
20	3.060	3.122	3.064
30	4.600	4.673	4.698
40	5.965	6.069	6.494
50	7.154	7.466	7.935
100	12.787	12.786	12.532
(Q)	30	28	100
(dBm)	-20.0	-21.0	-17.8

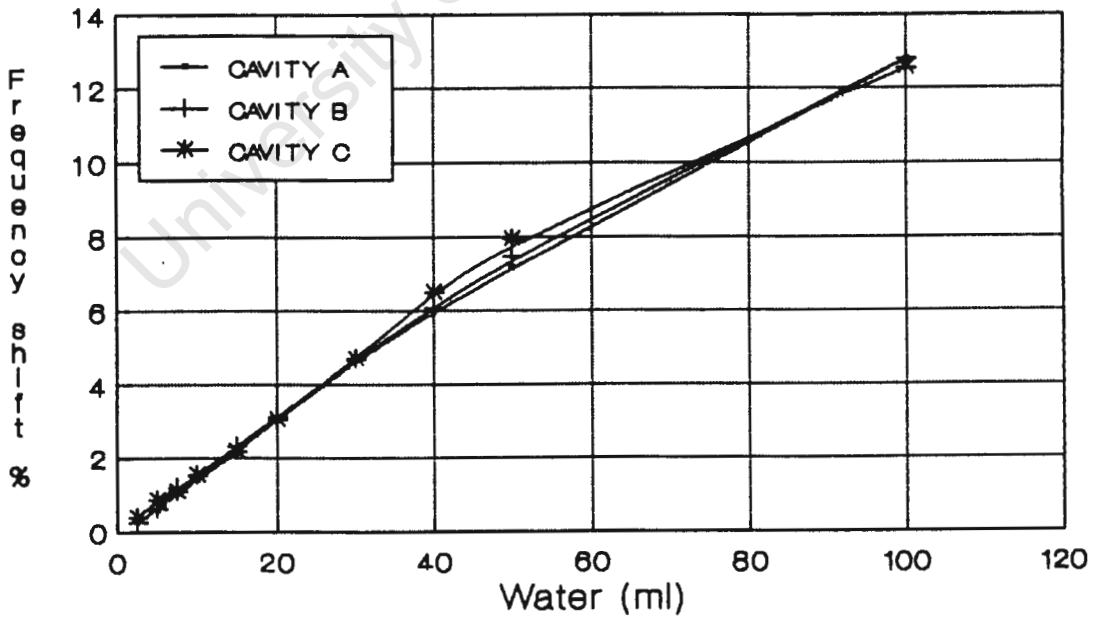

Table 5.31 and Figure 5.32: Percent frequency shift for kimberlite gravel for cavities A-C.

Gravel	Cavity A	Cavity B	Cavity C
(MHz)	513.0	515.7	493.0
(Q)	190	147	160
(dBm)	-12.0	-14.0	-12.2
20g	0.097%	0.097%	0.182%
50	0.234	0.272	0.335
100	0.487	0.582	0.609
150	0.760	0.912	0.913
200	1.033	1.222	1.146
250	1.267	1.494	1.602
300	1.520	1.804	1.765
350	1.754	2.056	2.059
400	1.969	2.328	2.343
450	2.242	2.638	2.718
500	2.495	2.890	3.100
550	2.749	3.220	3.628
(Q)	82	62	55
(dBm)	-19.0	-22.0	-20.7

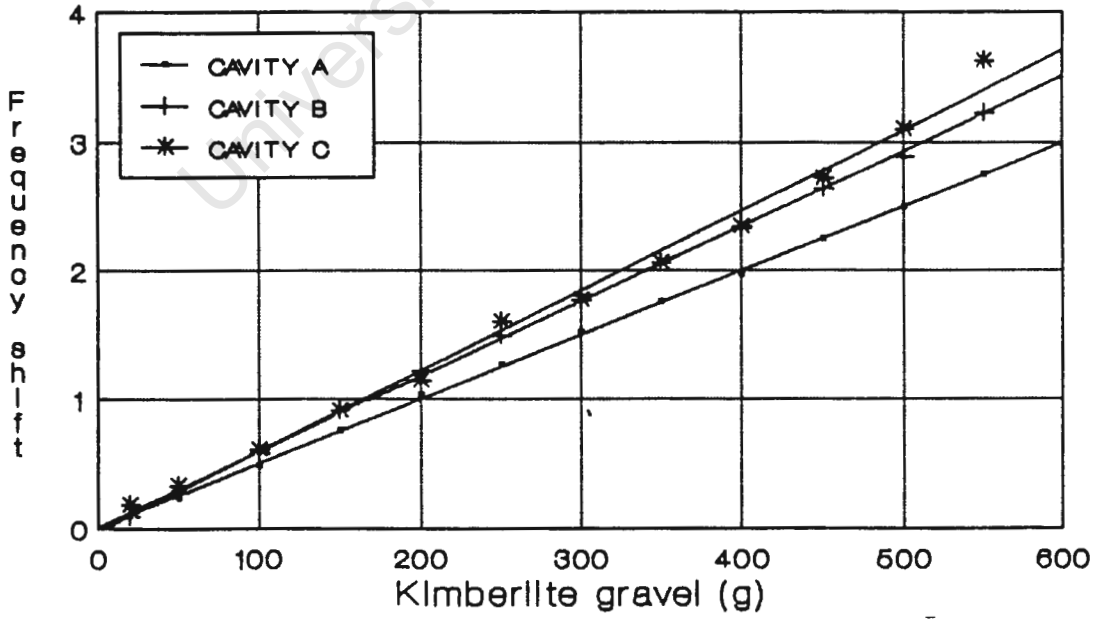

Table 5.33 and Figure 5.34: Percent frequency shift for kimberlite and water mixture for cavities A-C.

Moisture	Cavity A	Cavity B	Cavity C
(MHz) (Q) (dBm)	497.9 82 -19.9	498.05 63 -21.7	474.8 55 -23.0
0.452% 0.901 1.345 1.786 2.655 3.509 5.172 6.780 8.333	0.190% 0.341 0.603 0.934 1.557 2.119 3.585 4.559 5.593	0.151% 0.331 0.622 0.873 1.426 2.108 3.413 4.467 5.662	0.190% 0.390 0.590 0.864 1.495 2.045 3.444 4.844 6.203
15.385 (Q) (dBm)	10.118 29 -31.2	10.742 20 -33.3	11.384 29 -30.2

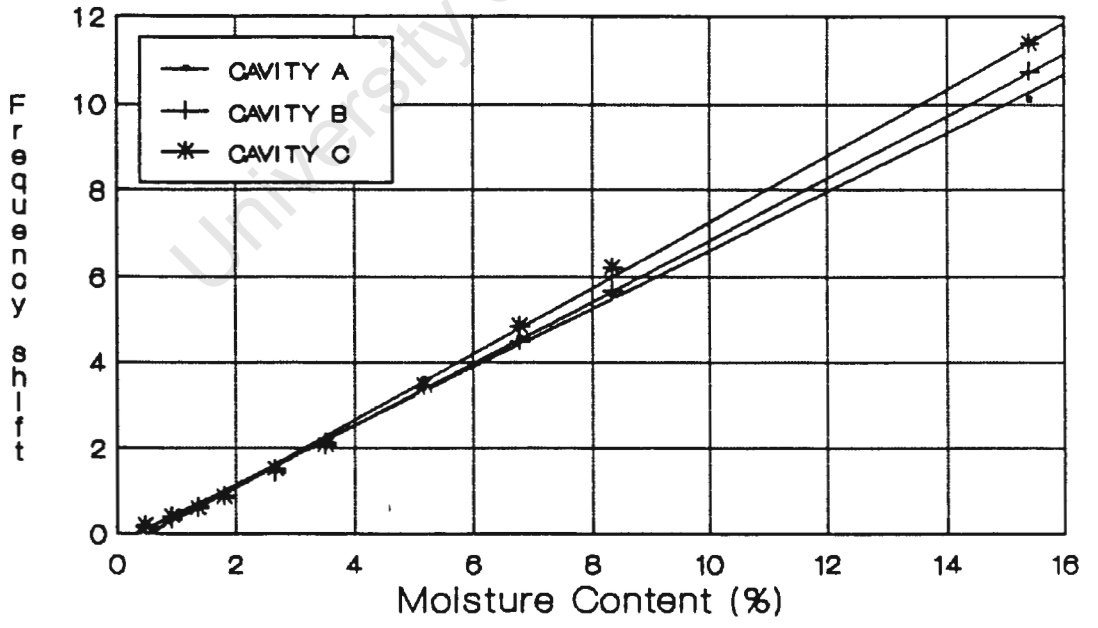

Note that the percentage shifts for Table 5.33 are given relative to the cavity frequency loaded with gravel. Thus the shifts shown are for the moisture alone, not the water and gravel.

From the results in Tables 5.29, 5.31 and 5.33 and Figures 5.30, 5.32 and 5.34 it can be seen that Cavity C seems to offer the greatest sensitivity for all three cases, while being loaded least easily. This is because the slot in this cavity is furthest from the center of the cavity, where the E-field concentration is a maximum, so causing the least distortion. Cavity A suffers from high attenuation as the slot orientation is in the same direction as the E-field maximum. This means that the attenuation is constant and high along the whole length of the slot. Since the sample size was small, only occupying one third the area of the slot, this is not clearly seen from the results. Cavity B has the maximum attenuation at the centre and then decreases outwards. Again due to the size of the sample holder this effect was not exaggerated. The most important point to note is the high frequency shifts that were recorded for these cavities. Compared to the 1% to 2% frequency shifts that were seen for the previous open structure devices, now there was over 10% shift for 15% moisture content. Best fit curves of moisture content verses frequency shift show a slope sensitivity range from 0.680, for the worst case (Cavity A), to 0.768 for Cavity C. What is also striking about the results is the high linearity, with all three cavities having a correlation coefficients of above 0.999. Thus the results for the rectangular waveguide resonant cavities show beyond doubt that they are the most promising devices.

Since the cavity being used only had two slots in it, a full size design would be undesirably large. This is because the conveyor belt runs through the narrowest side of the resonant cavity. Ideally the cavity should be separated into two sections thus enabling a smaller cavity to be used with one half placed above the belt and the other below. However, this would have the disadvantage of radiation leakage occurring through the gap between the two halves of the cavity. This will result in a distortion of the field distribution and a reduction in the quality factor will inevitably result. A sketch of the form of the E-field pattern is shown in Figure 5.35. The H-field is not shown as only the E-field couples to the rocks, as they are dielectrics.

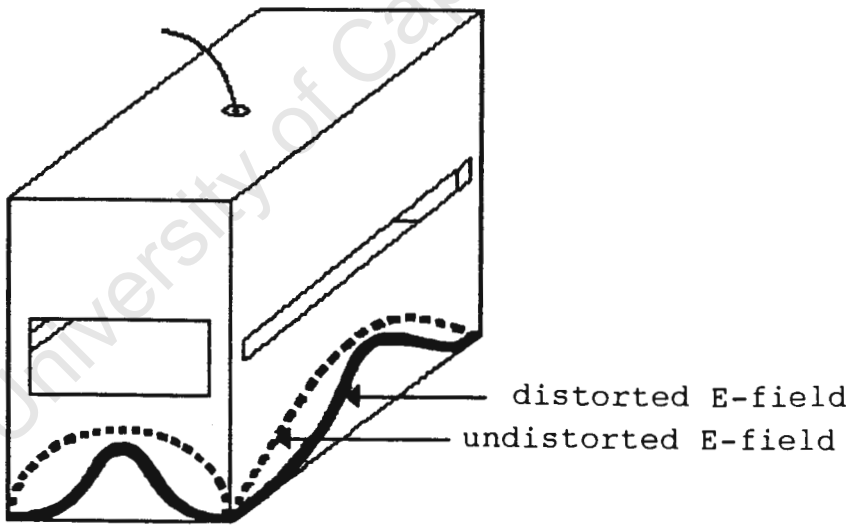

Figure 5.35: E-field distortion due to extra gap.

Experiments were performed to try and establish whether sufficient accuracy of moisture measurement could be achieved if the gap was small.

Noting the above points, Cavity C was then altered as follows. Two extra slots were cut into it, also in the same horizontal plane but this time in the opposite walls to the existing slots. This almost splits the cavity into two but the corner strips were left intact to maintain the structure. This "multi-gapped" cavity is shown in Figure 5.36.

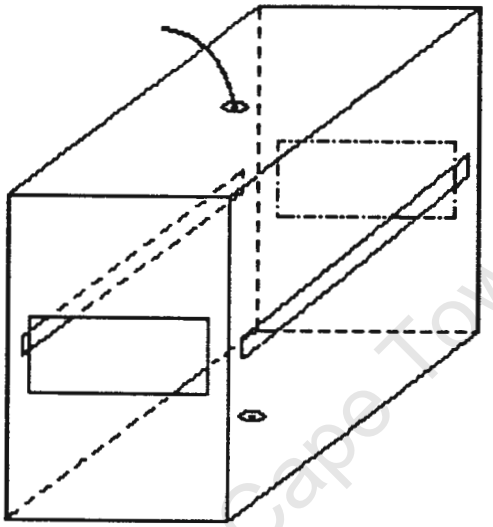

Figure 5.36: "Multi-gapped" resonant cavity.

This cavity was also tested using the water, gravel, and water/gravel mixture samples. The extra-gap width was adjusted for four different cases of 1, 2, 5 and 10cm. The results are given in Tables 5.37, 5.39 and 5.41 and are plotted in Figures 5.38, 5.40 and 5.42.

Table 5.37 and Figure 5.38: Percent frequency shift for water for the multi-gap cavity.

	No gap	1cm	2cm	5cm	10cm
(MHz)	492.75	500.3	500.0	500.8	505.2
(Q)	177	80	65	60	108
(dBm)	-12.6	-19.2	-19.8	-20.4	-13.8
2.5ml	0.406%	0.540%	0.380%	0.479%	0.475%
5.0	0.873	0.770	0.540	0.699	0.851
7.5	1.086	0.999	1.009	1.258	1.188
10	1.542	1.559	1.549	1.717	1.504
15	2.182	2.414	2.324	2.661	2.351
20	3.064	3.283	3.193	3.395	2.959
30	4.698	4.917	4.797	4.932	4.315
40	6.494	6.606	6.706	6.799	6.027
50	7.935	8.125	8.245	8.307	7.443
100	12.532	12.787	12.952	12.839	11.594
(Q)	100	48	48	80	51
(dBm)	-17.8	-24.5	-23.8	-23.3	-23.3

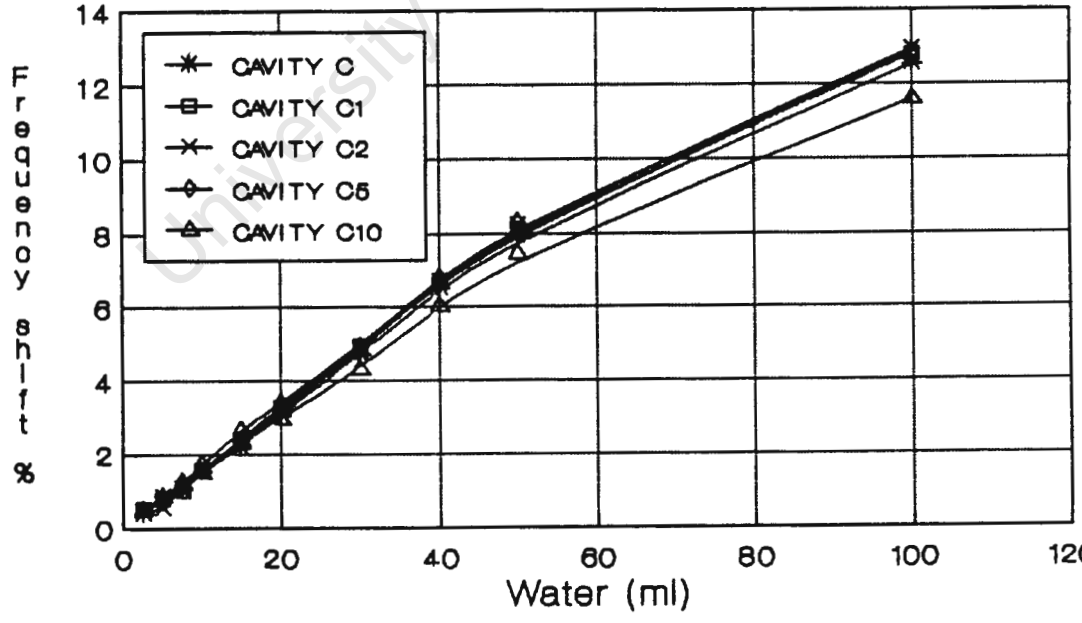

Table 5.39 and Figure 5.40: Percent frequency shift for kimberlite gravel for the multi-gap cavity.

	No gap	1cm	2cm	5cm	10cm
(MHz)	493.0	500.1	500.3	500.0	505.3
(Q)	160	74	54	57	144
(dBm)	-12.2	-18.3	-20.7	-21.7	-16.7
20g	0.182%	0.140%	0.139%	0.159%	0.138%
50	0.335	0.330	0.290	0.350	0.317
100	0.609	0.570	0.610	0.630	0.633
150	0.913	0.880	0.849	0.940	0.970
200	1.146	1.210	1.149	1.180	1.168
250	1.602	1.510	1.499	1.180	1.168
300	1.765	1.740	1.709	1.800	1.672
350	2.059	2.140	2.089	2.110	1.989
400	2.343	2.380	2.409	2.420	2.296
450	2.718	2.699	2.718	2.760	2.513
500	3.100	3.215	3.154	3.098	2.906
550	3.628	3.520	3.695	3.758	3.306
(Q)	55	39	34	36	56
(dBm)	-21.7	-24.5	-26.3	-25.2	-21.9

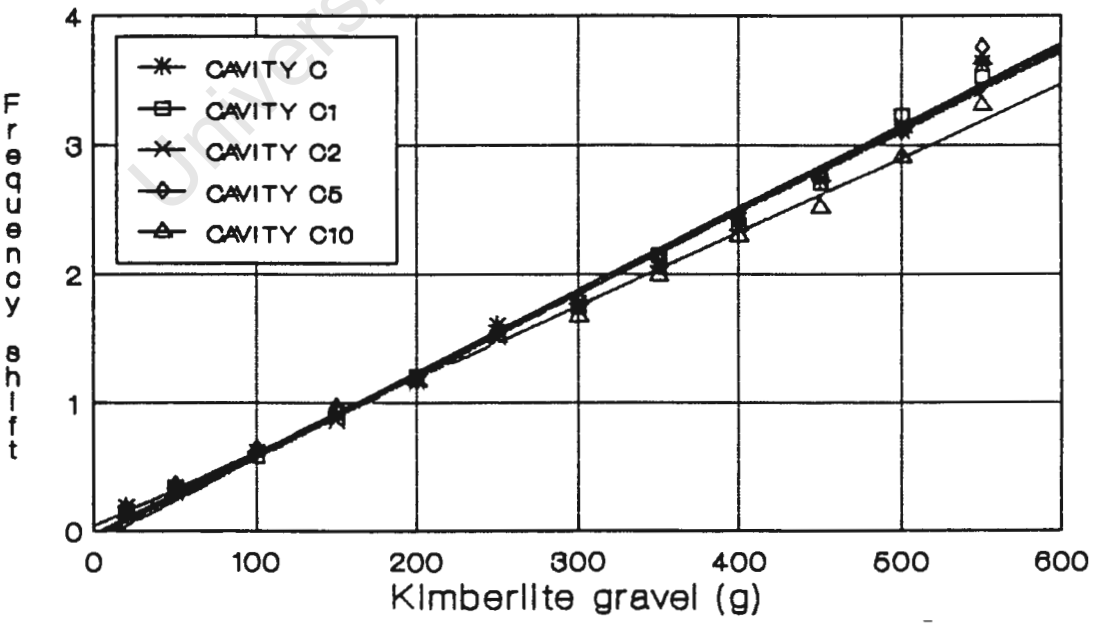

Table 5.41 & Figure 5.42: Percent frequency shift for kimberlite and water mixture for multi-gap cavity.

	No gap	1cm	2cm	5cm	10cm
(MHz) (Q) (dBm)	474.8 55 -23.0	481.95 39 -25.8	481.85 36 -26.8	481.3 38 -25.7	488.55 53 -22.8
0.452% 0.901 1.345 1.786 2.655 3.509 5.172 6.780 8.333	0.190% 0.390 0.590 0.864 1.495 2.053 3.444 4.844 6.203	0.197% 0.415 0.716 1.006 1.494 2.075 3.351 4.959 6.121	0.166% 0.291 0.664 0.882 1.557 2.148 3.393 4.939 6.112	0.073% 0.353 0.665 0.945 1.538 2.150 3.449 4.914 6.160	0.215% 0.399 0.686 0.931 1.545 2.231 3.132 4.391 5.250
15.385 (Q) (dBm)	11.384 29 -30.2	11.744 22 -33.1	11.809 21 -33.6	11.344 28 -30.2	10.695 19 -34.0

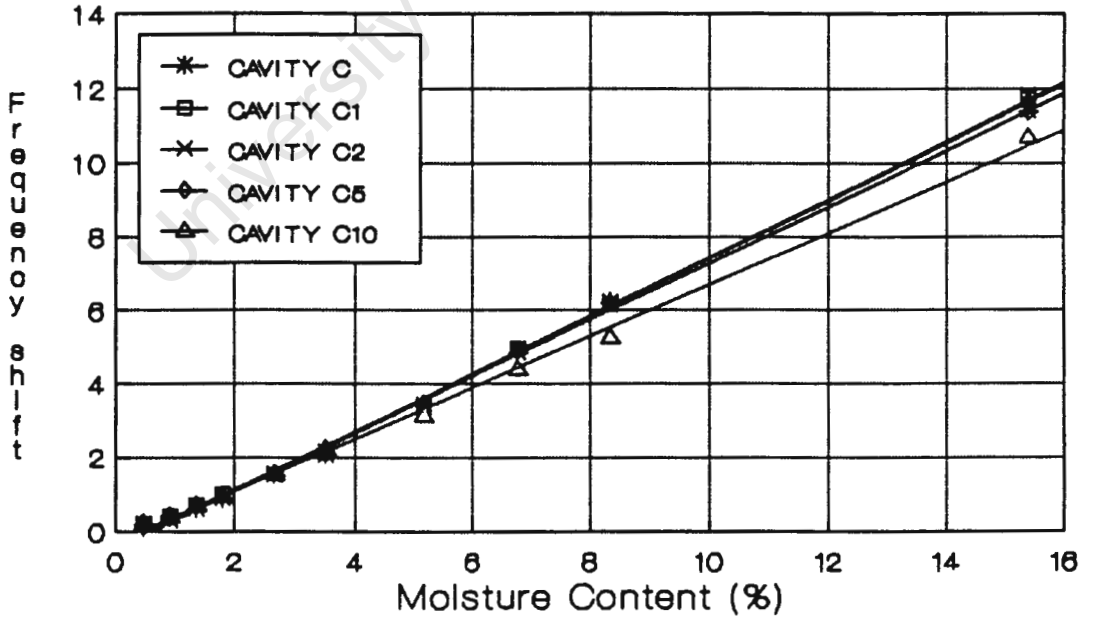

From the results in Tables 5.37, 5.39 and 5.41 and the graphs in Figures 5.38, 5.40 and 5.42 the following points can be made.

1. The quality factors of most of the multi-gapped cavities are lower than that of the original cavity. This was expected since these cavities radiate much more than before due to the extra gaps. However, for the 10cm gap the quality factor is almost equal to the no-gap case. This is because the cavity is not resonant in the TE_{01} mode, but rather in a higher order mode, due to the large discontinuity at the centre.

2. The transmission loss was low in the unloaded no gap and 10cm case, because these cavities radiate least. The low radiation for the 10cm gap case is explained in point 1. However, once loaded this cavity shows the largest loss as it is now forced to operate in the fundamental mode. This now means that it has a higher radiation than the other cavities.

3. The attenuation due to the loads themselves is basically the same for all the cavities, except for the 10cm gap case. Again this is due to the higher radiation, so allowing the cavity to be loaded.

4. The most striking result, however, is to notice that the sensitivities of the extra gap cavities are very similar, in fact sometimes better, than the case for no gap. The performance of the 10cm gap was the worst, particularly when heavily loaded. This is due to the large gap which radiated the most. This time the slope for the

moisture sensitivity ranged from 0.700 for the 10cm case to 0.791 for the 2cm gap. Again all five cases showed exceptional linearity with the minimum correlation coefficient of 0.9988 for the 10cm case. Thus the concept of separating the cavities is very promising, particularly if the gap is kept small.

The split cavity concept was then taken one step further by separating the two halves completely. The sections were then held apart by wooden struts, which are electrically insulating. The cavity was then tested for separation gaps of 1, 1.5 and 2cm. The results are given in Tables 5.43, 5.45 and 5.47 and plotted in Figures 5.44, 5.46 and 5.48.

Table 5.43 and Figure 5.44: Percent frequency shift for water for the split cavity.

	No gap	1.0cm	1.5cm	2.0cm
(MHz)	492.75	523.7	519.1	514.1
(Q)	177	83	82	71
(dBm)	-12.6	-17.0	-17.2	-17.3
2.5ml	0.406%	0.191%	0.270%	0.331%
5.0	0.873	0.458	0.694	0.759
7.5	1.086	0.821	1.060	1.011
10.0	1.542	1.298	1.560	1.420
15.0	2.182	2.654	2.716	2.237
20.0	3.064	3.704	3.699	3.404
30.0	4.698	5.748	5.317	5.524
40.0	6.494	7.180	7.263	7.139
50.0	7.935	8.803	8.804	8.559
100.0	12.532	15.116	15.026	14.486
(Q)	100	59	54	51
(dBm)	-17.8	-23.6	-24.1	-24.3

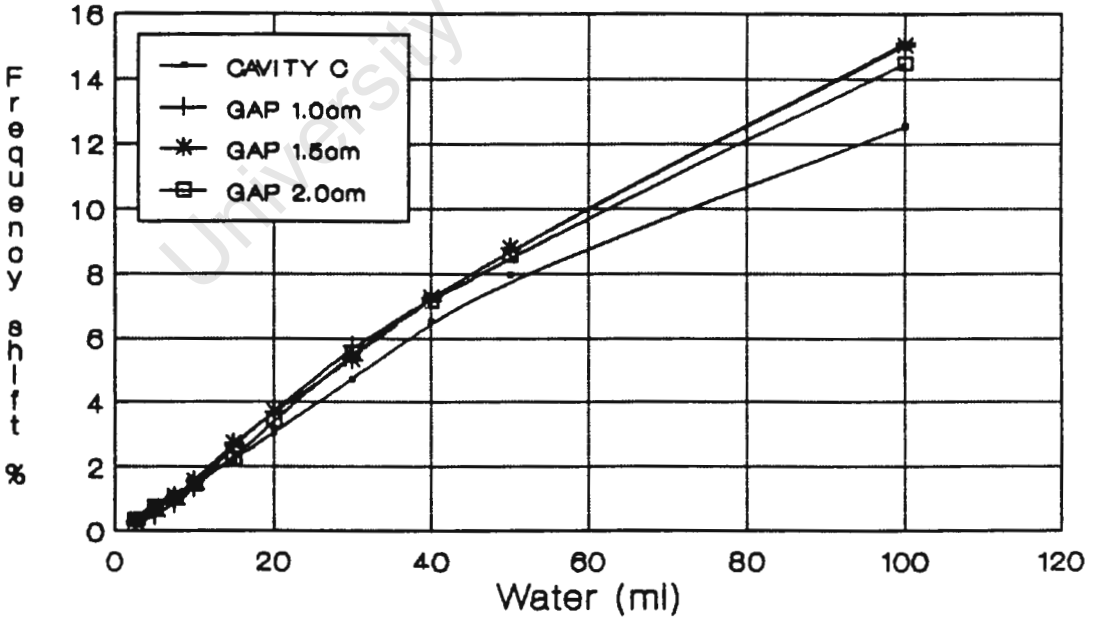

Table 5.45 and Figure 5.46: Percent frequency shift for kimberlite gravel for the split cavity.

	No gap	1.0cm	1.5cm	2.0cm
(MHz)	493.0	523.4	518.2	513.4
(Q)	160	103	86	79
(dBm)	-12.2	-21.0	-20.0	-22.0
20g	0.182%	0.115%	0.154%	0.156%
50	0.335	0.325	0.328	0.351
100	0.609	0.745	0.714	0.701
150	0.913	1.165	1.061	1.091
200	1.146	1.528	1.447	1.480
250	1.602	1.911	1.853	1.870
300	1.765	2.293	2.142	2.162
350	2.059	2.713	2.509	2.513
400	2.343	3.076	2.895	2.863
450	2.718	3.458	3.223	3.194
500	3.100	3.802	3.589	3.506
550	3.628	4.203	3.956	3.915
(Q)	55	43	40	41
(dBm)	-21.7	-26.0	-27.0	-27.0

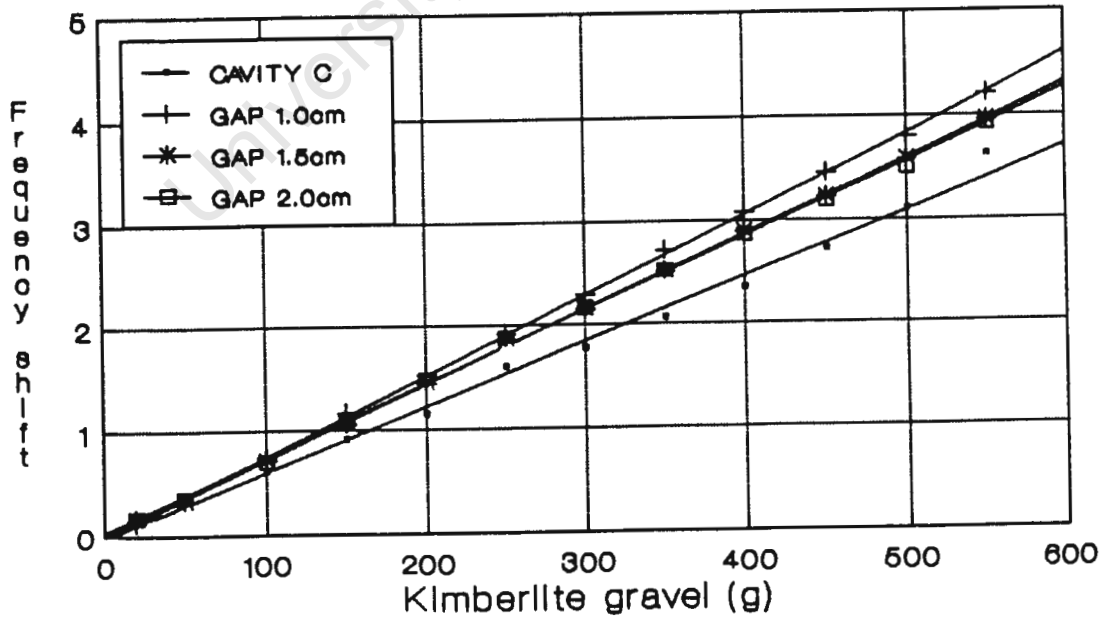

Table 5.47 & Figure 5.48: Percent frequency shift for kimberlite and water mixture for the split cavity.

	No gap	1.0cm	1.5cm	2.0cm
(MHz) (Q) (dBm)	474.8 55 -23.0	498.8 46 -26.2	495.3 44 -26.5	491.8 42 -27.0
0.452% 0.901 1.345 1.786 2.655 3.509 5.172 6.780 8.333	0.190% 0.390 0.590 0.864 1.495 2.053 3.444 4.844 6.203	0.321% 0.391 0.642 0.872 1.644 2.356 3.960 5.373 6.736	0.252% 0.474 0.797 1.030 1.746 2.403 3.846 5.310 6.824	0.325% 0.641 0.824 1.057 1.728 2.501 3.853 5.307 6.771
15.385 (Q) (dBm)	11.384 29 -30.2	13.362 24 -33.1	13.234 25 -33.3	12.932 28 -33.2

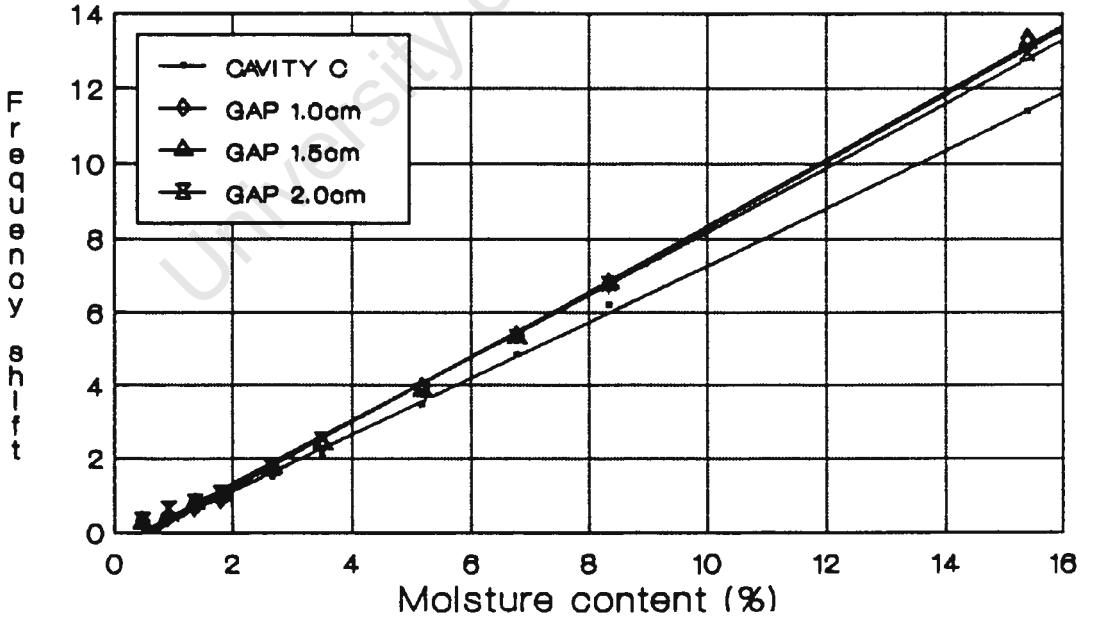

From the results in Tables 5.43, 5.45 and 5.47 and the graphs in Figures 5.44, 5.46 and 5.48 the following observations can be made.

1. As in the case of the multi-gapped cavities, the transmission loss and quality factors of the no-gap case are better than the separated cases. This is again due to the increased radiation for the latter cases.

2. The sensitivity shown by the separated cavities is better than for the no-gap case. This is probably due to increased radiation, due to the slot, reducing loading problems and hence increasing sensitivity. The moisture sensitivity for these cases almost gives an exact correlation between moisture content and frequency shift, with the slopes varying from 0.854 to 0.891. The linearity was again a strong feature of the responses.

3. For the cases of light load, the no-gap cavity is more sensitive than the separated ones. This is because the field is more concentrated in the no-gap case so being forced through the sample, thus providing greater sensitivity.

5.4.3. Conclusions for resonant cavities:

In view of the results for resonant cavities, the following conclusions can be drawn.

1. Although dielectric constant determination is extremely accurate using almost closed resonant cavities with a small non-radiating slot, employing the perturbation technique, such a system is not viable as an industrial moisture

meter for moisture measurement of kimberlite. This is due to the large size of the cavity structure. However, compromising accuracy for cavity volume has allowed the development of a viable system.

2. The principle of separating the almost closed cavity proved to be the most viable system since this allowed the two cavity halves to be positioned on either side of the conveyor belt. This is ideal for an industrial on-line moisture meter.

3. The greater sensitivity of the split cavity compared to the multi-gap cavity is most likely due to the field distortion of the discontinuities caused by the metal corner struts of the multi-gap cavity.

4. In the case of the water/gravel mixture tests, it is seen that the sensitivity is not as great as the water alone measurements. This is particularly noticeable at the low moisture readings. This is due to the initial absorption by the kimberlite gravel, which is highly porous. This means that the water does not behave as free water, but is rather bound into the gravel, so reducing its freedom of rotation [12]. In addition, after initial absorption, a single water layer forms around the gravel which is particularly strongly bound to the gravel. Only once this layer is complete and multi layers start forming does the water start behaving like free water [43]. Thus as the water volume increases the sensitivity approaches that of the water alone case, since this water is not bound to the gravel and behaves more like free water.

5. The graphs for the water alone measurements show that this response is not as linear as for the other cases. It is seen that for the increased volume of water the sensitivity starts to decrease. This is because the water acts as a complete body, unlike the mixture case, so allowing the strong cohesion bonds between the water molecules to reduce the freedom of rotation, and hence the sensitivity.

6. Although resonant cavities provided the most promising results of all the tested devices, they were not developed further. This is because the project was merely a feasibility study to determine if the moisture content of rocks could be established on-line. The high loading of the system, which reduced the amplitude and quality factor, despite using a small sample, would be alleviated using a full scale model. This is due to the lower operating frequency, which would increase the penetration and sensitivity. Thus a new on-line method for determining the moisture content of rocks has been developed using a split rectangular waveguide resonant cavity.

5.5. CONCLUSIONS FOR FREQUENCY SHIFT TECHNIQUE

From the tests and results of the frequency shift method, the following conclusions can be drawn.

5.5.1. Open resonant structures do not have a sufficiently strong and uniform field pattern to allow accurate and significant moisture measurements to be made. This is due to low quality factors which reduce the accuracy [29]. In addition, the weak fields are

easily loaded by both water and rocks, so not allowing one to separate the frequency shift due to the various individual components. Finally, the weak field also causes low sensitivity.

5.5.2. A partially-closed structure, in the form of a hybrid loop-gap resonator, provided more promising results than the open resonant structures. This was particularly noticeable at higher frequencies, where the structure was quite small and hence the E-field more uniform. However, even this device was not effective enough in providing a final structure, as the moisture sensitivity was not high enough for accurate readings. When the structure was developed to its full size, this was even more prominent, due to the E-field being confined mainly to the gap and not spreading strongly and uniformly through the rest of the structure.

5.5.3. Finally an almost closed structure, a rectangular waveguide resonant cavity, provided very promising results. Although the initial resonant cavity design was not adequate for on-line moisture measurement of rocks due to size constraints, the separated cavity proved to be a suitable structure as well as having strong sensitivity. This is due to the almost closed structure which keeps the field concentrated on the measured sample. The sensitivity approached 1% frequency shift per 1% moisture content. Although the small sample size, which only occupied one third of the slot volume, was able to load the cavity quite heavily, a full size structure, which would operate at a lower frequency so providing greater penetration and sensitivity, would overcome this problem. Since this was only a feasibility study, development of this system was not taken further.

CHAPTER 6

CONCLUSIONS

In view of the experiments performed and the results obtained, the following conclusions can be drawn:

6.1. Although 23GHz was confirmed as a moisture sensitive frequency, the attenuation of the host material at this frequency was also very high. This meant that the signal was not detectable after passing through the sample. A more sensitive receiver would not solve this problem as reflected signals from indirect paths would generate incorrect moisture values. Thus an attenuation alone system was not considered viable for this project. However, for the case of a uniform height, even surface, homogeneous and low density material, such a system could be used very effectively.

6.2. Phase techniques were not considered viable as this system also requires a direct path through the measured material. The attenuation is again very high, so reducing the potential of this method. The inherent complexity of the system would result in long development times and high component cost.

6.3. Open resonant devices have the ideal structure for on-line applications since the sample can pass by unhindered. However, the weak and non-uniform fields result in low quality factors and allow the device to be easily loaded by both water and rocks. Thus these systems show low and inconsistent sensitivity.

6.4. Although a hybrid loop-gap resonator provided a stronger field with a higher quality factor than the open resonant structures, this field was mainly confined to the parallel gap. This resulted in high moisture sensitivity near the gap, but due to the non-uniform field the sensitivity decreased rapidly away from the gap. Hence this system could not be used as a rock moisture meter.

6.5. A rectangular waveguide resonant cavity provided a strong predictable field due to its closed structure. This resulted in the greatest sensitivity of all the devices tested. Due to the closed structure, however, it was impossible to pass a large volume of rocks through the cavity. Splitting the cavity into two halves and placing one half above the sample and the other half below, provided both high sensitivity and a suitable structure. Thus a new on-line rock moisture meter has been developed using a split rectangular waveguide resonant cavity.

CHAPTER 7

RECOMMENDATIONS

As a result of the findings and the conclusions presented in this thesis, the following recommendations are made:

7.1. In the case of a uniform height, even surface, homogeneous, low density material Eg. paper or grain, an attenuation alone moisture meter can be developed. An operating frequency of 23GHz will highlight the moisture very strongly so eliminating the need for the usual density compensation. However, calibration curves and an averaging system would be required for each measured material.

7.2. For the on-line moisture determination of rocks, a split rectangular waveguide resonant cavity has provided excellent results. This has a practical structure while still providing accurate moisture sensitivity and high linearity. Although a full scale model was not developed, the lower operating frequency will provide greater penetration as well as increasing sensitivity. Thus this device can be used as an on-line rock moisture meter.

LIST OF REFERENCES

[1] Carr-Brion K.G., The on-line determination of moisture in bulk solids - an overview, On-line moisture measurement of bulk solids for process control seminar publication, pp 1-3, Westminster, UK, March 1988.

[2] Ray R.D., The automatic determination of moisture in coal, The British Coal Utilisation Research Association, Vol 24, No 3, pp 117-137, 1960-Part 2.

[3] Klein A., Comparison of rapid moisture meters, Aufbereitungs-Technik, Nr 1, pp 10-16, 1987.

[4] Kress-Rogers E., Kent M., Microwave measurement of powder moisture and density, Journal of Food Engineering, Vol 6, pp 345-376, 1987.

[5] Meyer W., Schilz W., A microwave method for density independent determination of the moisture content of solids, J. Phys. D: Appl. Phys., 13, pp 1823-1830, 1980.

[6] Zender C.B., Application of the combination microwave gamma ray gauge to wood chip weight and moisture measurement, Pulp and Paper Magazine of Canada, Vol 10, pp 678-688, 1967.

[7] Klein A., Microwave determination of moisture content compared with capacitive, infra-red and conductive measurement methods. Comparison of on-line measurements at coal preparation plants, Proc. 14th Europ. Microwave Conf., pp 661-666, September 1984.

[8] Hall D.A., Morris G.F., Scott C., The continuous determination of moisture in coal, Mining and Minerals Engineering, Vol 5(10), pp 30-40, 1969.

[9] Scott J.H., Carroll R.D., Cunningham D.R., Dielectric constant and electrical conductivity measurement of moist rock: a new laboratory method, Journal of Geophysical Research, Vol 72, No 20, pp 5101-5115, 1967.

[10] Iskander M.F., DuBow J.B., Time- and frequency-domain techniques for measuring the dielectric properties of rocks: a review, Journal of Microwave Power, 18(3), pp 55-74, 1983.

[11] Sen P.N., Dielectric anomaly in inhomogeneous materials with application to sedimentary rocks, Applied Physics Letters, Vol 39, No 8, pp 667-668, 1981.

[12] Badzioch S., Cornford G.B., Determination of moisture in coal, The British Coal Utilisation Research Association, Vol 16, No 3, pp 77-89, 1952.

[13] Meyer W., Schilz W., High frequency dielectric data on selected moist materials, Journal of Microwave Power, 17(1), pp 67-81, 1982.

[14] Harvey A.F., Microwave engineering, Academic press, London, pp 1074-1075, 1963.

[15] Kraszewski A., Kulinski S., Madziar J., Zielkowski K., Microwave on-line moisture content monitoring in low-hydrated organic materials, Journal of Microwave Power, 15(4), pp 267-275, 1980.

[16] Jacobsen R., Meyer W., Schrage B., Density independent moisture meter at X-band, Proc. 10th Europ. Microwave Conf., pp 216-220, Warszawa, Poland, September 1980.

[17] Kent M., Meyer W., Density independent moisture metering in fish meal industry, Proc. 11th Europ. Microwave Conf., pp 448-453, September 1981.

[18] Klein A., Microwave moisture determination of coal.- A comparison of attenuation and phase measurement, Proc. 10th Europ. Microwave Conf., pp 526-530, Warszawa, Poland, September 1980.

[19] Hoppe W., Meyer W., Schilz W., Density-independent moisture metering in fiberous materials using a double cut-off Gunn-oscillator, IEEE MTT-S International Microwave symposium digest, pp 419-421, 1980.

[20] Kraszewski A., Kulinski S., An improved microwave method of moisture content measurement and control, IEEE Trans. on Industr. Electr. and Control Instrum., IECI-23(4), pp 364-370, 1976.

[21] Voss W.A.G., Microwave instruments for material control, Journal of Microwave Power, 4(3), pp 210-216, 1969.

[22] Klein A., Schicker W., Schiek B., Microwave moisture measurements with reduced sensitivity to particle size and shape, Proc. 12th Europ. Microwave Conf., pp 593-598, September 1982.

[23] Ostwald O., Schiek B., Chaloupka H., A new approach for a quantitive microwave moisture-measurement, Proc. 10th Europ. Microwave Conf., pp 211-215, Warszawa, Poland, September 1980.

[24] Chaloupka H., Ostwald O., Schiek B., Structure independent microwave moisture measurement, Journal of Microwave Power, 15(4), pp 221-231, 1980.

[25] Lytle R.J., Measurement of earth medium electrical characteristics: techniques, results and applications, IEEE Trans. on Geo. Science Electron, Vol 12, No 3, pp 81-101, 1974.

[26] Bosisio R.G., Giroux M., Automatic field measurements in microwave applicators, Journal of Microwave Power, 4(3), pp 152-156, 1969.

[27] Kumar A., Smith D.G., Microwave properties of yarns and textiles using a resonant microwave cavity, IEEE Trans. on Inst. Meas., IM-26(2), pp 95-98, 1977.

[28] Lakshminarayana M.R., Partain L.D., Cook W.A., Simple microwave technique for independent measurement of sample size and dielectric constant with results for a gunn oscillator system, IEEE Trans. Microwave Theory Tech., MTT-27(7), pp 661-665, 1979.

[29] Stuchly M.A., Stuchly S.S., Coaxial line reflection methods for measuring dielectric properties of biological substances at radio and microwave frequencies - a review, IEEE Trans. on Inst. Meas., IM-29(3), pp 176-183, 1980.

[30] Bosisio R.G., Giroux M., Couderc D., Paper sheet moisture measurement by microwave phase perturbation techniques, Journal of Microwave Power, 5(1), pp 25-34, 1970.

[31] Stuchly M.A., Brady M.M., Stuchly S.S., Gajda G., Equivalent circuit of an open-ended coaxial line in a lossy dielectric, IEEE Trans. on Inst. Meas., IM-31(2), pp 116-119, 1982.

[32] Church R.H., Webb W.E., A measurement technique for determining the dielectric properties of low loss minerals, Journal of Microwave Power, Symposium summaries, pp 113-115, 1986.

[33] Webb W.E., Church R.H., Measurement of dielectric properties of minerals at microwave frequencies, Report of investigations 9035, United States Bureau of Mines, 1986.

[34] Mercer S.R., Rock differentiation using microwave irradiation, Unpublished MSc thesis, University of Cape Town, 1987.

[35] Aldera M.A., A 10GHz rock differentiation system, Unpublished BSc thesis project, University of Cape Town, 1986.

[36] Private communication with De Beers Diamond Research Laboratories.

[37] Parkhomenko E.I., Electrical properties of rocks, Plenum press, New York, pp 11-51 and 185-236, 1967.

[38] Kalinski J., Further possibilities of the modulated subcarrier technique for microwave attenuation measurements in industrial applications, IEEE Trans. on Inst. Meas., IM-21, pp 291-300, 1972.

[39] Kumar A., Smith D.G., Microwave properties of yarns and textiles using a resonant microwave cavity, IEEE Trans. on Inst. Meas., IM-26(2), pp 95-98, 1977.

[40] Nelson S.O., Fanslow G.E., Bluhm D.D., Frequency dependence of the dielectric properties of coal, Journal of Microwave Power, 15(4), pp 277-282, 1980.

[41] Briggs W.E., Lewis J.E., Tranquilla J.M., Dielectric properties of New Brunswick oil shale, Journal of Microwave Power, 18(1), pp 75-82, 1983.

[42] Mehdizadeh M., Ishii T.K., Hyde J.S., Froncisz W., Loop-gap resonator: a lumped mode microwave resonant structure, IEEE Trans. Microwave Theory Tech., MTT-31(12), pp 1059-1064, 1983.

[43] Wilkes J.M., Waldie A.H., Analysis and mathematical modelling of an on-line cotton moisture measuring system, Textile research Journal, pp 29-39, January 1987.

BIBLIOGRAPHY

Aldera M.A., A 10GHz rock differentiation system, Unpublished BSc thesis project, University of Cape Town, 1986.

Badzioch S., Cornford G.B., Determination of moisture in coal, The British Coal Utilisation Research Association, Vol 16, No 3, pp 77-89, 1952.

Benson I.B., Edgar R.F., New development in moisture measurement using diffuse infrared reflectance, On-line moisture measurement of bulk solids for process control seminar publication, pp 9-20, Westminster, UK, March 1988.

Bosisio R.G., Giroux M., Automatic field measurements in microwave applicators, Journal of Microwave Power, 4(3), pp 152-156, 1969.

Bosisio R.G., Giroux M., Couderc D., Paper sheet moisture measurement by microwave phase perturbation techniques, Journal of Microwave Power, 5(1), pp 25-34, 1970.

Boulanger R.J., Boerner W.M., Hamid M.A.K., Comparison of microwave and dielectric heating systems for the control of moisture content and insect infestation of grain, Journal of Microwave Power, 4(3), pp 194-208, 1969.

Briggs W.E., Lewis J.E., Tranquilla J.M., Dielectric properties of New Brunswick oil shale, Journal of Microwave Power, 18(1), pp 75-82, 1983.

Carr-Brion K.G., The on-line determination of moisture in bulk solids - an overview, On-line moisture measurement of bulk solids for process control seminar publication, pp 1-3, Westminster, UK, March 1988.

Chaloupka H., Ostwald O., Schiek B., Structure independent microwave moisture measurement, Journal of Microwave Power, 15(4), pp 221-231, 1980.

Chouikhi S.M., Use of RF wave reflection method for moisture content determination in powered and granulated products, On-line moisture measurement of bulk solids for process control seminar publication, pp 21-24, Westminster, UK, March 1988.

Church R.H., Webb W.E., A measurement technique for determining the dielectric properties of low loss minerals, Journal of Microwave Power, Symposium summaries, pp 113-115, 1986.

Grant J.P., Clarke R.N., Symm G.T., Spyron N.M., A critical study of the open-ended coaxial line sensor technique for RF and microwave complex permittivity measurement,

Hall D.A., Morris G.F., Scott C., The continuous determination of moisture in coal, Mining and Minerals Engineering, Vol 5(10), pp 30-40, 1969.

Hall D.A., Sproson J.C., Gray W.A., The rapid determination of moisture in coal using microwaves, Part 2: plant trials, J.Inst.Fuel, Vol 45, pp 163-167, March 1972.

Harvey A.F., Microwave engineering, Academic press, London, pp 1074-1075, 1963.

Hoppe W., Meyer W., Schilz W., Density-independent moisture metering in fiberous materials using a double cut-off Gunn-oscillator, IEEE MTT-S International Microwave symposium digest, pp 419-421, 1980.

Iskander M.F., DuBow J.B., Time- and frequency-domain techniques for measuring the dielectric properties of rocks: a review, Journal of Microwave Power, 18(3), pp 55-74, 1983.

Jacobsen R., Meyer W., Schrage B., Density independent moisture meter at X-band, Proc. 10th Europ. Microwave Conf., pp 216-220, Warszawa, Poland, September 1980.

Kalinski J., Further possibilities of the modulated subcarrier technique for microwave attenuation measurements in industrial applications, IEEE Trans. on Inst. Meas., IM-21, pp 291-300, 1972.

Kalinski J., Automatic phase control system for microwave industrial on-line moisture-attenuation-voltage (MAV) converter, IEEE Trans. on Industr. Electr. and Control Instrum., IECI-23(4), pp 425-427, 1976.

Kalinski J., Self-adjusting microwave homodyne circuit for on-line simultaneous attenuation and phase measurement, Proc. 7th Europ. Microwave Conf., pp 267-272, Copenhagen, Denmark, September 1977.

Kalinski J., An industrial microwave attenuation monitor (MAM) and its application for continuous moisture content measurements, Journal of Microwave Power, 13(3), pp 275-281, 1978.

Keller G.V., "Supplementary guide to the literature on Electrical properties of rocks and minerals" in Electrical properties of rocks, Parkhomenko E.I., Plenum press, New York, pp 286-293, 1967.

Kent M., Complex permittivity of white fish meal in the microwave region as a function of temperature and moisture content, J. Phys. D: Appl. Phys., 3, pp 1275-1283, 1970.

Kent M., Complex permittivity of protein powders at 9.4 GHz as a function of temperature and hydration, J. Phys. D: Appl. Phys., 5, pp 394-409, 1972.

Kent M., Meyer W., Density independent moisture metering in fish meal industry, Proc. 11th Europ. Microwave Conf., pp 448-453, September 1981.

Kent M., Meyer W., Density independent microwave moisture meter using stripline sensors, 16th Microwave Power Symposium, Toronto, 1981.

Kent M., Microwave measurement for moisture content and bulk density, On-line moisture measurement of bulk solids for process control seminar publication, pp 43-47, Westminster, UK, March 1988.

King R.J., Microwave homodyne systems, Peter Peregrinus LTD, England, pp 308-309, 1978.

Klein A., Microwave moisture determination of coal.- A comparison of attenuation and phase measurement, Proc. 10th Europ. Microwave Conf., pp 526-530, Warszawa, Poland, September 1980.

Klein A., Schicker W., Schiek B., Microwave moisture measurements with reduced sensitivity to particle size and shape, Proc. 12th Europ. Microwave Conf., pp 593-598, September 1982.

Klein A., Microwave determination of moisture content compared with capacitive, infra-red and conductive measurement methods. Comparison of on-line measurements at coal preparation plants, Proc. 14th Europ. Microwave Conf., pp 661-666, September 1984.

Klein A., Comparison of rapid moisture meters, Aufbereitungs-Technik, Nr 1, pp 10-16, 1987.

Klein A., On-line microwave meter for determining the moisture content of bulk materials on conveyor belts, On-line moisture measurement of bulk solids for process control seminar publication, pp 37-42, Westminster, UK, March 1988.

Kraszewski A., Kulinski S., An improved microwave method of moisture content measurement and control, IEEE Trans. on Industr. Electr. and Control Instrum., IECI-23(4), pp 364-370, 1976.

Kraszewski A., Kulinski S., Madziar J., Zielkowski K., Microwave on-line moisture content monitoring in low-hydrated organic materials, Journal of Microwave Power, 15(4), pp 267-275, 1980.

Kress-Rogers E., Kent M., Microwave measurement of powder moisture and density, Journal of Food Engineering, Vol 6, pp 345-376, 1987.

Kumar A., Smith D.G., Microwave properties of yarns and textiles using a resonant microwave cavity, IEEE Trans. on Inst. Meas., IM-26(2), pp 95-98, 1977.

Lakshminarayana M.R., Partain L.D., Cook W.A., Simple microwave technique for independent measurement of sample size and dielectric constant with results for a gunn oscillator system, IEEE Trans. Microwave Theory Tech., MTT-27(7), pp 661-665, 1979.

Lytle R.J., Measurement of earth medium electrical characteristics: techniques, results and applications, IEEE Trans. on Geo. Science Electron, Vol 12, No 3, pp 81-101, 1974.

Maris P.I., On-line moisture measurement of whole grain and flour, On-line moisture measurement of bulk solids for process control seminar publication, pp 33-36, Westminster, UK, March 1988.

McFarlane I., Moisture measurement using light emitting diodes, On-line moisture measurement of bulk solids for process control seminar publication, pp 5-8, Westminster, UK, March 1988.

Mehdizadeh M., Ishii T.K., Hyde J.S., Froncisz W., Loop-gap resonator: a lumped mode microwave resonant structure, IEEE Trans. Microwave Theory Tech., MTT-31(12), pp 1059-1064, 1983.

Mercer S.R., Rock differentiation using microwave irradiation, Unpublished MSc thesis, University of Cape Town, 1987.

Meyer W., Dielectric measurement on polymeric materials by using superconducting microwave resonators, IEEE Trans. Microwave Theory Tech., MTT-31(2), pp 116-119, 1982.

Meyer W., Schilz W., A microwave method for density independent determination of the moisture content of solids, J. Phys. D: Appl. Phys., 13, pp 1823-1830, 1980.

Meyer W., Schilz W., High frequency dielectric data on selected moist materials, Journal of Microwave Power, 17(1), pp 67-81, 1982.

Nelson S.O., Fanslow G.E., Bluhm D.D., Frequency dependence of the dielectric properties of coal, Journal of Microwave Power, 15(4), pp 277-282, 1980.

Nelson S.O., Observations on the density dependence of dielectric properties of particulate materials, Journal of Microwave Power, 18(2), pp 143-152, 1983.

Ostwald O., Schiek B., Chaloupka H., A new approach for a quantitive microwave moisture-measurement, Proc. 10th Europ. Microwave Conf., pp 211-215, Warszawa, Poland, September 1980.

Parkhomenko E.I., Electrical properties of rocks, Plenum press, New York, pp 11-51 and 185-236, 1967.

Pink C.D., Liquid level measurement using a coplanar transmission line, Unpublished MSc thesis, University of Cape Town, 1989.

Ray R.D., The automatic determination of moisture in coal, The British Coal Utilisation Research Association, Vol 24, No 3, pp 117-137, 1960-Part 2.

Schafer G.E., A modulated subcarrier technique of measuring microwave phase shifts, IRE Trans. on Instrumentation, Vol I-9, pp 217-219, 1960.

Scott J.H., Carroll R.D., Cunningham D.R., Dielectric constant and electrical conductivity measurement of moist rock: a new laboratory method, Journal of Geophysical Research, Vol 72, No 20, pp 5101-5115, 1967.

Sen P.N., Dielectric anomaly in inhomogeneous materials with application to sedimentary rocks, Applied Physics Letters, Vol 39, No 8, pp 667-668, 1981.

September R.J, A microwave moisture meter, Unpublished BSc thesis project, University of Cape Town, 1984.

Stuchly M.A., Stuchly S.S., Coaxial line reflection methods for measuring dielectric properties of biological substances at radio and microwave frequencies - a review, IEEE Trans. on Inst. Meas., IM-29(3), pp 176-183, 1980.

Stuchly M.A., Brady M.M., Stuchly S.S., Gajda G., Equivalent circuit of an open-ended coaxial line in a lossy dielectric, IEEE Trans. on Inst. Meas., IM-31(2), pp 116-119, 1982.

Tiuri M., Heikkila S., Microwave instrument for accurate moisture measurement of timber, Proc. 9th Europ. Microwave Conf., pp 702-705, Brighton, England, September 1979.

Voss W.A.G., Microwave instruments for material control, Journal of Microwave Power, 4(3), pp 210-216, 1969.

Voss W.A.G., A note on moisture content, Journal of Microwave Power, 4(3), pp 165, 1969.

Webb W.E., Church R.H., Measurement of dielectric properties of minerals at microwave frequencies, Report of investigations 9035, United States Bureau of Mines, 1986.

Wilkes J.M., Waldie A.H., Analysis and mathematical modelling of an on-line cotton moisture measuring system, Textile research Journal, pp 29-39, January 1987.

Williams K.F., Williams R.B., Measurement of the moisture content of particulate solids in ironmaking processes, On-line moisture measurement of bulk solids for process control seminar publication, pp 25-31, Westminster, UK, March 1988.

Zender C.B., Application of the combination microwave-gamma ray gauge to wood chip weight and moisture measurement, Pulp and Paper Magazine of Canada, Vol 10, pp 678-688, 1967.

APPENDIX A: Transmitter/receiver waveguide cavity design

When designing the waveguide cavity the following considerations had to be made:

1. The waveguide slot should have standard K-band dimensions (a = 10.67mm and b = 4.32mm).

2. The bolt holes are also standardised, thus the position of these are fixed.

3. The flange width and height of K-band attachments are specified as 22.2mm, thus setting the cavity width. The height, however, was increased to 27mm for ease of manufacture.

4. The length of the cavity should be about half a wavelength so that the microwave device can be mounted approximately a quarter of a wavelength from a short circuit plate. This would make the cavity length 8.24mm, but machining this would be impossible as the RF choke still has to be included. The next option is to set the diode three quarters of a wavelength from a short circuit. This makes the total cavity length 1½ wavelengths long, i.e 24.7mm. Thus the length of the cavity was made 22mm so that general K-band frequencies could be used, and fine tuned later.

5. The RF choke consists of three, quarter wavelength sections, of 4mm each. These alternate from low, high and then low impedance, so that the signal sees an effective very high impedance. This is due to quarter wavelength impedance transformations. Finally the RF choke is insulated from the main cavity.

6. The choke is held in place by a threaded section, but this is also isolated from the choke itself by an insulation washer.

7. Attached to the RF choke is the D.C post. The post diameter is 2mm so that the microwave diode, whose connection mounting is 1.5mm in diameter, can fit snugly in it.

8. The lower matching post diameter is 7mm, and 1mm thick.

The full design is given below:

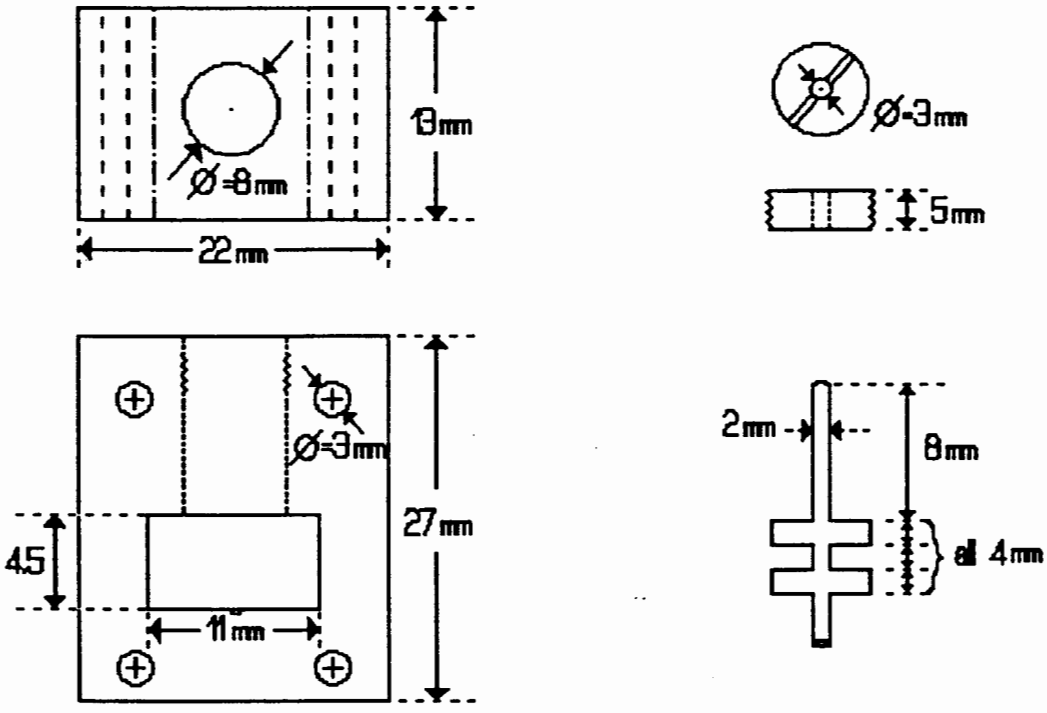

APPENDIX B: Band-stop filter design for microstrip

As in the band-pass case, the filter could not be designed for 100MHz, so 600MHz was used instead.
Using the relationship that h = 3mm for 10GHz, then for 600MHz h = 50mm. This was then reduced to 30mm for better field strength.
At 600MHz, λ = 0.5m. Thus $\lambda/4$ = 12.5cm.
The impedances chosen were 100Ω and 200Ω. Higher impedances were not considered as the width of the sections would then get too narrow.
Since the dielectric is air (ϵ = 1) the w/h ratio is

w/h = 0.1 for 200Ω thus w = 3mm

w/h = 1.7 for 100Ω thus w = 51mm

using the Wheeler charts wide strip approximation.

A three section filter was used to get a reasonable insertion loss. The layout is given below:

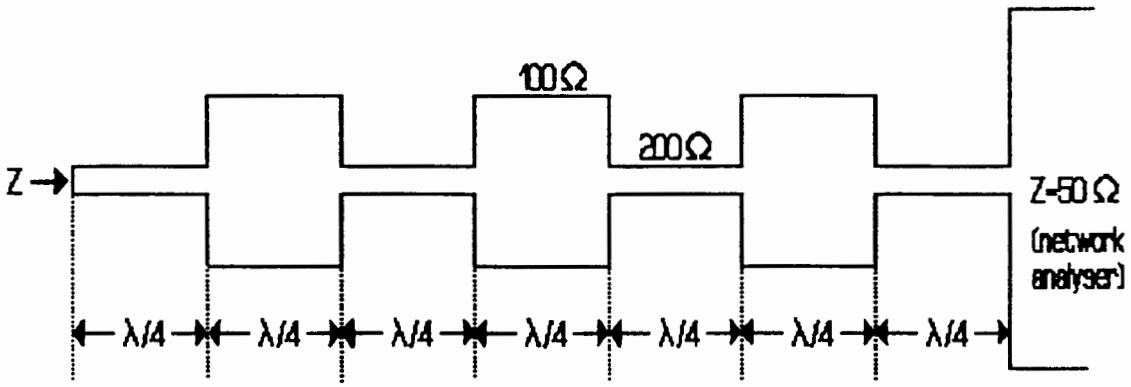

Using the relationship

$$Z_{in} = Z_{01}^2 / Z_{term}$$

for quarter wavelength impedance transformations, the total impedance looking into the filter is given by

Z = 205kΩ

Since the impedance of the network analyser is 50Ω, the V.S.W.R = s = 4096.

The reflection coefficient ≡ μ = (s-1) / (s+1) = 0.9995
The reflected power ≡ μ^2 = 0.9990
Hence the insertion loss ≡ 1 - μ^2 = 30.1dB
The layout shown before was too bulky, so the layout was adjusted as seen below:

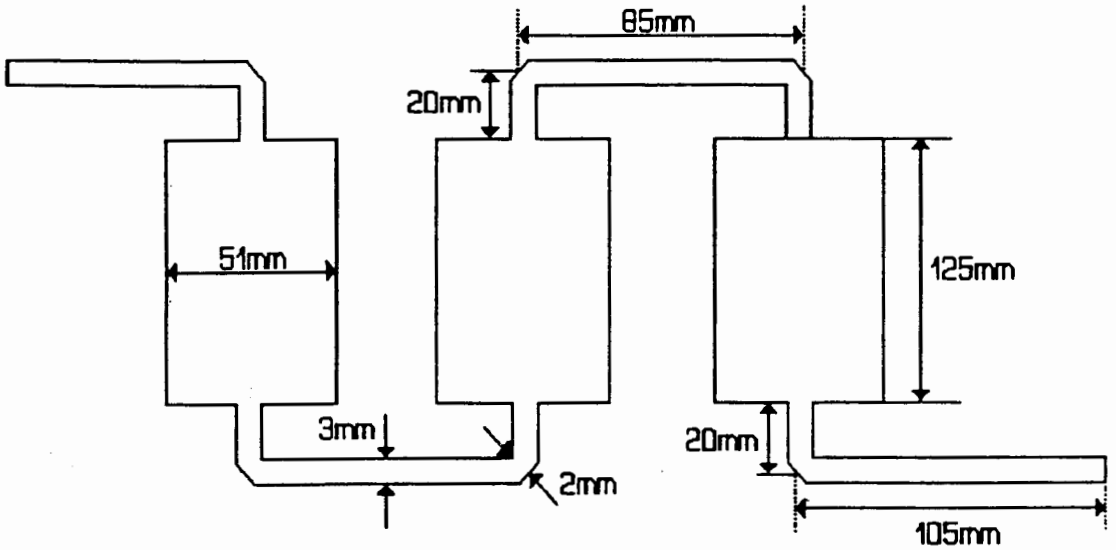

The filter was made out of brass foil and attached to expanded polystyrene, to maintain the shape. The filter was powered by the Network Analyser, so SMA connectors were used.
The 200Ω end sections were tapered, keeping w/h = 0.1. This maintains the impedance at 200Ω all the way to the ground plane so that the SMA connector could be well earthed.